AD-A115 233 TEXAS A AND M UNIV COLLEGE STATION DEPT OF CHEMISTRY F/G 20/6
RECENT ADVANCES IN MULTICOMPONENT FLUORESCENCE ANALYSIS.(U)
APR 82 I M WARNER, L B MCGOWN N00014-80-C-0703
UNCLASSIFIED TR-6 NL

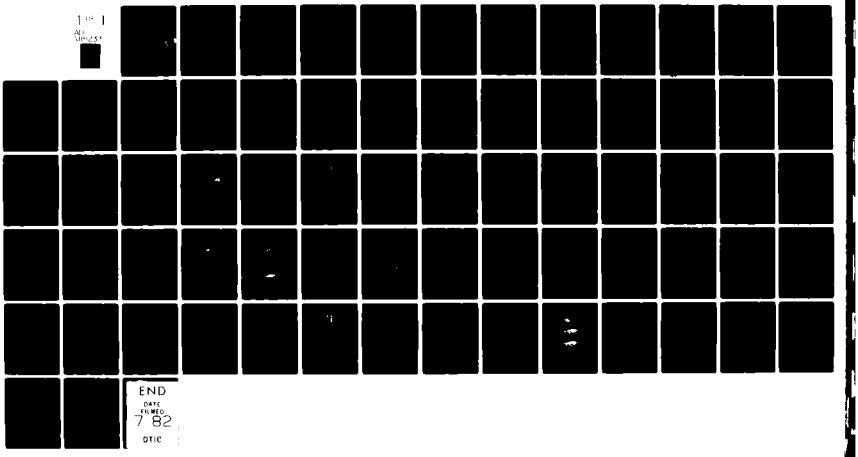

END
DATE FILMED
7 82
DTIC

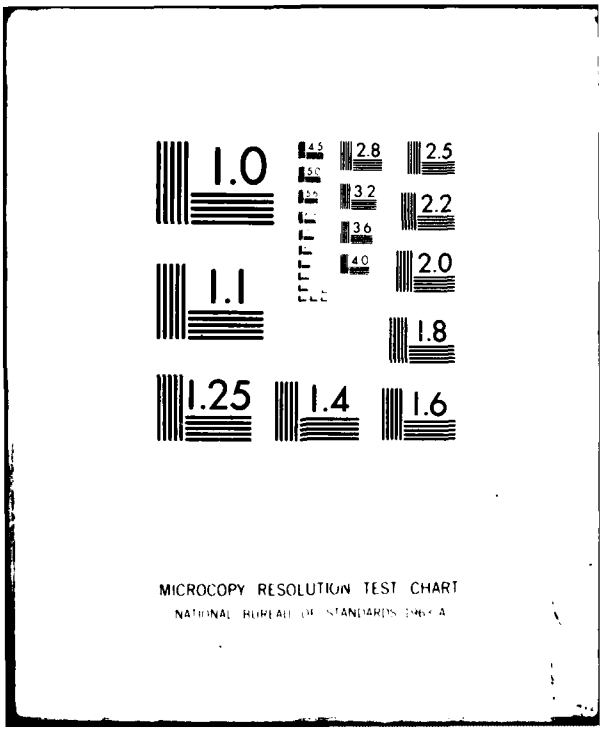
1.0
1.1
1.25
1.4
1.6
1.8
2.0
2.2
2.5
2.8
3.2
3.6
4.0
MICROCOPY RESOLUTION TEST CHART
NATIONAL BUREAU OF STANDARDS 1963-A

SECURITY CLASSIFICATION OF THIS PAGE (When Data Entered)

REPORT DOCUMENTATION PAGE

READ INSTRUCTIONS BEFORE COMPLETING FORM

1. REPORT NUMBER: 6	2. GOVT ACCESSION NO.: AD-A115233
3. RECIPIENT'S CATALOG NUMBER:	
4. TITLE (and Subtitle): Recent Advances in Multicomponent Fluorescence Analysis	5. TYPE OF REPORT & PERIOD COVERED: Interim Technical Report
	6. PERFORMING ORG. REPORT NUMBER:
7. AUTHOR(s): Isiah M. Warner and Linda R. McGown	8. CONTRACT OR GRANT NUMBER(s): N00014-80-C-0703
9. PERFORMING ORGANIZATION NAME AND ADDRESS: Department of Chemistry, Texas A&M University, College Station, TX. 77843	10. PROGRAM ELEMENT, PROJECT, TASK AREA & WORK UNIT NUMBERS: NR-051-747
11. CONTROLLING OFFICE NAME AND ADDRESS: Chemistry Program, Office of Naval Research, 800 North Quincy St. - Arlington, Va. 22217	12. REPORT DATE: April 20, 1982 13. NUMBER OF PAGES: 69
14. MONITORING AGENCY NAME & ADDRESS (if different from Controlling Office): Martial Davonst-ONR, Administrative Contracting Office, Room 582, Federal Building - 300 East 8th St., Austin, TX. 78701	15. SECURITY CLASS. (of this report): Unclassified 15a. DECLASSIFICATION/DOWNGRADING SCHEDULE:

16. DISTRIBUTION STATEMENT (of this Report)

Approved for PUblic Release: Distribution Unlimited

17. DISTRIBUTION STATEMENT (of the abstract entered in Block 20, if different from Report)

18. SUPPLEMENTARY NOTES

Prepared for Publication in CRC Critical Reviews in Analytical Chemistry

19. KEY WORDS (Continue on reverse side if necessary and identify by block number)

Multicomponent Analysis, Fluorescence

20. ABSTRACT (Continue on reverse side if necessary and identify by block number)

Numerous advances in fluorescence spectroscopy have been made in the past few years. Many of these advances have come in the form of improved instrumentation and new data reduction strategies. Primary emphasis of these new strategies is to develop new systems for multicomponent analysis. This manuscript described a number of recent advances in fluorescence spectroscopy with primary emphasis on multicomponent techniques. Methods for increasing sensitivity of fluorescence analysis are also discussed, along with a few new ideas for use in conventional instrumentation. However, most of the review (Cont on Back)

DD FORM 1 JAN 73 1473

82 06 07 063

SECURITY CLASSIFICATION OF THIS PAGE (When Data Entered)

OFFICE OF NAVAL RESEARCH

Contract N00014-80-C-0703

Task No. NR 051-747

TECHNICAL REPORT NO. 6

Recent Advances in Multicomponent Fluorescence Analysis

by

Isiah M. Warner and Linda B. McGown

Prepared for Publication

in

CRC Critical Reviews in

Analytical Chemistry

Department of Chemistry
Texas A&M University
College Station, Texas 77843

April, 1982

RECENT ADVANCES IN MULTICOMPONENT FLUORESCENCE ANALYSIS

Authors: **Isiah M. Warner**
Department of Chemistry
Texas A & M University
College Station, Texas

Linda B. McGown
Department of Chemistry
California State University
Long Beach, California

Referee: Gary D. Christian
Department of Chemistry
University of Washington
Seattle, Washington

TABLE OF CONTENTS

I. INTRODUCTION

An increasing number of researchers are recognizing the distinct advantages offered by molecular fluorescence spectroscopy as an analytical tool. This increase is evident from the large number of manuscripts and monographs published in this area. In the area of fluorescence instrumentation alone, the number of referenced articles in the biennial "Fundamental Reviews" of *Analytical Chemistry* increased from 82 in 1976 to 156 in 1978. This widespread use of fluorescence analysis arises from its selectivity and sensitivity. The selectivity of fluorescence assay is derived from the dependence of the emission intensity both on the wavelength of the exciting radiation and on the wavelength of detection for the emitted radiation. Thus, it is often possible to find optimal spectral regions where the effects of background or interfering fluorescence are minimized. Moreover, the use of phosphorescence spectra and exploitation of differences in lifetimes and polarization can provide even greater selectivity. The sensitivity advantage of fluorescence arises from the direct detection of the emitted photons to give an emission signal. This is in contrast to absorption spectroscopy, in which a small difference between two large signals is measured. Consequently, with the use of state-of-the-art detectors, the sensitivity of fluorescence methods will often surpass the sensitivity of similar absorption methods by three orders of magnitude.

Numerous advances in the area of fluorescence spectroscopy have been made in the past few years. These advances have come largely in the form of improved instrumentation and new data reduction strategies. A detailed account of each of these improvements is beyond the scope of this review. Therefore, our treatment will be limited to those techniques which have proved to be either novel concepts or novel applications of established concepts. Broader, more general, coverage of many areas of fluorescence spectroscopy can be found in any number of review articles,[1-4] and more specific accounts in detailed reviews by Bridges,[5] Gibson,[6] Guilbault,[7] Klainer,[8] and others.[9-12] Although our discussion will focus on the two major areas of fluorescence spectroscopy mentioned above (new developments in instrumentation and new data reduction strategies), we do feel that the application and refinement of the more traditional methods of fluorimetry warrant some discussion. These advances will be discussed in Section II and will emphasize improvements in the sensitivity of fluorescence assay. Section III focuses on the development of novel instrumental methods for multicomponent fluorescence analysis, including discussions of time- and phase-resolved methods, synchronous excitation, selective modulation, total luminescence spectroscopy, and several other techniques.

The rapid data acquisition capabilities provided by advanced fluorescence instrumentation have caused an increased need for new data reduction strategies. In Section IV we will describe some of the new data reduction strategies being developed to meet this need in multicomponent fluorescence analysis.

Finally, although the major concern of this manuscript is multicomponent fluorescence analysis, we will also discuss multicomponent phosphorescence methods, many of which can be modified to provide multicomponent fluorescence capabilities.

II. GENERAL ADVANCES IN FLUORESCENCE INSTRUMENTATION

Many advances in fluorescence spectroscopy have been directed towards increasing sensitivity, including improvements in signal-to-noise ratio (S/N), background reduction, and data acquisition and manipulation. Adaptations and modifications for improving the sensitivity of the traditional fluorescence instrumental configuration, shown in Figure 1, are discussed in this section.

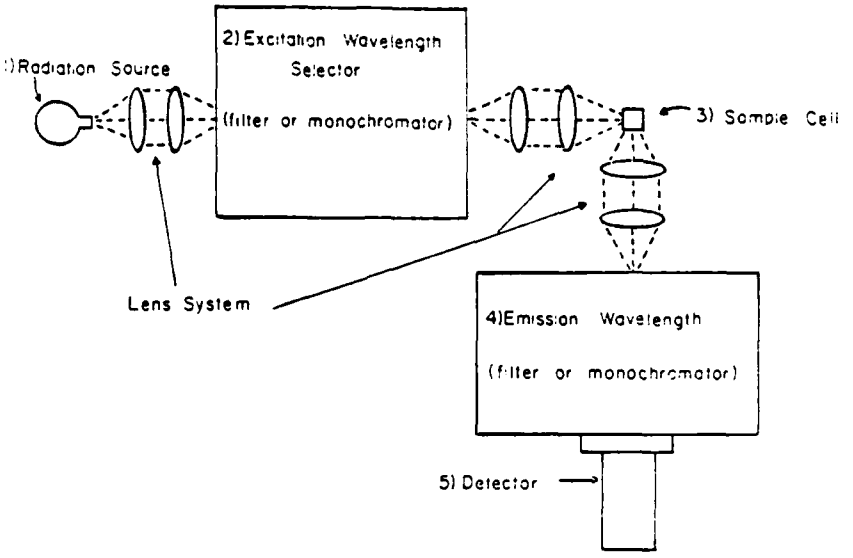

FIGURE 1. Diagram of a conventional fluorimeter.

A. *General and Theoretical Discussions of Signal-To-Noise Enhancement*

A theoretical comparison of pulsed-source excitation-gated detection with continuous wave source excitation for both atomic and molecular luminescence spectroscopy has been presented by Boutilier et al.[13] The investigators suggest that the S/N advantages of the pulsed-source excitation-gated methods are not necessarily large enough in all cases to justify the necessarily more complicated apparatus. Mathematical expressions for signals and for noise sources are developed for each of three measurement methods, including continuous wave excitation and measurement (cw/cw), pulsed source-gated detection with no time resolution (p/g), and pulsed source-gated detection with time resolution (p/g/t) (Figure 2). Noise sources considered include detector shot noise, background shot and flicker noise, scatter shot and flicker noise, source-induced background shot and flicker noise, and analyte luminescence shot and flicker noise. Signal/noise ratios for realistic experimental conditions are then calculated using the appropriate expressions.

The investigators note that the less expensive cw/cw system is rarely used in analytical fluorescence spectroscopy, and conclude that such systems are analytically useful only in cases where source scatter, source-induced background, and nonsource-induced background are small, i.e., not much greater than the analyte signal. For molecular fluorescence spectroscopy, p/g systems are useful if source-induced fluorescence background is small. However, as p/g/t systems become available they will prove to be more useful due to their ability to discriminate against source-induced background.

Cooney has investigated detector and other instrumental effects on the S/N ratio.[14] Comparisons are made between photomultiplier tubes with various image devices, including image dissector, silicon vidicon, silicon intensified target vidicon, intensified silicon intensified target vidicon, and secondary electron conduction vidicon detectors. The comparison is based on theoretically developed equations for the S/N ratio for each device, calculating the S/N ratio for analytically important situations. His conclusions are that the silicon vidicon is not useful for molecular luminescence spectroscopy, but the integrating image devices are useful in the visible range, since they combine the

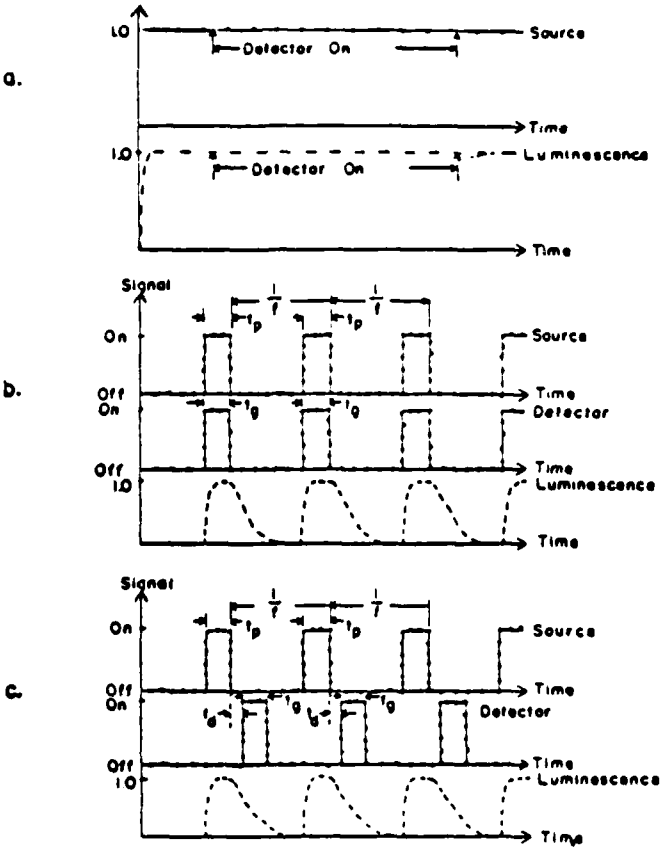

FIGURE 2. Schematic representation of excitation measurement systems used in atomic and molecular luminescence. (a) C w. cw (cw excitation with cw detection). (b) P g (pulsed excitation with gated detection and no time delay). In this case, the source turns on and off at a certain repetition rate, f. The source on time is t_p (seconds). The detection gate time is t_g (seconds). The lifetime of the luminescence of the analyte is τ_L (seconds). The lifetime of the luminescence of any source-induced fluorescence background is τ_f (seconds). The lifetime of the source scatter is τ_s (seconds). Recall lifetime is defined for a first-order process (exponential decay) as the time for the intensity to decrease by 1/e from the initial value. The luminescence decay of allowing source termination is actually a convolution of the decay processes having lifetimes of τ_L, τ_f, and τ_s. (c) P g t (pulsed excitation with gated detection and with time resolution). The discussion in (b) applies here except that there is a delay of t_d (seconds) between the termination of excitation and the initiation of the measurement process. Key: solid line, source temporal profile normalized to unity; dashed line with dots, detector temporal profile normalized to unity; dashed line, luminescence profile normalized to unity assuming steady state is reached. (From Boutilier, G. D., Bradshaw, J. D., Weeks, S. J., and Winefordner, J. D., *Appl. Spectrosc.*, 31, 307, 1977. With permission.)

multichannel time advantage over scanning devices with S/N ratios which approach those of PMT tubes. These considerations will be dealt with more fully in the next section.

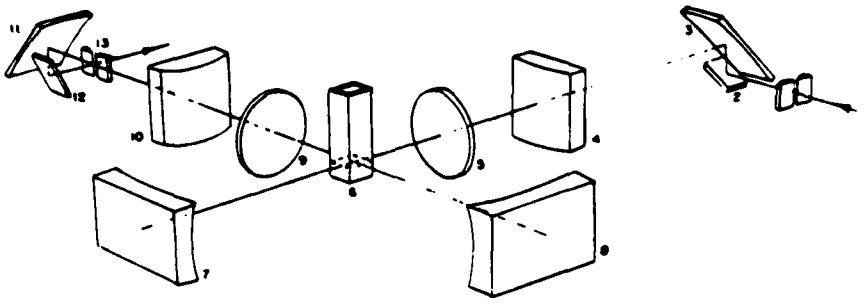

FIGURE 3. Image rotation system. Exciting light emerging from exit slit 1 of excitation monochromator strikes plane mirror 2, goes up to concave mirror 3, passes through cylindrical lens 4 and spherical lens 5 to cuvette 6 and retromirror 7. Fluorescence light from the cuvette and retromirror 8 passes through spherical lens 9 and cylindrical lens 10 to image rotating concave 11 and flat 12 mirrors and fluorescence monochromator entrance slit 13. (Reprinted with permission from White, J. U., *Anal. Chem.*, 48, 2089, 1976. Copyright 1976 American Chemical Society.)

B. Improvements through Modification of Instrumentation and Configuration

Lim and Miller[15] discussed the use of polarizers to improve detection limits in fluorimetry by reducing interference due to scattered light. Such reduction is particularly useful in biological samples such as blood, and in solutions of macromolecules. The investigators demonstrated the use of some new arrangements of polarizers that had not been previously studied, and suggest that their results show that the use of polarizers may have a wider applicability in fluorimetric analysis than previously suspected. Specifically, improved detection limits were found, using their new polarizer configurations, for aqueous solutions of quinine sulfate, riboflavin, and warfarin, and for warfarin in plasma. The improvements ranged from 10- to 100-fold in terms of pg $m\ell^{-1}$ detection limits. First-order Rayleigh scattered light is reduced by single, horizontally oriented polarizers, and second-order scattering is removed using crossed polarizers, although this configuration severely reduces fluorescence intensities. It is noted that the detection limit of warfarin in plasma using polarizers is better than the limit in pure aqueous solution without using polarizers.

Studies by White[16] demonstrated that a 30-fold increase in sensitivity of fluorescence spectrophotometers can be achieved by rotating the monochromator slit images 90°. Concave retromirrors are used behind the sample to reimage the cuvette on itself, collecting all the light passing through the sample and directing it through the sample again. Thus, the sample is viewed along the passing excitation slit image, and sensitivity is increased by more efficient use of the emitted light. Figure 3 shows the image rotation system used for the studies. Signals can be increased by a factor of 3.8, and an overall increase in signal/noise of 30 was observed for a Raman spectrum of methanol.

An instrumental modification which has only recently been applied to routine (and affordable) fluorescence analysis is double-beam spectrophotometry. Anacreon and Ohnishi[17] described a moderately priced commercial double-beam spectrophotometer, also discussed by Porro and Terhaar[18] in a review article. Sample fluorescence is corrected for background scatter and unwanted fluorescence using a reference beam passing through a reference (blank) cell. Since the reference beam intensity is monitored and then automatically subtracted from that of the sample beam instrumentally, time is saved and measurement precision is increased. Sensitivity is sacrificed due to the time-sharing nature of the electrooptical system; however, this decreased S/N ratio can often be tolerated in practical applications of fluorescence since the technique is inherently so sensitive. The optical paths for the sample and reference beams are equivalent, and are

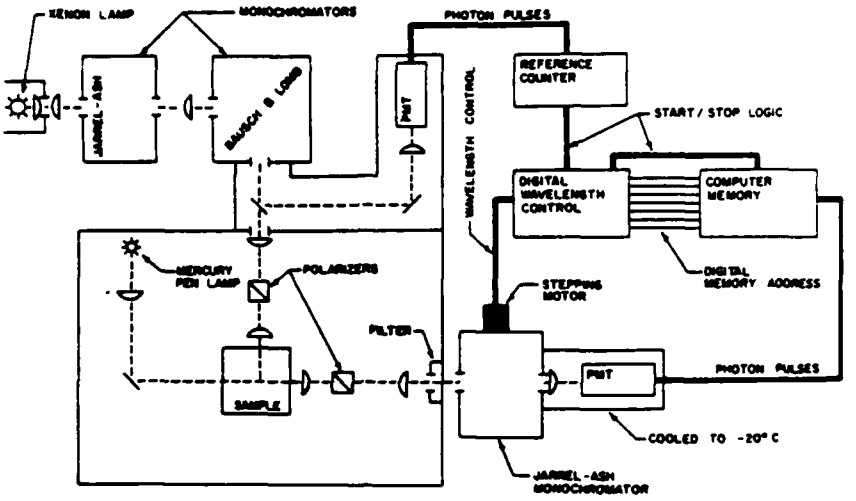

FIGURE 4. Block diagram of system for single photon counting. (From Jameson, D. M., Spencer, R. D., and Weber, G., *Rev. Sci. Instrum.*, 47, 1034, 1976. With permission.)

split by an optical chopper. Both beams are measured at right angles to the exciting light using a photomultiplier detector. The two signals are amplified, discriminated via phase sensitive demodulation, and finally the difference between the two is taken electronically. More discussion on this technique is given in Section III.F.

C. Improvements in Detection and Electronics

Single photon counting detection was combined with repetitive scanning to improve S/N ratios in studies done by Jameson et al.[19] Strong fluorophores were detectable on this system at the picomolar level. The instrumental set-up is shown in Figure 4. The double monochromator arrangement is used to reduce stray light levels. Data manipulation via computer interfacing allows background subtraction after blank and sample data are collected (Figure 5), providing a means for extracting very small sample signals from background for the sufficiently sensitive instrument.

Glushko et al.,[20] developed a method for increasing S/N ratios of weak fluorescence signals using drift-free integration to enhance the analog signals obtained. A gain in sensitivity of an order of magnitude is obtained using high resolution voltage-to-frequency conversion, followed by even counting. It is pointed out that, although weak signals are best measured by discrete photon counting systems, appreciable advantages in sensitivity for weak signals can be inexpensively obtained using the enhanced analog technique described, avoiding conversion to photon counting instrumentation.

Finally, another electronic approach to enhancing S/N ratios for spectrofluorimeters, described by Wehrly et al.,[21] utilizes a bipolar averaging circuit. One hundred signals are averaged at variable sampling rates (a few seconds or longer for collection of the 100, or less time with modifications). The exciting light is also monitored as a reference signal for adjusting phototube dark currents and amplifier offsets. Figure 6 shows a fluorescence emission spectrum before and after the signal averaging is applied.

III. MULTICOMPONENT FLUORESCENCE INSTRUMENTATION

The large number of variable parameters in fluorescence spectroscopy provides a

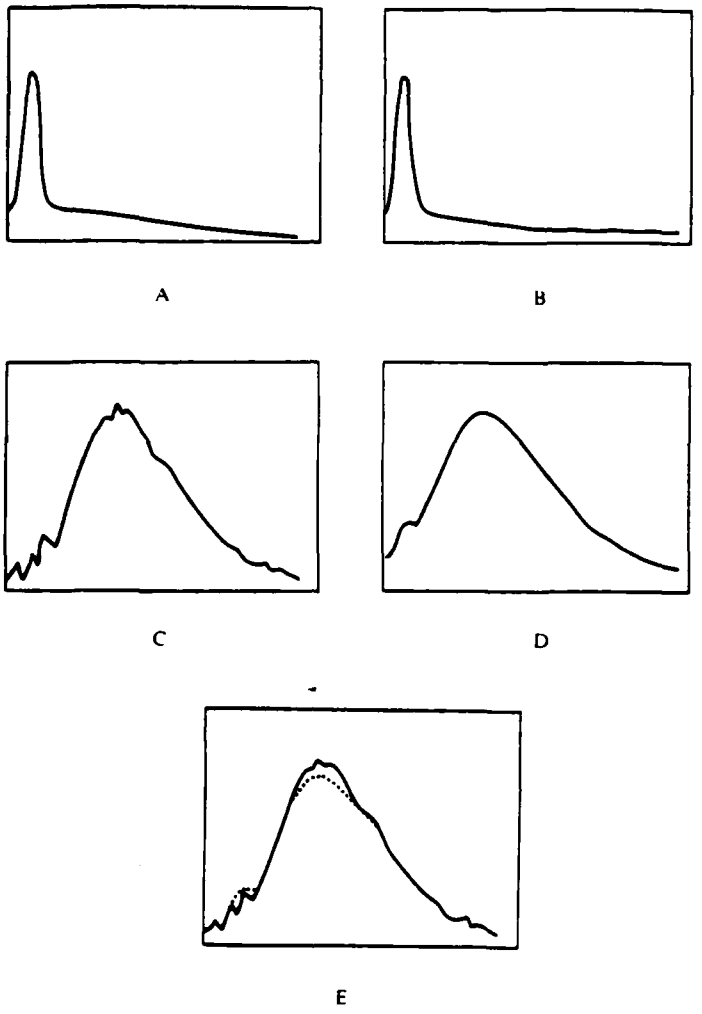

FIGURE 5. Extracting small sample signals from background. (A) Background emission of 0.2 *N* H_2SO_4 scanned from 371 to 560 nm. Excitation at 340 nm. Raman appears at 385 nm. (B) Background plus 10^{-11} *M* quinine sulfate. (C) Spectrum B minus spectrum A: 10^{-11} *M* quinine sulfate. (D) 10^{-14} *M* quinine sulfate. (E) Overlay of spectra C and D. (From Jameson, D. M., Spencer, R. D., and Weber, G., *Rev. Sci. Instrum.*, 47, 1034, 1976. With permission.)

wide variety of approaches to the analysis of multicomponent mixtures. For example, the fluorescence intensity can be defined as a function of the wavelength of excitation and monitored wavelength of emission. Mathematically, this can be expressed as

$$I_f = f(\lambda_{ex}, \lambda_{em}) \quad (1)$$

where I_f is the intensity of fluorescence and λ_{ex} and λ_{em} are the wavelengths of the exciting and emitted radiation, respectively. If one were to pulse the excitation radiation, and monitor the fluorescence intensity as a function of time after the termination of the

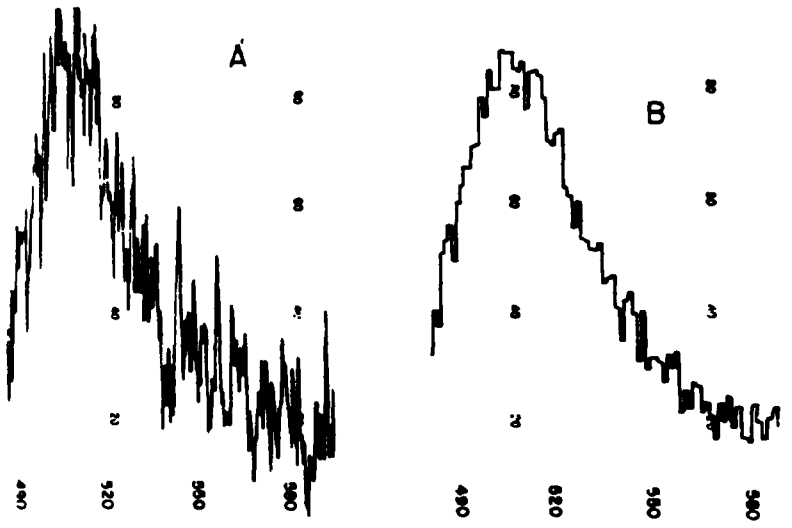

FIGURE 6. Signal-averaged spectrum of fluorescein. Fluorescence emission spectra of 10^{-10} *M* fluorescein in carbonate buffer. Excitation wavelength is 480 nm. Emission scanned from 490 to 580 nm. (A) Direct acquisition. (B) Average of 100 signals at each wavelength. (Reprinted with permission from Wehrly, J. A., Williams, J. F., Jameson, D. M., and Kolb, D. A., *Anal. Chem.*, 48, 1424, 1976. Copyright 1976 American Chemical Society.)

excitation beam, an exponential decay would be observed. This is because the fluorescence decay process obeys first-order rate kinetics. Thus, the fluorescence equation as a function of time would have the form

$$\frac{I_f(t)}{I_f(o)} = e^{-kt} \qquad (2)$$

where $I_f(o)$ is the fluorescence intensity at time zero, and $I_f(t)$ is the fluorescence intensity at a time t after termination of the excitation source. The constant k is a summation of all the first-order rate processes which compete for deactivation of the excited molecule. Included in this constant are the rate constants for radiative decay, intersystem crossing, and collisional quenching where the number of quencher molecules is assumed to be large compared to the number of excited molecules.

Use of the three individual parameters (λ_{ex}, λ_{em}, time) and combinations of them provide a variety of approaches to the development of novel multicomponent fluorescence instrumentation. Most of the discussion in this section will describe instrumentation which exploits one or more of these three variables. Of course, it is to be realized that the addition of other parameters, e.g., fluorescence polarization, could provide an even greater variety of instrumental approaches.

Although this section will be concerned with new developments in fluorescence instrumentation, we will first briefly discuss conventional fluorescence instruments. More detailed information can be obtained by consulting one of several different monographs.[22-25] As depicted previously in Figure 1, the conventional fluorimeter consists of an excitation source, an excitation wavelength selector, a sample cuvette, an emission wavelength selector, and a detector. The radiation source for most research instruments is the xenon arc lamp. For the excitation and emission wavelength selector, a

grating system is usually chosen over the less expensive filter systems. The photomultiplier tube is the preferred detection system in emission studies because of its high gain, low noise and relatively broad spectral sensitivity.

A. Time-Resolved Techniques

Since emission decay rates vary from molecule to molecule, an obvious approach to multicomponent analysis is to exploit these differences in emission lifetimes. A few years ago, this was most easily performed using phosphorescence emission since the phosphorescence decay is usually very long lived (lifetime $\gtrsim 1$ msec). With such relatively long-lived processes, devices such as electromechanical shutters could easily be employed as mechanical pulsers for the lamp source and for "gating out" the interference of the shorter-lived fluorescence signal. A number of experiments have employed such techniques.[26-31] Although this technique is not new, it does warrant discussion since new applications of the technique are continuing to be developed. Moreover, it serves as a background for the more widely used nanosecond time-resolved fluorescence techniques. Perhaps the first published application of time-resolved phosphorimetry to multicomponent analysis was that of Keirs et al. in 1957.[32] This early work showed that it was possible to examine the components in a mixture by proper choice of the wavelengths of excitation and emission, using the decay times of the various components.

More recent work by Winefordner's group has explored the possible advantages of using a pulsed-source phosphorimeter for time resolution phosphorimetry.[33-36] In one of these articles, Fisher and Winefordner[36] provide an extensive comparison of pulsed-source and continuous operating mechanical phosphoroscope systems. A number of advantages of pulsed-source phosphorimetry are cited, including lower detection limits and greater discrimination of short-lived phosphors. Figure 7 gives a block diagram of their pulsed-source phosphorimeter. Two types of readout methods were used to observe the emission of rapidly decaying phosphors. In the first, the phototube was operated continuously, and the integrated phosphorescence intensity examined by an electronic gate. The gate could be scanned to display the decay curve. The second method employed a continuously operating phototube with a fast multichannel readout device capable of signal averaging. The second method was preferred for ease of data processing. Three major methods of processing the data were presented, all of which assume that the unknown molecules absorb and emit independently of each other. The first method is called the "multiple analytical curve method" and is essentially the same as that originally used by Keirs et al.[32] For a binary mixture, this method requires obtaining analytical working curves at two different time intervals, t_1 and t_2. In the original work by Keirs et al., the two variables were λ_1 and λ_2, i.e., two different wavelengths of emission. In either case, the concentration of each component in the binary mixture can be obtained by the simultaneous solution of two equations. Of course, this method is applicable to higher-order mixtures. However, n equations are always required for n unknowns.

The second method employed is called an "exponential method." This method requires prior measurement of the decay times of the components in the mixture. The phosphorescence intensity of each component is then expressed as an exponential decay function of the time after termination of the exciting light. Assuming that the absorption and emission processes of each molecule are independent, one can analyze a binary mixture at delay times t_1 and t_2. Again, this provides n equations for n unknowns which can be solved simultaneously.

The third method used by Fisher and Winefordner is a logarithmic technique used in nuclear decay studies. The technique consists of a semilogarithmic plot of decay rate vs. time. For a multicomponent sample, different linear portions will be observed corresponding to components having different half-lives. Extrapolation of these linear

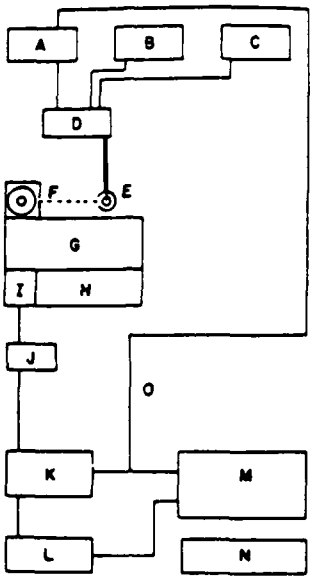

FIGURE 7 Block diagram of pulsed source phosphorimeter (A) Pulse generator (Model 100, Datapulse Inc., Culver City, Calif.). (B) 300-V power supply (Model C-281, Lambda Electronics, Melville, L.I., N. Y.). (C) 1400-V power supply (Model 403 M, John Fluke Mfg., Co., Seattle, Wash.). (D) Trigger circuit. (E) Xenon flashtube compartment (laboratory constructed). (F) Sample cell compartment (identical to amino phosphoroscope accessory minus rotating phosphoroscope can). (G) Emission monochromator (Model EU-700, Heath Co., Benton Harbor, Mich.). (H) Phototube power supply (Model EU-701-30, Heath Co., Benton Harbor, Mich.). (I) RCA 1P28 photomultiplier tube. (J) Load resistors (500 Ω to 3 MΩ) and fast-switching diodes. (K) Oscilloscope (Model 545, Tektronix, Inc., Orlando, Fla.). (L) Preamplifier (Model 465A, Hewlett-Packard, Orlando, Fla.). (M) Signal averager (Biomac Model 1000, Data Laboratories, Ltd., London, England), or Boxcar Integrator (Model 160, Princeton Applied Research, Princeton, N.J.). (N) Strip chart potentiometric recorder (Model TR, E. H. Sargent, Chicago, Ill.). (O) Synchronization for oscilloscope and signal averager. (Reprinted with permission from Fisher, R. P. and Winefordner, J. D., *Anal. Chem.*, 44, 948, 1972. Copyright 1972 American Chemical Society.)

portions back to time zero after activation (or excitation) provides the initial decay intensity of each component.

All three of these data processing techniques were applied to the analysis of various mixtures of phosphors. The results of the analysis of binary mixtures of 4-bromoacetophenone and benzaldehyde are shown in Table 1.[16] The results of the multiple analytical curve method (first method) and the exponential method (second method) are

Table 1
ANALYSIS OF TWO BINARY MIXTURES BY THE MULTIPLE ANALYTICAL CURVE METHOD AND THE EXPONENTIAL METHOD

Binary Mixtures I: 2.5×10^{-6} *M* 4-bromoacetophenone (A)
1.5×10^{-6} *M* benzaldehyde (B)

	Mean value found	Rel std dev (%)	Error (%)
	Multiple Analytical Curve Method		
C_A	3.09×10^{-6} *M*	4	24
C_B	1.30×10^{-6} *M*	15	13
	Exponential Method		
C_A	2.53×10^{-6} *M*	2	1
C_B	1.98×10^{-6} *M*	12	32

Binary Mixture II: 1.0×10^{-6} *M* 4-bromoacetophenone (A)
3.5×10^{-6} *M* benzaldehyde (B)

	Multiple Analytical Working Curve Method		
C_A	0.85×10^{-6} *M*	35	15
C_B	3.18×10^{-6} *M*	26	9
	Exponential Method		
C_A	0.76×10^{-6} *M*	25	24
C_B	3.45×10^{-6} *M*	21	1

compared. Table 2 shows the results of the analysis of a ternary mixture by the logarithmic decay method (third method).[36] The technique of pulsed source-time resolved phosphorimetry was later applied to the analysis of halogenated biphenyls[37] and to the analysis of drugs[38] using a more intense flash lamp source.

The rate of decay for a fluorescence signal after termination of the exciting source also follows first-order kinetics. However, while the phosphorescence lifetimes are usually larger than a millisecond, the fluorescence lifetimes are usually in the range of fractions of microseconds to nanoseconds. Basically, the components of a time-resolved fluorimeter are similar to the components of a time-resolved phosphorimeter. Obviously, the much faster fluorescence decay rates require more sophisticated electronics. A typical nanosecond fluorimeter has been described by Badea and Georghiou.[39] Figure 8 shows a block diagram of their system. The system is a pulsed sampling type fluorimeter, which uses a boxcar averager for short data acquisition times. The exciting nanosecond light source has a repetition rate of about 10 kHz for an electrode gap of 0.5 mm and an applied voltage of 15 kV. The fluorimeter is also equipped for baseline sampling, allowing correction for dc drifts. Corrections are made for exciting light intensity fluctuations by incorporating a beam splitter and a second photomultiplier tube for ratioing the

Table 2
ANALYSIS OF A TERNARY MIXTURE BY THE LOGARITHMIC DECAY METHOD

Ternary Mixture I: 2.3×10^{-6} *M* 4-bromoacetophenone (A), $\tau \approx 6.8$ msec
2.3×10^{-6} *M* benzaldehyde (B), $\tau \approx 2.2$ msec
2.3×10^{-6} *M* benzophenone (C), $\tau \approx 4.8$ msec

	Mean value found	Rel std dev (%)	Error (%)
C_A	2.9×10^{-6} *M*	30	26
C_B	2.1×10^{-6} *M*	38	10
C_C	3.1×10^{-6} *M*	13	35

Reprinted with permission from Fisher, R. P. and Winefordner, J. D., *Anal. Chem.*, 44, 948, 1972. Copyright 1972 American Chemical Society.

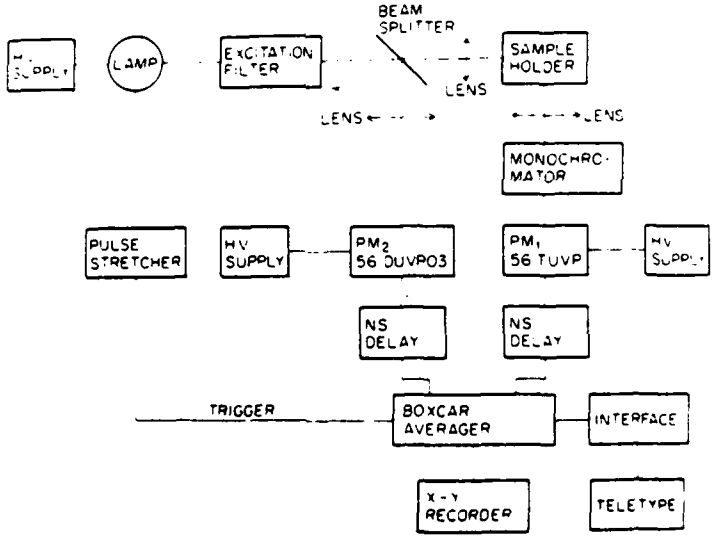

FIGURE 8 Block diagram of a nanosecond fluorimeter. The photomultipliers are manufactured by Amperex. The triggering signal was stretched by a Tektronix rise-time limiter. The input to each channel was delayed by about 80 nsec. (From Badea, M. G. and Georghiou, S., *Rev. Sci. Instrum.*, 47, 314, 1976. With permission.)

fluorescence signal with the exciting light signal. Although not shown in this diagram, the system also contained an interface to an IBM 360 computer for data analysis. Although many nanosecond fluorimeters do not have all of the features described for this system, the basic components are common to all nanosecond fluorimeters. Other time-resolved fluorimeters have been described,[40-42] and comprehensive reviews of nanosecond fluorescence spectroscopy of macromolecules have been written by Yguerabide,[43] Weissler,[44] and Cundill and Palmer.[45]

Table 3
CALCULATION OF LIFETIMES OF SIMULATED CURVES BY DECONVOLUTION AND GRAPHICAL METHODS[a]

Lifetime (nsec)			
	Calculated		Error (%) of graphical method
Theoretical	Deconvolution	Graphical	
4.00	4.00	3.92	2.0
3.00	2.97	3.05	2.7
2.00	2.00	2.15	7.5
1.00	1.01	1.26	25.0
0.50	0.50	1.07	114.0

[a] Simulated source lifetime, 1.10 nsec; width at half-maximum, 3.2 nsec; counts in peak channel, 12,000.

From Shaver, L. A. and Love, L. J. C., *Appl. Spectrosc.*, 29, 485, 1975. With permission.

A number of works can be cited which demonstrate the possible applications of time-resolved fluorimetry for multicomponent analysis.[46-48] However, the discussion here will be limited to the works of Love and co-workers[49,50] and a review by Love and Shaver.[51] Shaver and Love[49] have quantitatively evaluated errors in luminescence lifetime calculations obtained by the graphical slope method, in comparison to mathematical deconvolution methods which are more complex and require a digital computer with relatively large memory capacity. This work evaluated the accuracy of each technique for calculation of the lifetime of a fluorescence specie. Table 3 shows some typical results obtained in this study,[49] calculating lifetimes of computer-simulated excited fluorophores by the deconvolution and graphical methods. The source lifetime was fixed at 1.10 nsec for these results. As one would expect, the more time-consuming deconvolution method is more accurate under all conditions. However, the authors concluded that, under certain conditions, the graphical slope method might be preferred since its computer requirements are less stringent. For example, fluorophores with lifetimes of 3 to 5 nsec in the presence of a pulsed-light source with a lifetime in the 1 to 3 nsec range can be deconvoluted with an error of 5% or less. On the other hand, serious errors are encountered when graphical slope-calculated lifetimes are within 2 nsec of the pulsed-source lifetime.

Another study by Love and co-workers[50] has evaluated solvent effects on the fluorescence decay times and quantum yields of atabrine and its homologues. This study was designed to elucidate the excited state properties which allow differentiation between similar species. The effects of molecular structure and microenvironment on the excited singlet state properties of an atabrine-based homologous series were determined. The structures of atabrine and related species which were studied are presented in Figure 9. The effects of solvent polarity on the important parameters of the excited molecules, such as lifetimes, quantum yields, and transition energies, were extensively evaluated. Typical results are displayed in Table 4. These results seem to indicate that increase in the carbon chain length in the solvents 0.1 *N* hydrochloric acid and methanol/acetic acid causes a decrease in the observed lifetime, τ, with no apparent trend in the natural lifetime, τ_o. Of the solvents examined, the best, in terms of increased quantum yield for analyzing any of the members of the atabrine-based series, is an acetic acid/chloroform mixture.

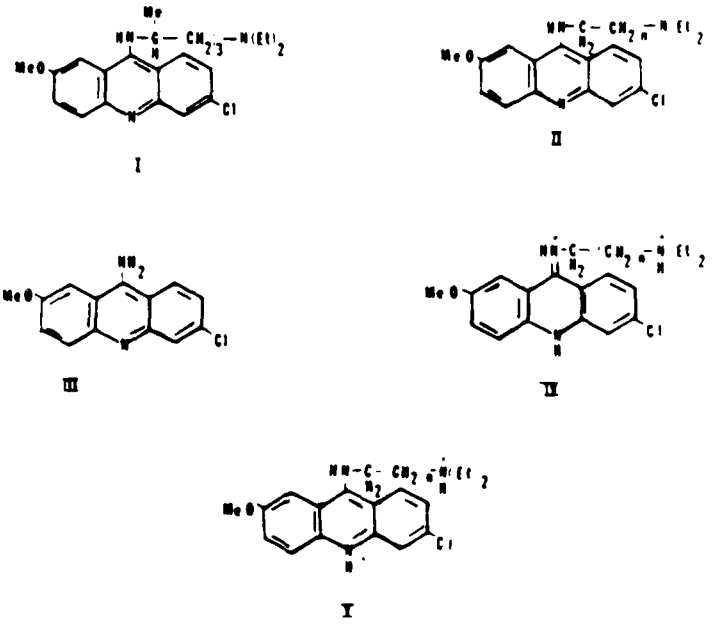

FIGURE 9 Structure of atabrine and related species. I, atabrine (base form). II, homologous series $n = 1$ to $n = 7$ (base form). III, parent compound (base form). IV, homologous series (acid form). V, proposed excited state species (acid form). (Reprinted with permission from Love, L. J. C., Upton, L. M., and Ritter, A. W., *Anal. Chem.*, 50, 2059, 1978. Copyright 1978 American Chemical Society.)

Table 4
LIFETIMES (nsec) AND QUANTUM YIELDS FOR SPECIES IV (see Figure 9) IN SOLUTIONS OF DIFFERENT POLARITIES

	0.1 *N* HCl			Acetic acid/methanol			Acetic acid/chloroform		
Compound	τ	ϕ	τ_0	τ	ϕ	τ_0	τ	ϕ	τ_0
III	20.1	—	—	19.9	0.865	23	14.0	0.210	67
I	3.2	0.056	57	3.8	0.057	67	13.1	0.316	41
II, $n = 1$	12.7	0.234	54	15.0	0.358	42	10.7	0.265	40
II, $n = 2$	6.7	0.090	74	7.4	0.135	55	12.7	0.340	37
II, $n = 3$	3.6	0.075	48	4.0	0.089	45	12.9	0.317	41
II, $n = 4$	2.9	0.027	107	3.3	0.062	53	13.4	0.398	34
II, $n = 5$	2.3	0.027	85	2.7	0.057	47	14.3	0.510	28
II, $n = 6$	1.6	0.013	123	2.1	0.050	42	13.5	0.389	35
II, $n = 7$	1.3	0.015	87	2.7	0.068	40	14.2	0.222	64

Reprinted with permission from Love, L. J. C., Upton, L. M., and Ritter, A. W., *Anal. Chem.*, 50, 2059, 1978. Copyright 1978 American Chemical Society.

A number of other references should be cited, although they will not be discussed here in detail. Aaron et al.[52] have reported the applications of fluorescence and phosphorescence lifetimes to the analytical study of important hallucinogens. A critical evaluation of time-resolved fluorescence for the analysis of multicomponent fluorescent mixtures has been reported in a dissertation by Shaver.[53] Finally, a number of studies in

the picosecond time domain[54-56] are providing new avenues of study for fluorescence kinetic studies.

B. Phase-Resolved Techniques

In our previous discussion we described one method of measuring the time decay of fluorescence and phosphorescence. An alternative method which has been previously employed for fluorescence decay studies is the phase fluorimetric method. Although one might consider phase fluorimetry and phosphorimetry as time-resolved techniques, we have elected to discuss them separately. The phase method is based on the fact that if a luminescing sample is excited with a modulated light signal of angular frequency w, the emitted light will also modulate with the same frequency. However, the emission will suffer a phase lag, θ, which at a given exciting light frequency, is often characteristic of the emitting molecule. The phase lag is then related to the angular frequency and lifetime τ of the molecule by

$$\tan \theta = w \tau \tag{3}$$

Another useful parameter for the phase-resolved technique is the modulation factor M with respect to the exciting light. This parameter is also related to the phase lag and angular frequency and is described by the expression

$$M = \frac{1}{\sqrt{1 + w^2 \tau^2}} = \text{Cos } \theta \tag{4}$$

These two equations are equally applicable to phosphorescence or fluorescence decay. The luminescence lifetime of the species can thus be calculated using the phase change equation or the degree of modulation. The emission decay is assumed to follow a simple first-order relationship. Therein lies the major disadvantage of phase fluorometry since this assumption is not always valid. However, the use of Equations 3 and 4 in combination will demonstrate the validity (or lack of validity) of the exponential decay assumption. Consequently, phase fluorimetry (or phosphorimetry) is a widely accepted technique, and a number of applications to molecular luminescence studies can be cited. For example, Spencer and Weber[57] have described the use of a cross-correlation phase fluorimeter for measurement of subnanosecond fluorescence lifetimes. The cross-correlation technique requires the mixing of the photocurrent produced by fluorescence with a fixed high frequency close to that of the modulated exciting light signal. The phase lag is then measured in the resulting amplified difference signal. Some of the advantages of this approach as described by Spencer and Weber are increased sensitivity, increased S/N ratio and signal isolation, and ability to use numerical time-interval counting for increased accuracy through averaging. The utility of the technique was demonstrated through the determination of the fluorescence lifetimes of NADH (nicotinamide-adenine dinucleotide), FMN (flavin mononucleotide), and FAD (flavin-adenine dinucleotide). Another study by Weber[58] has described the theory and application of differential phase fluorimetry to the detection of an isotopic molecular rotation. A wide-range, high-accuracy phase fluorimeter has been described by Schurer et al.[59] A number of similar investigations are cited by Itoh,[60] Pohoski and Zachara,[61] Reseuitz and Lippert,[62] and Hauser and Heidt.[63]

The application of the technique to multicomponent analysis is perhaps best exemplified by the work of Mousa and Winefordner.[64] This study demonstrated the possible use of the technique in analytical phosphorimetry. Using the terminology of Mousa and Winefordner, the total intensity of the sinusoidally varying luminescence signal at any time t can be expressed as

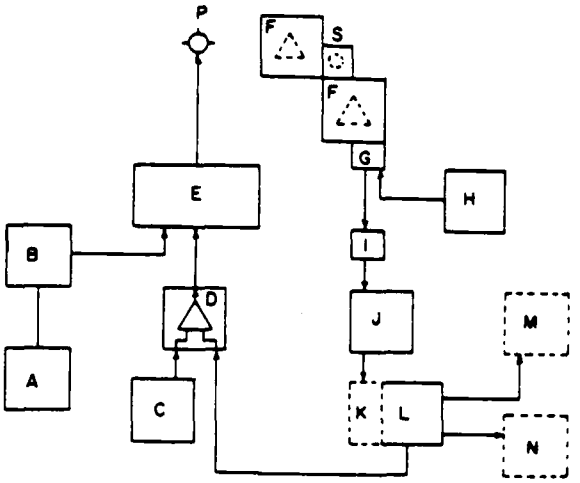

FIGURE 10. Block diagram of instrumental system for phase fluorimetry. A = 0-40V, 0-30A DC power supply (Harrison Model 6268A); B = starter circuit; C = 0-100V, 0-0.2A DC power supply (Harrison Model 6116A); D = summing operational amplifier and current booster (Heath Model EUW-19); E = modulation circuit; F = excitation and emission monochromator; G = photomultiplier tube and housing; H = high voltage power supply; I = load resistors; J = differential amplifier (Tektronix Model 1A7A); K = amplifier (optional) (PAR Model 211); L = lock-in amplifier; M = strip-chart recorder (optional); N = X-Y recorder (optional); P = xenon arc lamp; S = sample compartment. (Reprinted with permission from Mousa, J. J. and Winefordner, J. D., *Anal. Chem.*, 46, 1195, 1974. Copyright 1974 American Chemical Society.)

$$I_f = M_p k_p I_o'' \cos(wt - \theta_p) + k_f I_o'' \cos wt \qquad (5)$$

where M_p is the degree of modulation for phosphorescence, $k_p = 2.3\phi_p$ bc, and $k_f = 2.3\phi_f$ bc. The terms ϕ_p and ϕ_f are the quantum efficiencies of phosphorescence and fluorescence, respectively. The parameter I_o'' is the amplitude of the exciting light and w is its angular frequency. In Equation 5, it is assumed that the ac component of the fluorescence is negligible since M_f is unity and θ_f is zero over the frequency range of 2 to 1000 Hz used for this study.

Figure 10 displays a block diagram of the instrumental system used by Mousa and Winefordner for this study. They employed two methods for resolving the overlapping phosphorescence spectra of a binary mixture. One method is called the "phase method", in which the frequency of modulation is held constant and the instrumental phase angles for standards of each of the components in the mixture is measured. Then the phase of the reference signal used for nulling out unwanted signals in the lock-in amplifier is adjusted so that it is $90° + \phi_{p1}$, where ϕ_{p1} is the instrumentally measured phase angle of one of the measured standards. The resultant output signal is then characteristic of the other component (component 2) in the mixture. Similarly, a signal characteristic of component 1 can be obtained by adjusting the reference phase angle to $90° + \phi_{p2}$. The other method is called the "frequency method". This method involves setting the reference signal at $90° + \theta_s$, where θ_s is a selected phase angle. A standard of one of the components in the mixture is run and the frequency of modulation is adjusted until the phase angle of the

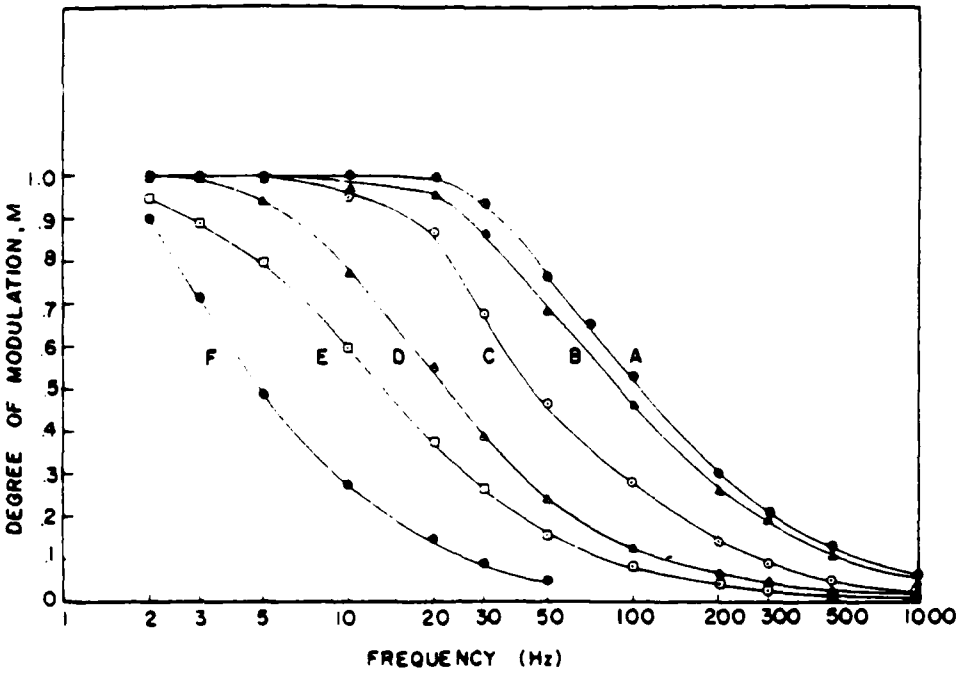

FIGURE 11. Variation of experimentally determined degree of modulation, M, with the frequency of modulation for several phosphors. A = anthraquinone, τ_P = 3.0 msec; B = 4-iodobiphenyl, τ_P = 3.5 msec; C = benzophenone, τ_P = 6.0 msec; D = 4,4'-dibromobiphenyl, τ_P = 12 msec; E = 4-bromobiphenyl, τ_P = 17. msec; F = 3-bromobiphenyl, τ_P = 55. msec. (Reprinted with permission from Mousa, J. J. and Winefordner, J. D., *Anal. Chem.*, 46, 1195, 1974. Copyright 1974 American Chemical Society.)

standard is equal to ϕ_1. The result is that the signal from this standard is nulled out at frequency, f_1. A similar frequency, f_2, is found using the standard of the second component. The characteristic signals of component 2 and component 1 are obtained by determining the spectra of the mixture at f_1 and f_2, respectively, while holding the phase angle constant.

The experimentally determined degree of modulation, M, and the phase shift angle θ, were measured for several phosphors. These experimental curves agree qualitatively with theoretical behavior as shown in Figures 11 and 12. As one would predict from Equation 4, the M values approach unity at low frequencies and zero at higher frequencies. One can also use these data and Equation 4 to calculate the lifetimes of these phosphors (see Table 5). These lifetime values were calculated using the M value corresponding to the 50 Hz frequency since this value generally corresponded to the steepest portion of the curve. One can also use a similar computation to derive the lifetimes from the phase shift data of Figure 12.

The analytical usefulness of this technique lies mainly in its ability to deconvolute spectral mixtures. In their study, Mousa and Winefordner used a number of synthetic binary mixtures. These mixtures were spectrally resolved using the phase method of nulling out one of the components. One of the binary systems studied was a mixture of benzophenone and 4-bromobiphenyl. The results of this experiment are shown in Figure 13. Spectrum A of this figure corresponds to a spectrum of the mixture measured at the peak output phase setting. Spectra B and C were obtained by nulling out the signals of 4-bromobiphenyl and benzophenone, respectively. Thus, the resulting mixture spectra

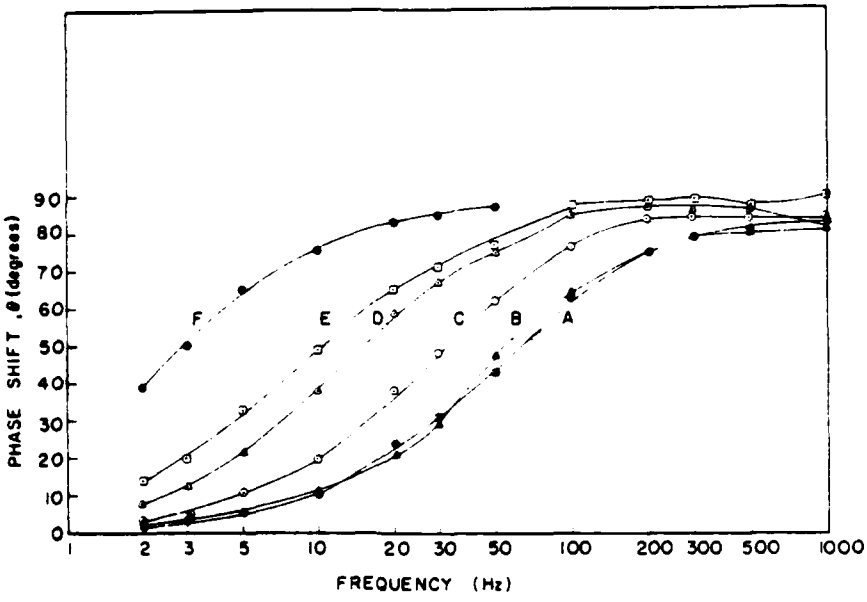

FIGURE 12. Variation of experimentally determined phase shift angle, θ, with the frequency of modulation for several phosphors. A = anthraquinone, τ = 3.0 msec; B = 4-iodobiphenyl, τ = 3.5 msec; C = benzophenone, τ = 6.0 msec; D = 4,4'-dibromobiphenyl, τ = 12 msec; E = 4-bromobiphenyl, τ = 17 msec; F = 3-bromobiphenyl, τ = 55 msec. (Reprinted with permission from Mousa, J. J. and Winefordner, J. D., *Anal. Chem.*, 46, 1195, 1974. Copyright 1974 American Chemical Society.)

Table 5
PHOSPHORESCENCE LIFETIMES FROM PHASE AND MODULATION DATA[a]

Molecule	Lifetime (msec)[b]		
	Phase[c]	Modulation[c]	Time resolved[d]
Benzophenone	5.9	6.1	7
Anthraquinone	3.0	2.7	3.6
4-Iodobiphenyl	3.5	3.3	3.2
4-Bromobiphenyl	14	20	17
3-Bromobiphenyl	55	59	58
4,4'-Dibromobiphenyl	12	13	12

[a] Solvent: ethanol.
[b] Relative errors in lifetimes are ± 10%.
[c] All values calculated from measurements at 50 Hz.
[d] Data taken from References 8 and 9 of Reference 64.

Reprinted with permission from Mousa, J. J. and Winefordner, J. D., *Anal. Chem.*, 46, 1195, 1974. Copyright 1974 American Chemical Society.

for B and C are characteristic of benzophenone and 4-bromobiphenyl. This study also explored the use of the frequency method where the reference phase angle was set at a value 90° away from a selected phase angle θ_s. The frequency of modulation was then adjusted to null out the signal of the selected component in the mixture. Figure 14 shows

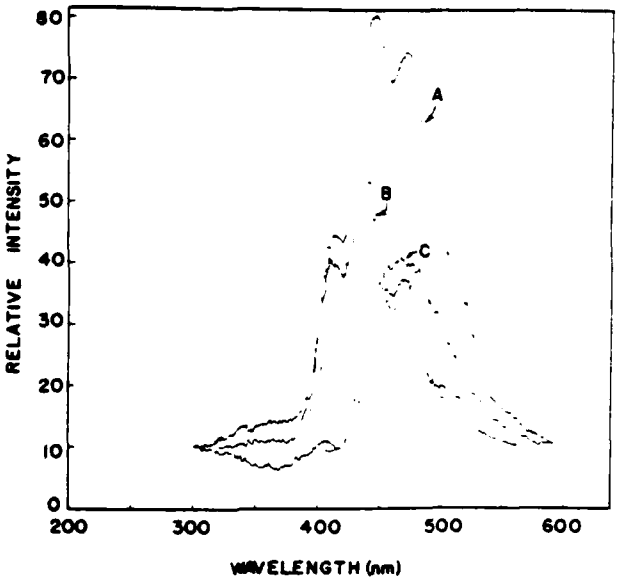

FIGURE 13. Phase-resolved emission spectrum of a mixture of 2.2×10^{-5} *M* benzophenone and 2.9×10^{-5} *M* 4-bromobiphenyl at 25 Hz. Excitation wavelength is 275 nm. A = mixture spectrum at peak phase angle, $\phi_R = 270° + 39°$; B = mixture spectrum, $\phi_R = 0° + 26°$, C = mixture spectrum, $\phi_R = 180° + 52°$; (---) = spectrum of benzophenone standard, $\phi_R = 270° + 52°$; (----) = spectrum of 4-bromobiphenyl standard $\phi_R = 270° + 26°$. (Reprinted with permission from Mousa, J. A. and Winefordner, J. D., *Anal. Chem.*, 46, 1195, 1974. Copyright 1974 American Chemical Society.)

the results of this study. Spectrum B of this figure corresponds to the acquired spectrum of benzophenone obtained by nulling out the signal of 4-bromobiphenyl. Similarly, Spectrum A corresponds to 4-bromobiphenyl obtained by nulling out the signal contributed by benzophenone.

Quantitative analysis of binary mixtures was also demonstrated by obtaining calibration curves of each component in the mixture. Figure 15 shows the results. Curves A1 and B1 correspond to measurements at the peak phase angle for 4-iodobiphenyl and 4-bromobiphenyl, respectively. Curves A2 and B2 were obtained by nulling out the signal of the interfering analyte. The results obtained indicated that the best calibration is obtained when the concentrations of the analytes are less than 10^{-9} *M*. Thus, inner filter effects must be considered as is often the case in fluorescence analysis. Other quantitative data were reported, including the determination of a weaker phosphorescence in the presence of a larger signal, and the use of the frequency method for obtaining quantitative results.

The technique of phase-resolved phosphorimetry as described above has the advantage of being independent of the degree of overlap of the components. However, a serious disadvantage is that the technique requires *a priori* knowledge of the components in the mixture. This is a serious deficiency since many analyses require the identification of unknown species.

C. Selective Modulation

The technique of selective modulation fluorimetry was first introduced by O'Haver and Parks.[65] The principle of the technique can best be explained by use of the diagram

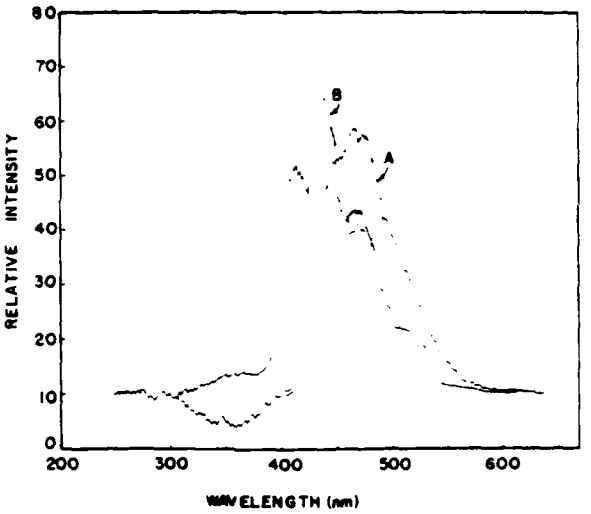

FIGURE 14. Frequency method resolved emission spectrum of a mixture of 2.2×10^{-5} *M* benzophenone and 2.9×10^{-5} *M* 4-bromobiphenyl. Excitation wavelength is 275 nm. A = emission spectrum of mixture, frequency = 37.5 Hz, $\phi_R = 180° + 40°$; B = emission spectrum of mixture, frequency = 14.7 Hz, $\phi_R = 180° + 40°$; (---) = emission spectrum of benzophenone standard; (-·-) = emission spectrum of 4-bromobiphenyl standard. (Reprinted with permission from Mousa, J. J. and Winefordner, J. D., *Anal. Chem.*, 46, 1195, 1974. Copyright 1974 American Chemical Society.)

presented in Figure 16. This diagram depicts the hypothetical excitation spectra for two hypothetical molecules A and B present in a binary mixture. Clearly, selective excitation of either of the components is not possible because of the extensive spectral overlap. However, suppose that the excitation monochromator is capable of rapidly scanning back and forth (modulating) over the interval $\Delta\lambda$. Since the emission is proportional to the amount of light absorbed and we are rapidly varying this absorption, the emission intensities of the components will also be modulated. However, with the spectral interval as specified in Figure 16, it should be clear that the emission of B will be modulated with the same frequency (1F) as the modulation frequency of the excitation monochromator. It should also be clear that the A component will be modulated at twice the frequency (2F) of the excitation monochromator. Therefore, the use of a lock-in amplifier detector would allow one to electronically isolate the signal of component A from component B and vice versa.

O'Haver and Parks defined several general considerations for the selective modulation technique in their studies. These considerations are (1) the amplitude of the 1F modulated component is usually greater than that of the 2F component; (2) to spectrally isolate A in the 1F modulation mode from B requires that B have a maximum or a minimum which falls on a sloping portion of A; and (3) the conditions for obtaining a pure spectrum of A in the presence of B require the determination of the exact conditions for nulling out B through a previously prepared standard. Then, pure A from the mixture can be obtained by analyzing the mixture under the predetermined standard conditions. Another consideration which should be taken into account is the relationship between $\Delta\lambda$ and peak separation. The authors found that for two symmetrical overlapping peaks,

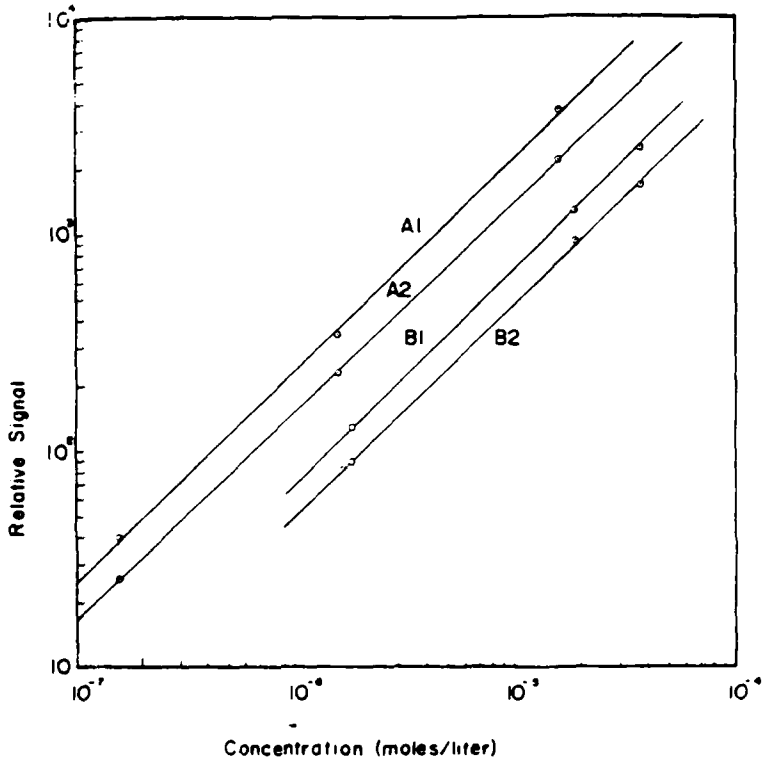

FIGURE 15. Analytical curves for 4-bromobiphenyl and 4-iodobiphenyl at the peak phase setting for each molecule and at the phase setting where one component is phased out. A1 = analytical curve for 4-iodobiphenyl, $\phi_R = 270° + 55°$. A2 = analytical curve for 4-iodobiphenyl, $\phi_R = 0° + 12.5°$. B1 = analytical curve for 4-bromobiphenyl, $\phi_R = 270° + 12.5°$; B2 = analytical curve for 4-bromobiphenyl, $\phi_R = 180° = 55°$ (Reprinted with permission from Mousa, J. J. and Winefordner, J. D., *Anal. Chem.*, 46, 1195, 1974 Copyright 1974 American Chemical Society.)

the optimum $\Delta\lambda$ is about twice the peak separation. In addition to modulated emission spectra, modulated excitation spectra can be acquired by modulating the emission monochromator and scanning the excitation monochromator.

Selective modulation has some features in common with derivative spectrometry. However, the differences as outlined by the authors are (1) normal spectra, not derivative spectra, are obtained by selective modulation; (2) much larger wavelength modulations (80 nm or more) can be used in selective modulation; (3) entire emission (or excitation) spectra of individual components can be recovered from a mixture; and (4) selective modulation is limited to luminescence spectrometry.

A block diagram for the selective modulation instrument used by O'Haver and Parks is shown in Figure 17. The instrument is completely computerized and has been described previously.[66] The programmable ramp generator depicted in this diagram provides repetitive scanning, variable scan rate, and adjustable wavelength limits. Modulation was accomplished by applying a 15-Hz pseudotriangular waveform to the motor. A variable potentiometer was used to attenuate the waveform and control the $\Delta\lambda$ interval.

Several examples demonstrating the utility of this approach were described by the authors. For example, consider the diagram in Figure 18, which illustrates the overlap of

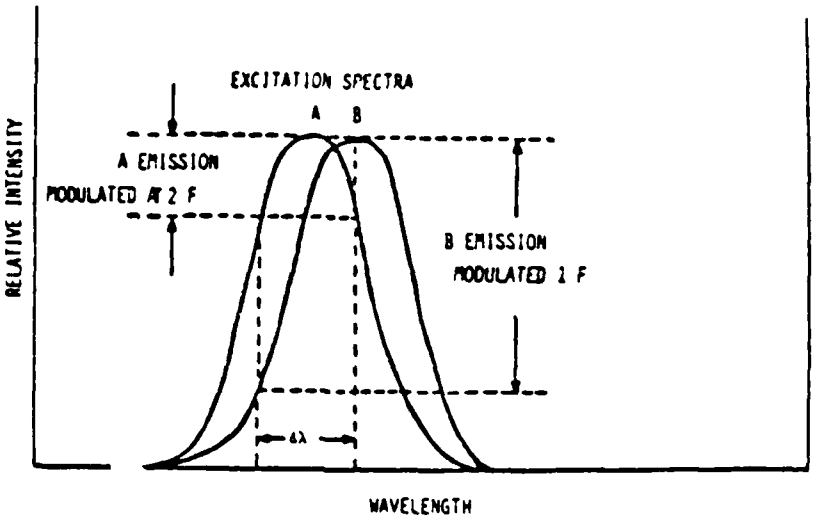

FIGURE 16. The principle of selective modulation. A and B are the excitation spectra of two hypothetical molecules in a mixture. Modulation of the excitation wavelength over the indicated interval $\Delta\lambda$, at a modulation frequency of F Hertz, will modulate the fluorescence intensity of B at the same frequency, while the fluorescence intensity of A will be modulated at twice this frequency (i.e., 2F). (Reprinted with permission from O'Haver, T. C. and Park, W. M., *Anal. Chem.*, 46, 1886, 1974. Copyright 1974 American Chemical Society.)

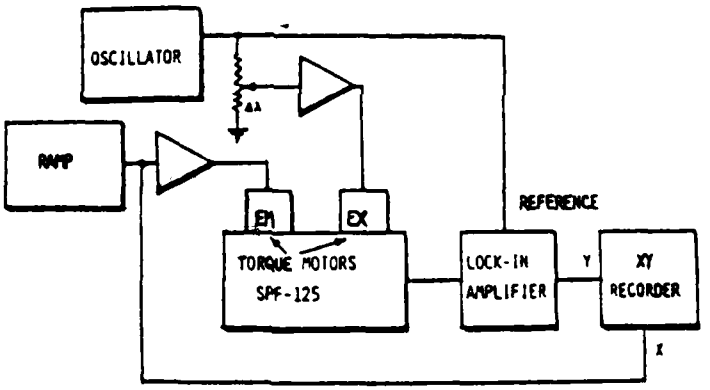

FIGURE 17. Block diagram of the selective modulation system in the excitation modulation mode. For operation in the emission modulation mode, the control lines to the torque motors are interchanged. (From O'Haver, T. C., Green, G. L., and Keppler, B. R., *Chem. Instrum.*, 4, 197, 1973. With permission.)

the emission and excitation spectra of the compounds chrysene and benz(a)anthracene. Possible modulation intervals are also shown. Table 6 summarizes the possible modulation conditions for the analysis of binary mixtures of chrysene and benz(a)anthracene. It should be clear from Figure 18 that determination of benz(a)anthracene in the presence of chrysene by selective excitation is a difficult task, while selective excitation of chrysene in benz(a)anthracene is somewhat easier. However, one can use a selective

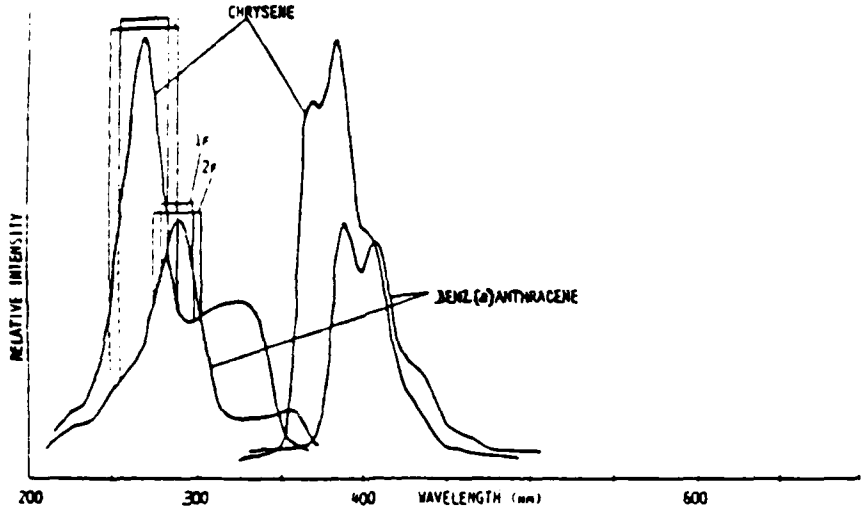

FIGURE 18 Fluorescence excitation and emission spectra of 1.0 ppm chrysene and 0.27 ppm benz(a)anthracene in cyclohexane at 25° C. The modulation intervals are designated by the vertical lines. $W_{em} = W_{ex} = 1.0$ mm (S = 10 nm). (Reprinted with permission from O'Haver, T. C. and Park, W. M., *Anal. Chem.*, 46, 1886, 1974. Copyright 1974 American Chemical Society.)

Table 6
MODULATION CONDITIONS FOR THE ANALYSIS OF BENZ(A)ANTHRACENE-CHRYSENE MIXTURES[a]

Analyte	Modulated wavelength	Detection mode	Center λ (nm)	Δλ (nm)
Benz(a)anthracene	Excitation	1F	270	30
	Excitation	2F	290	30
	Emission	1F	380	45
	Emission	2F	400	45
Chrysene	Excitation	1F	290	20
	Excitation	2F	270	40
	Emission	1F	400	45
	Emission	2F	380	45

[a] Modulation frequency 15 Hz.

From O'Haver, T. C., Green, G. L., and Keppler, B. R., *Chem. Instrum.*, 4, 197, 1973. With permission.

modulation approach to eliminate the interference of a selected component in the presence of the other. Consider the diagrams of Figures 19 and 20. Figure 19 corresponds to the selective modulation of benz(a)anthracene in the presence of chrysene in cyclohexane solution. The diagram shows the observed signals from pure benz(a)anthracene, the mixture sample, and a chrysene standard. The signals were obtained using the 1F detection mode shown in Table 6 and diagramed in Figure 18. Similar results were obtained for the selective modulations of chrysene in benz(a)anthracene as depicted in Figure 20. Again, the results, shown in Figure 20, were obtained using the 1F detection mode shown in Table 6. The authors also demonstrated the effectiveness of using this

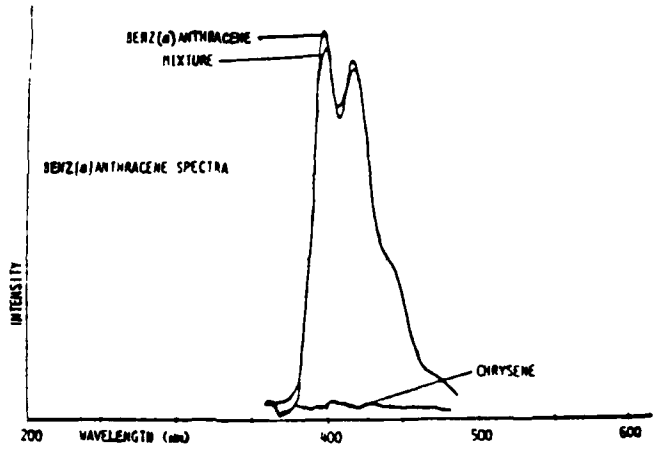

FIGURE 19. Selective modulation of 0.27 ppm benz[a]anthracene in the presence of 1.0 ppm chrysene in cyclohexane at 25° C. $W_{ex} = W_{em} = 1.0$ mm (S = 10 nm). IF, excitation modulation mode; $\Delta\lambda = 30$ nm at 270 nm. The spectra of chrysene and benz(a)anthracene alone are also given, as indicated. (Reprinted with permission from O'Haver, T. C. and Park, W. M., *Anal. Chem.*, 46, 1886, 1974. Copyright 1974 American Chemical Society.)

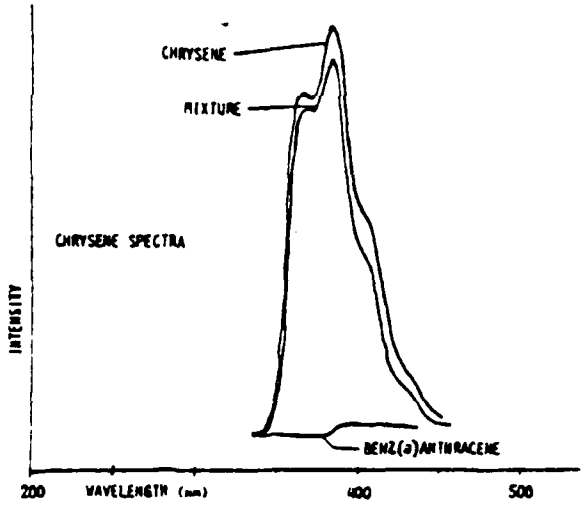

FIGURE 20. Selective modulation of 1.0 ppm chrysene in the presence of 0.27 ppm benz(a)anthracene in cyclohexane at 25°C. (Reprinted with permission from O'Haver, T. C. and Park, W. M., *Anal. Chem.*, 46, 1886, 1974. Copyright 1974 American Chemical Society.)

technique to generate analytical working curves to determine the unknown concentration of a given analyte in the presence of another. The effectiveness of this approach is amply demonstrated in Figure 21, while Figure 22 compares the concentration effects of chrysene on the benz(a)anthracene signal using selective modulation and selective

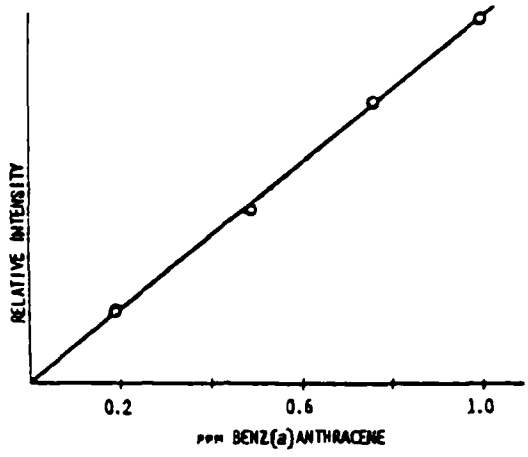

FIGURE 21. Selective modulation analytical curve for benz(a)anthracene in cyclohexane containing 1.0 ppm chrysene. Conditions are as in Figure 19. (Reprinted with permission from O'Haver, T. C. and Park, W. M., *Anal. Chem.*, 46, 1886, 1974. Copyright 1974 American Chemical Society.)

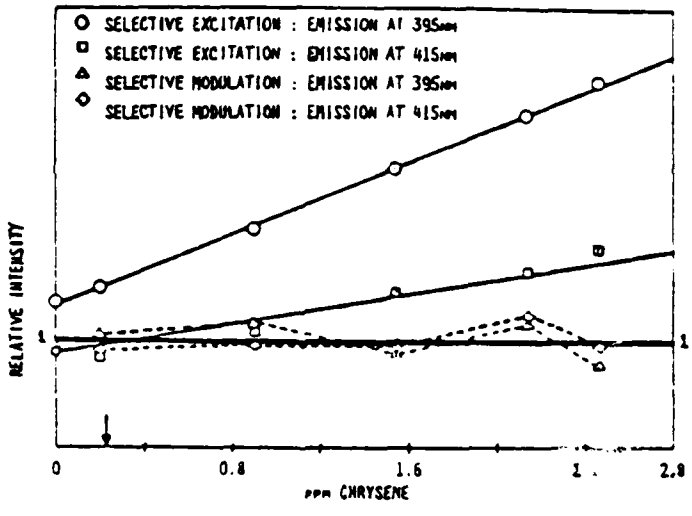

FIGURE 22. Effect of the concentration of chrysene on the selective excitation and selective modulation analytical signals of 0.27 ppm benz(a)anthracene in cyclohexane. (Reprinted with permission from O'Haver, T. C. and Park, W. M., *Anal. Chem.*, 46, 1886, 1974. Copyright 1974 American Chemical Society.)

excitation. Clearly, in this case the selective modulation approach provides better results.

The technique of selective modulation was demonstrated to be a new and interesting approach to analysis of simple multicomponent mixtures. However, as is the case with phase-resolved phosphorimetry, it suffers from the disadvantage that the identities and spectral properties of the mixture components must be known before separation can be

achieved. For additional information, a detailed study has been provided by Green and O'Haver[57] on derivative luminescence spectrometry.

D. Total Luminescence Spectroscopy

The many parameters of luminescence previously discussed indicate that a large amount of information and, consequently, greater specificity can be obtained by exploiting a number of these parameters simultaneously. One such technique is an instrumental one, first called "total luminescence spectroscopy" by Brownrigg et al.[58] and Giering at Baird Corporation.[59] The name "total luminescence" is somewhat of a misnomer since, quite often, only the fluorescence at room temperature is measured. However, the name has come to be synonymous with the approach, and it is futile to attempt to change it at this point. Generally, the total luminescence technique involves the acquisition of the fluorescence intensity of a sample as a function of multiple excitation and emission wavelengths. The acquired data set is then in matrix form with the elements of the matrix representing relative fluorescence intensity, while the position of each represents a given excitation and emission wavelength. Since, for most molecules in fluid solution, the fluorescence spectrum has been found to be independent of the excitation wavelength and the excitation spectra has been found to be independent of the monitored emission wavelength, we can represent the fluorescence matrix for a pure component in matrix form as

$$\underline{M} = \alpha \underline{x}\,\underline{y} \tag{6}$$

where α is a concentration-dependent parameter, $\underline{x}$ is the observed excitation spectrum represented as a column vector, and $\underline{y}'$ is a row vector representing the observed emission spectrum. In dilute solution, where synergistic effects such as energy transfer and quenching are negligible, the fluorescence matrix for multiple components is simply the sum of the contributing matrices, i.e.,

$$\underline{M} = \sum_{i=1}^{n} \alpha(i)\,\underline{x}(i)\,\underline{y}(i) \tag{7}$$

where n is the number of fluorescent species and i is an index of each. For illustration, consider the diagrams of Figure 23. The diagram in Figure 23a corresponds to the fluorescence matrix obtained for a hypothetical compound with assumed double Gaussian peaks corresponding to the emission spectrum. The wavelength distribution of this hypothetical spectrum is shown at the top of the emission axis in this diagram. Also shown is the Gaussian-distributed excitation spectrum with its wavelength distribution. The fluorescence matrix is shown here as a contour map with various contour lines representing isointensity data points. A similar matrix is given in Figure 23b for a second hypothetical compound with two bands each in its excitation and emission spectra. If these compounds were present in a binary mixture at the intensities (concentrations) depicted, then the fluorescence matrix would appear as shown in Figure 23c. Of course, the data can also be represented as an isometric projection of three dimensions (Figure 23d).

It should be apparent from our discussion above that the total luminescence spectrum has considerable utility for multicomponent fluorescence analysis. This utility has often been exploited in a simpler form through the use of selective excitation to isolate the emission of individual components.[70,71] However, several investigators have recognized the improved selectivity which can be obtained by acquiring and retaining large amounts of data as we have described for Figure 23. The most direct approach to acquiring the data is through a computerized conventional fluorimeter. For example, it is a simple task

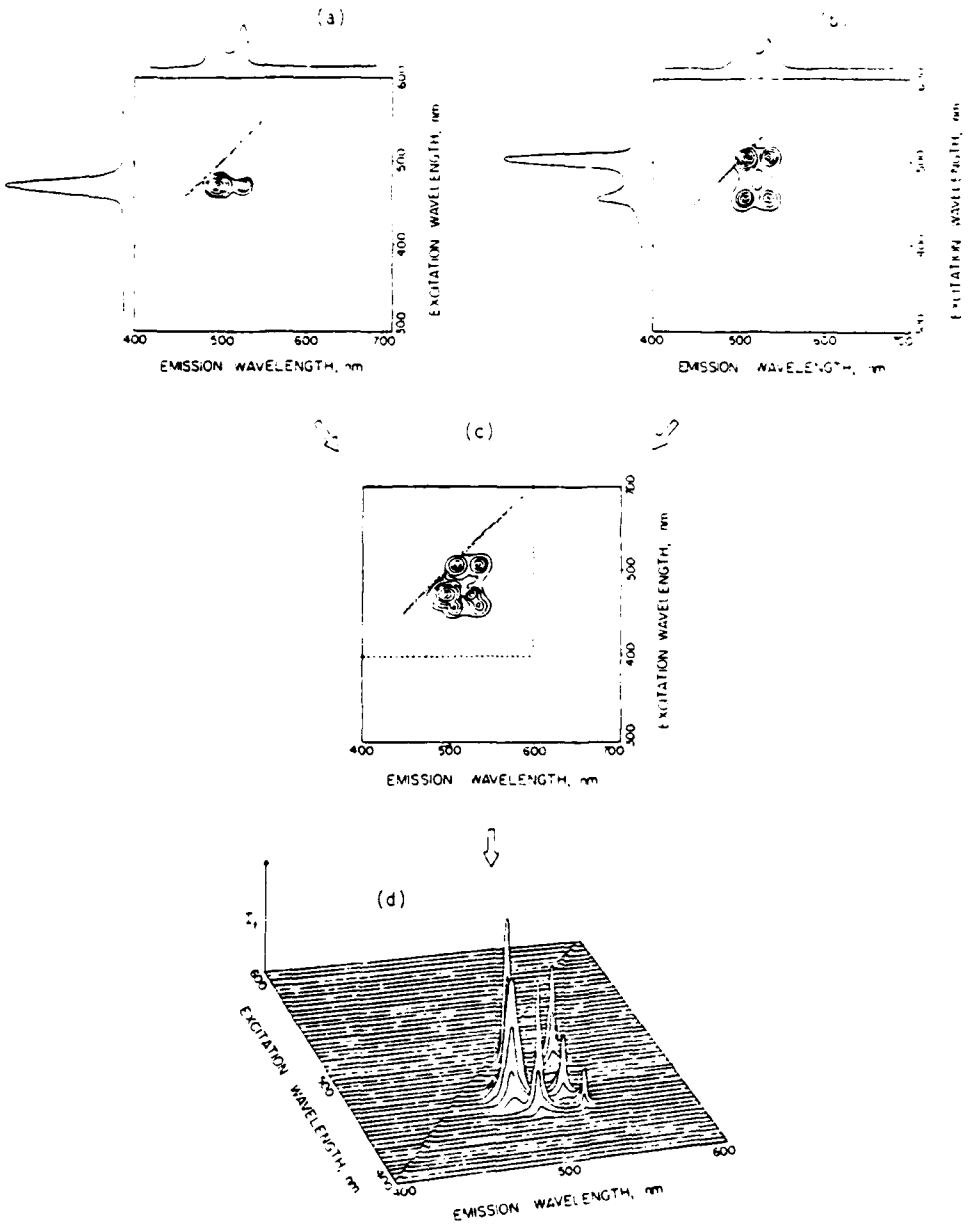

FIGURE 23. Fluorescence matrix for a hypothetical compound. (From Warner, I. M., Fogarty, M. P., and Shelly, D. C., *Anal. Chim. Acta*, 109, 361, 1979. With permission.)

through computer control to fix the wavelength of excitation and obtain and store the emission spectrum. The process can be repeated at several additional excitation wavelengths until the desired fluorescence matrix is obtained. This approach has been employed by several investigators including Giering,[69] Haugen et al.,[72] and others.[73,74] The problem with this approach is that even with computerized instrumentation, the task

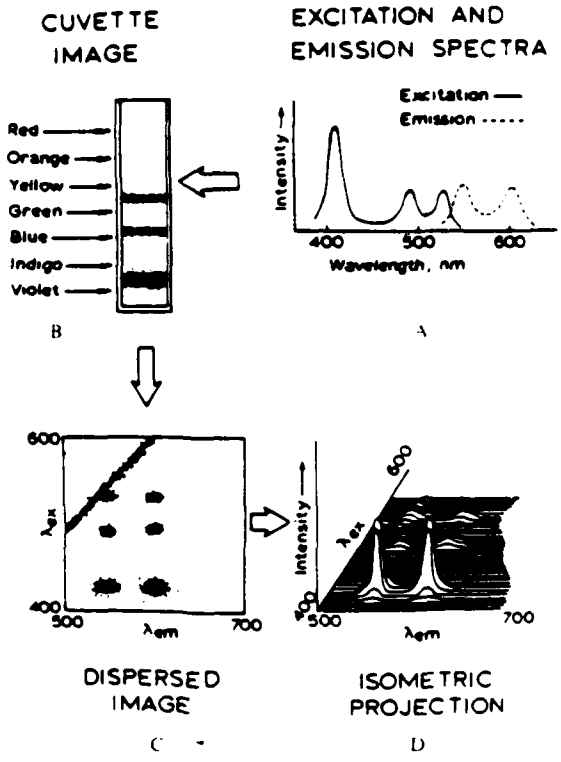

FIGURE 24. Production of the emission-excitation matrix for a hypothetical compound. (A) The hypothetical excitation and emission spectra. (B) The fluorescent cuvette as illuminated by the polychromatic beam. (C) The emission-excitation matrix produced at the exit slit aperature of the analyzing polychromator. (D) An isometric projection of the emission-excitation matrix of C. (From Warner, I. M., Callis, J. B., Davidson, E. R., and Christian, G. D., *Clin. Chem.*, 22, 1483, 1976. With permission.)

of obtaining the desired data can be time consuming and tedious (and may be plagued with instrument drift during the lengthy measurement periods). Recently, a commercially developed computerized fluorimeter designed to acquire total luminescence spectra has been described.[55] This system is described as requiring 1½ hr to record a complete total luminescence spectrum. The commercial development of such instrumentation is a further example of the usefulness of the total luminescence approach.

An alternative to the time-consuming mechanical scanning approach was first proposed and developed by Callis and co-workers.[56-58] This new instrument employs a novel concept of polychromatic sample illumination to eliminate the necessity of time-consuming mechanical scanning. Consider the diagram shown in Figure 24. In Figure 24A the dashed curve represents the emission spectrum of a hypothetical compound while the continuous curve represents its observed excitation spectrum. The polychromatic illumination can be achieved as shown in Figure 24B by exciting the cuvette simultaneously with spatially and spectrally resolved polychromatic light. This spatially resolved polychromatic source can be obtained by focusing a continuum source such as a xenon arc lamp into a monochromator which has been rotated on its side and

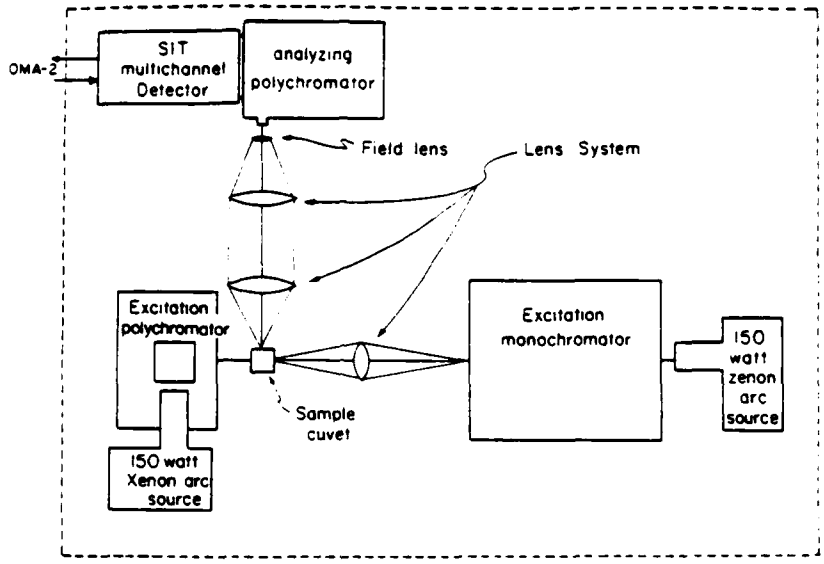

FIGURE 25. Optical layout of rapid scanning fluorimeter. (From Warner, I. M., Fogarty, M. P., and Shelly, D. C., *Anal. Chim. Acta*, 109, 361, 1979. With permission.)

has its exit slit removed.[76] Alternatively, a flat field polychromator can be used as the excitation source in a similar fashion.[79] In either case, the observed curvette image will be as shown in Figure 24B. The observed bands correspond to the relative excitation spectrum of the compounds, i.e., the fluorescence intensity as a function of the excitation wavelength. This cuvette image can then be focused onto the entrance slit of a polychromator or *monochromator with the exit slit removed*. Each fluorescence band will then be dispersed into its component emission wavelengths while the y axis information is spatially preserved. The resultant image (fluorescence matrix) at the exit plane of the analyzing polychromator is as shown in Figure 24C. Alternatively, the data can be displayed as an isometric projection as depicted in Figure 24D. It should be realized that this image is acquired over a given spectral region without the need for any mechanical scanning. Therefore, the time limitation in acquiring these data is from the detection system. The rapid acquisition of the two-dimensional spectral data is most easily achieved with a two-dimensional light transducer such as a multichannel detector (e.g., a television camera).[80-82] Such a detection system will provide the acquistion of a 256 × 256 fluorescence matrix in a time frame of less than 17 msec. This is a considerable improvement over the hours required on conventional instrumentation. A more versatile version of this "video fluorimeter" has been developed by Warner et al.[83] Figure 25 provides an optical layout of their system, which was designed to eliminate much unneeded transfer optics by use of a holographically ruled, flat field polychromator. Thus, a considerable improvement in spectral quality is realized. This improvement is nicely illustrated by the isometric projection of an ethanolic mixture of 3×10^{-6} *M* anthracene and 1×10^{-7} *M* perylene. The detection electronics of this system is provided by the EG & G Princeton Applied Research OMA-2 system. This detection system provides great versatility and a wide dynamic range for spectral data acquisition.

The video fluorimeter should continue to provide new avenues for multicomponent fluorescence analysis. However, a major difficulty of this system is in the handling of the large data base generated. This problem will be discussed later in our section on multicomponent data analysis.

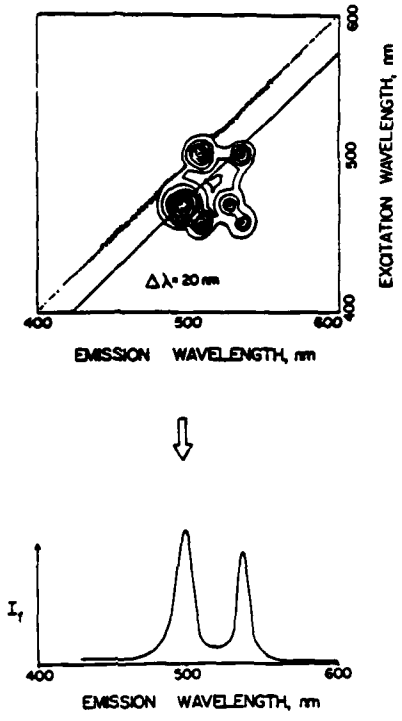

FIGURE 26 Total luminescence and synchronous spectrum of hypothetical binary mixture.

E. Synchronous Excitation Fluorescence

The synchronous excitation method was first introduced by Lloyd in 1971.[84,85] The technique is multicomponent in that spectral information can be acquired for most or all of the fluorescing species in a mixture. For example, consider the total luminescence contour depicted in Figure 26. This diagram corresponds to the emission-excitation matrix (EEM) of the hypothetical binary mixture described in the previous section of this manuscript. The synchronous spectrum of the mixture is shown at the bottom of the diagram. The synchronous excitation method differs from most conventional fluorescence methods in that the excitation and emission monochromators are scanned simultaneously with some constant interval difference "$\Delta\lambda$". Thus the synchronous excitation spectrum of Figure 26 corresponds to a plot of the fluorescence intensity along the line parallel to the scattered exciting light vs. wavelength of fluorescence. This spectrum shows two distinct wavelength maxima, one from each component. It should be clear from this diagram that one can vary the shape and number of components of the spectrum simply by varying the interval "$\Delta\lambda$" between the emission and excitation monochromator. It should also be apparent from the diagram that the spectral information provided by the synchronous spectrum is also contained in the total luminescence spectrum. Thus, as with any information set which is a subset of another, the synchronous spectrum of a mixture is more ambiguous than the total luminescence spectrum. However, the synchronous method has the advantage that it can easily be acquired on a simple fluorimeter capable of simultaneously scanning the excitation and emission monochromator.

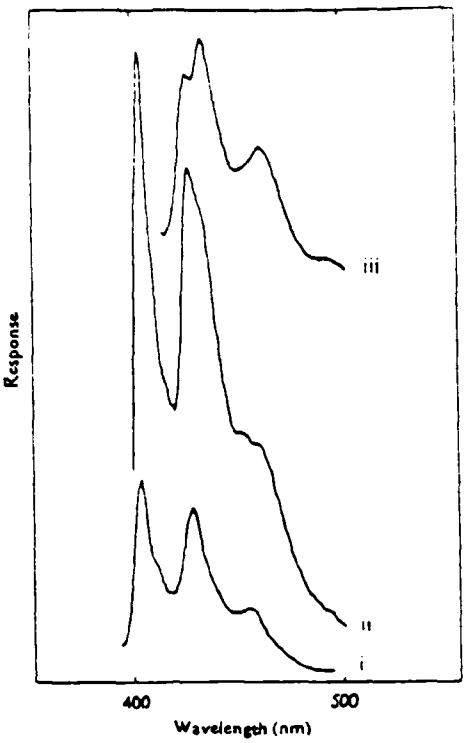

FIGURE 27. Emission spectra (uncorrected) of a liquid chromatography fraction containing benzo(k)fluoranthene, benzo(a)pyrene and perylene. (i) Excited at 308 nm. (ii) Excited at 385 nm. (iii) Excited at 404 nm. The solvent is one volume of diethyl ether in three of 40 to 60° light petroleum. (*Reprinted by permission from* Lloyd, J. B. F., *Nature*, 231, 64, 1971. © 1971 Macmillan Journals Limited.)

To illustrate the potential of the synchronous excitation method, consider the diagrams of Figures 27 and 28. Figure 27 displays the uncorrected emission spectra obtained at different excitation wavelengths of a mixture from a liquid chromatography fraction containing benzo(k)fluoranthene, benzo(a)pyrene, and perylene. The spectrum of each component of the mixture was obtained by selective excitation of the mixture, and Figure 28 shows the synchronous excitation spectra of the pure individual components as well as that of the chromatography fraction of Figure 27. Clearly, the synchronous excitation spectrum of the mixture provides information about each of the three components.

Since its development by Lloyd, the synchronous method has received wide use for the analysis of complex fluorescent mixtures. Most of Lloyd's applications of the technique have been in the area of forensic chemistry. For example, Lloyd has employed the technique to characterize rubbers, rubber contact traces, and tire prints.[86] In addition, he has explored the use of the technique in conjunction with quenching to characterize complex mixtures.[86] Results of this study showed that quenching could be used in combination with synchronous excitation to provide increased structural features where

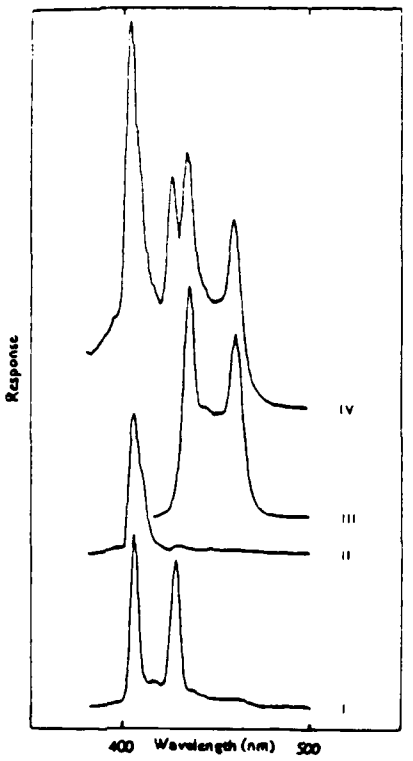

FIGURE 28. Emission spectra (uncorrected) synchronously excited at an interval of 23 nm. (i) Benzo(k)fluoranthene, (ii)Benzo(a)pyrene, (iii) Perylene. (iv) The chromatography fraction of Figure 27. The solvent is the same as in Figure 27. (Reprinted by permission from Lloyd, J. B. F., *Nature*, 231, 64, 1971. © 1971 Macmillan Journals Limited.)

much spectral similarity exists without the use of a quencher. For example, consider Figure 29 which shows the synchronously excited spectra of a naphthenic oil in cyclohexane and in chloroform. One notes considerable differences in the characteristics of the two spectra. The fingerprinting applicability of this approach is demonstrated in Figure 30. Two solutions of gear oils with similar spectral characteristics are compared. Although little differences between the two are noted in the cyclohexane solution, considerable differences are noted in the partly quenched chloroform solution. John and Soutar have also explored the use of synchronous excitation spectrofluorimetry for the identification of crude oils[97] with some degree of success.

More recently, Lloyd and Evett[98] have developed a theory for predicting peak wavelengths and intensities in synchronously excited fluorescence emission spectra. Using the assumption that the excitation and emission peak maxima could be represented as Gaussian peaks, they were able to predict the peak maxima in the synchronous spectrum with a reasonable degree of accuracy. That is, the mean difference between calculated and observed maxima in the synchronous spectrum was 1.95 nm.

Vo-Dinh[99] has also developed a methodology to improve the selectivity of the

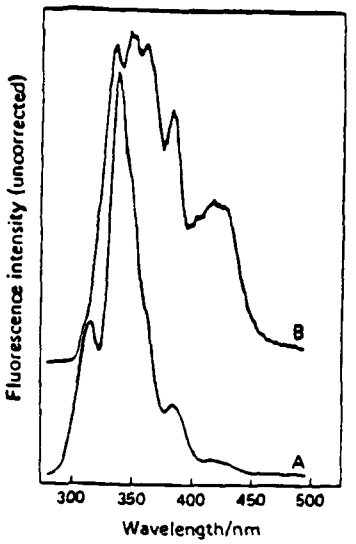

FIGURE 29. Synchronously excited spectra (30 nm) of a naphthenic oil (1 mg mℓ). (A) cyclohexane. (B) chloroform. B is at ten times greater sensitivity than A. (From Lloyd, J. B. F., *Analyst*, 100, 82, 1975. With permission.)

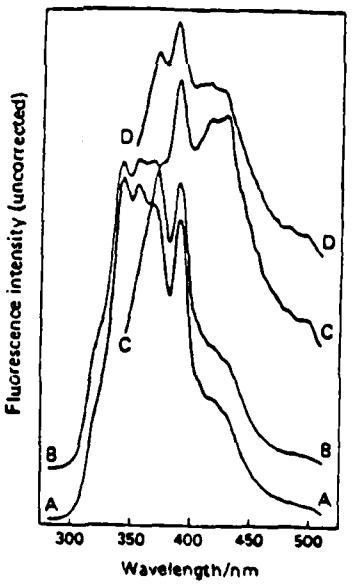

FIGURE 30. Synchronously excited spectra (30 nm) of solutions (0.2 mg mℓ) of gear oils. A and C are from one sample in cyclohexane and chloroform, respectively. B and D are from a second sample. (From Lloyd, J. B. F., *Analyst*, 100, 82, 1975. With permission.)

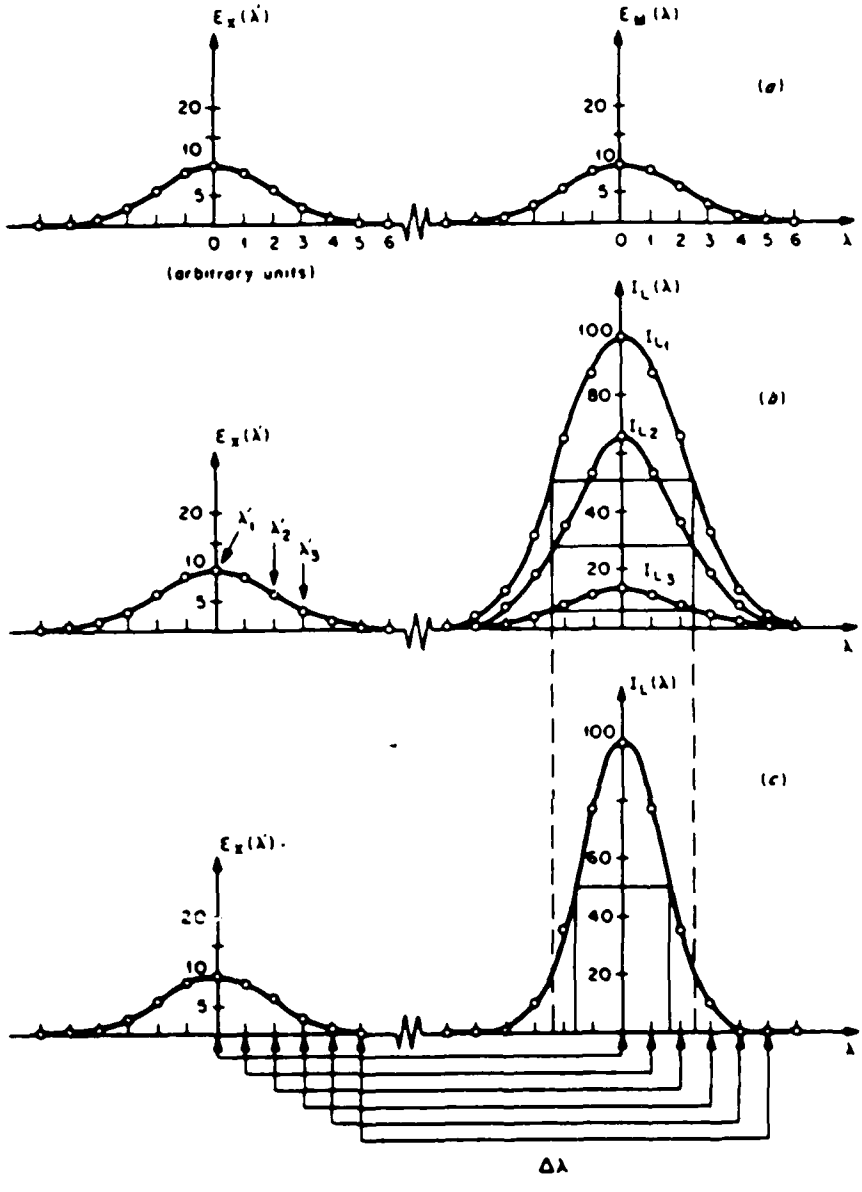

FIGURE 31. Schematic representation of the band-narrowing effect. (Reprinted with permission from Vo-Dinh, T., *Anal. Chem.*, 50, 396, 1978. Copyright 1978 American Chemical Society.)

synchronous excitation technique in luminescence spectrometry. In his discussion, Vo-Dinh presented an interesting observation which he termed the "band narrowing effect". Consider the diagram of Figure 31. In this diagram, the functions $E_x(\lambda')$ and $E_m(\lambda)$ represent the excitation and emission spectra, respectively, as Gaussian functions. Figure 31b shows how a variation in the monochromatic excitation from λ'_1 to λ'_2 to λ'_3 causes a corresponding variation in the fluorescence intensity while the peak width is

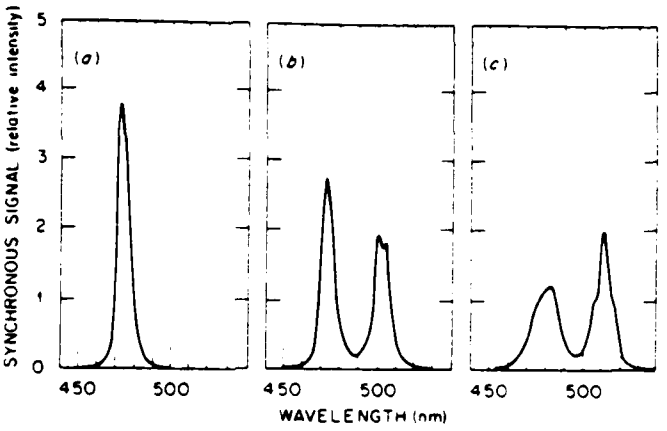

FIGURE 32. Effect of the wavelength interval on the synchronous fluorescence signal of tetracene (a) $\Delta\lambda$ = 3 nm, (b) $\Delta\lambda$ = 30 nm, (c) $\Delta\lambda$ = 45 nm. (Reprinted with permission from Vo-Dinh, T., *Anal. Chem.*, 50, 396, 1978. Copyright 1978 American Chemical Society.)

about the same. Figure 31c shows how band narrowing occurs in the synchronous spectrum. In this paper Vo-Dinh also demonstrated how simplification of the synchronous spectra can be produced by variation of $\Delta\lambda$. Figure 32 shows how the synchronous spectrum of tetracene varies as a function of $\Delta\lambda$. In regard to multicomponent analysis, it was demonstrated that the positions of synchronous signals could be predicted for a group of polynuclear aromatic compounds. This prediction is amply displayed in Figure 33 where λ and λ_x are the wavelength of emission and the longest wavelength of absorption, respectively. The shaded areas in this figure correspond to the predicted spectral regions in the synchronous spectrum of naphthalene, phenanthrene, anthracene, perylene, and tetracene which agreed well with data presented by Vo-Dinh.

Another interesting factor useful for improving selectivity in phosphorimetry has been suggested by Vo-Dinh and Gammage. Their approach is based on the synchronous excitation technique, employing the energy difference between the phosphorescence band and the absorption band of the compound.[90]

Recently, Latz et al.[91] have cautioned users on the limitations of synchronous spectrometry for multicomponent analysis. They demonstrated how the loss of information in synchronous spectrometry can lead to erroneous interpretation of data.

F. Miscellaneous Instrumental Techniques

A number of instrumental techniques are becoming useful or have recently been shown to be useful for multicomponent fluorescence analysis. While a complete discussion on each of these topics is not possible here, their usefulness as multicomponent techniques in fluorescence spectroscopy merits discussion. Therefore, a brief description of each is given here, and references to more extensive reviews are provided where applicable.

1. Double-Beam Fluorescence Spectroscopy

One of the few advantages often mentioned of absorption spectroscopy over fluorescence spectroscopy is its ability to compensate for blank interferences. In recent years, some investigators have recognized this inherent shortcoming of fluorescence spectroscopy; consequently, double-beam fluorescence spectroscopy has been developed.

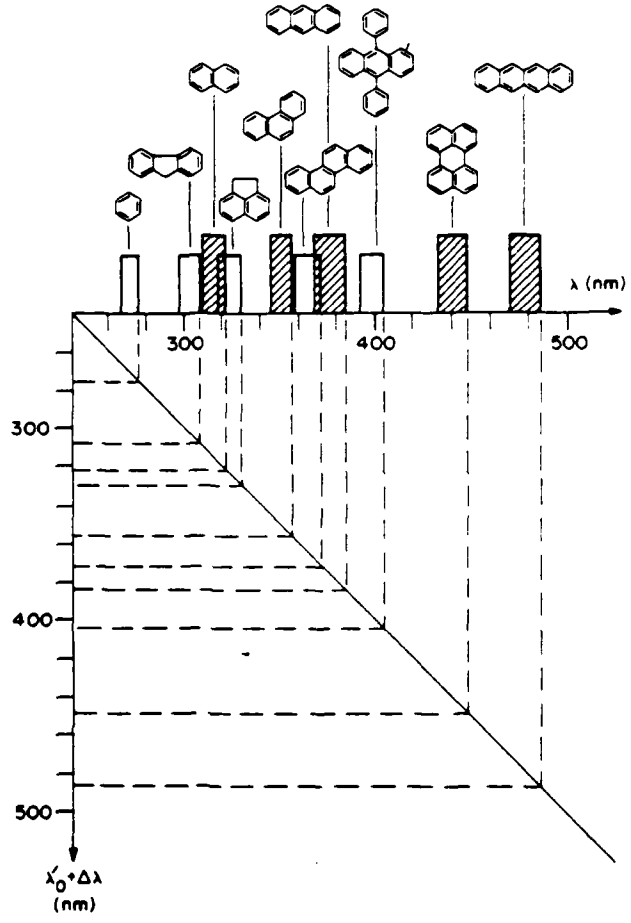

FIGURE 33. Data chart for synchronous spectra. (Reprinted with permission from Vo-Dinh, T., *Anal. Chem.*, 50, 396, 1978. Copyright 1978 American Chemical Society.)

One such double-beam system has been described by Anacreon and Ohnishi.[92] Their design incorporates several modes of operation into a single fluorimeter. Figure 34 provides an optical diagram of their fluorimeter. In this system, the radiation source is chopped similar to a double-beam spectrometer at a frequency of 60 Hz, then is focused onto the entrance slit of the excitation monochromator. The chopper is connected via a shaft to a sector mirror located after the exit slit of the excitation monochromator. This sector mirror is used to alternately excite the sample and the reference blank. Consequently, the emitted fluorescence which is viewed at right angles is also intermittently focused onto the entrance slit of the emission monochromator. Thus, the chopper allows temporal separation of both beams which are therefore alternately detected by the photomultiplier tube. Each of the two signals is then discriminated using a lock-in amplifier, and the reference signal is electronically subtracted from the sample signal.

To demonstrate the utility of this technique, Anacreon and Ohnishi gave several applications. For example, Figure 35 shows two overlapping Raman bands of distilled

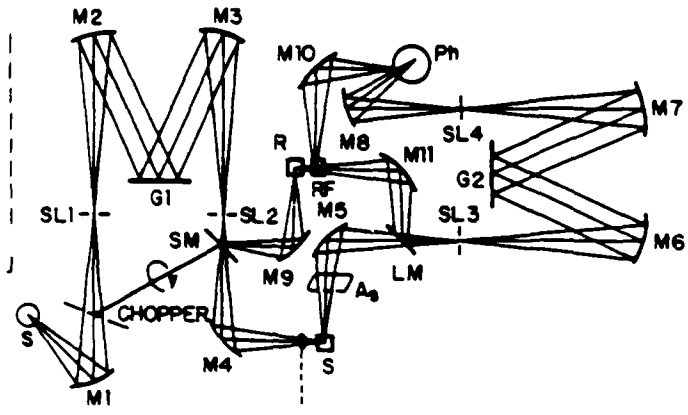

FIGURE 34. Optical layout of the double-beam system. SM, sector mirror; G, grating; LM, lattice mirror; M, mirror; A_s, absorption cell holder; Ph, photomultiplier; RF, reference cell holder; R, reference; SL_1 and SL_2, entrance slit and exit slit; S, sample. (From Anacreon, R. E. and Ohnishi, Y., *Appl. Opt.*, 14, 2921, 1975. With permission.)

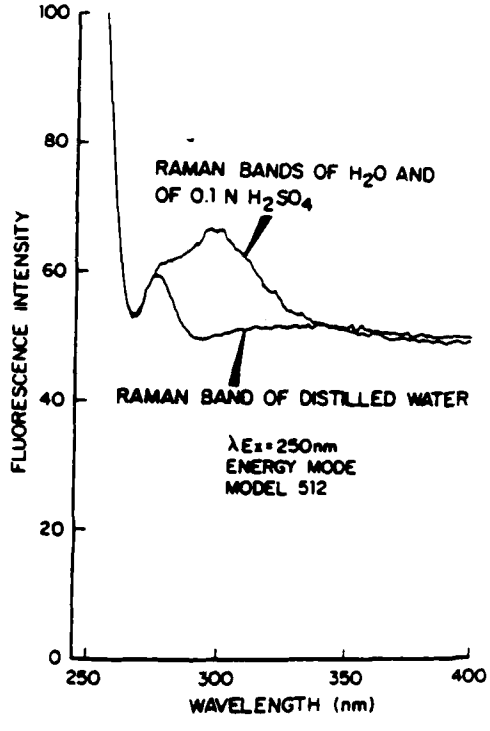

FIGURE 35. Overlapping Raman bands of H_2O and of H_2SO_4. (From Anacreon, R. E. and Ohnishi, Y., *Appl. Opt.*, 14, 2921, 1975. With permission.)

water and 0.1 *N* H_2SO_4. A second Raman spectrum of distilled water is also shown for comparison. Figure 36 shows the Raman band of H_2SO_4 alone obtained by subtracting the Raman band of distilled water in the double-beam mode. The flat spectrum obtained for distilled water in both beams is also shown. The utility of this approach is further

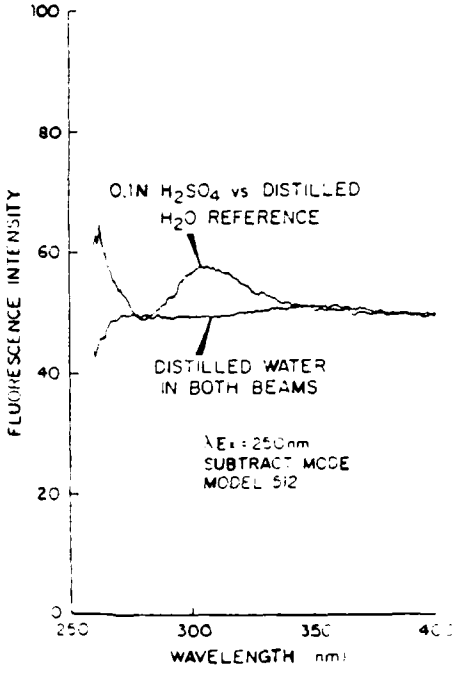

FIGURE 36 Double-beam spectrum of 0.1 N H_2SO_4 Raman band. (From Anacreon, R. E. and Ohnishi, Y., *Appl. Opt.*, 14, 2921, 1975. With permission.)

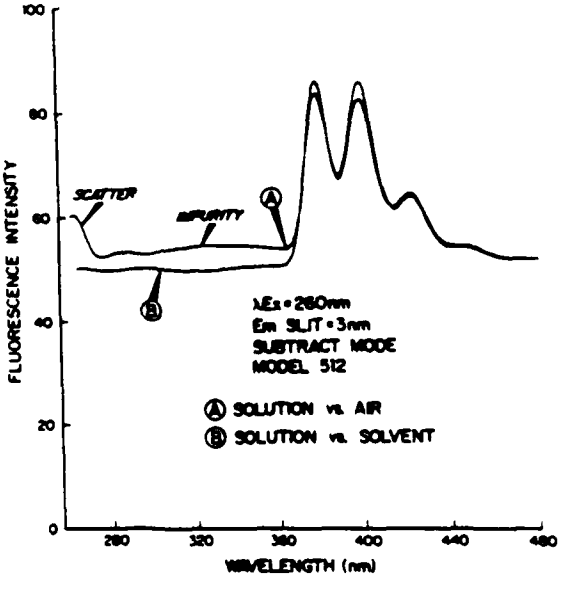

FIGURE 37 Double-beam fluorescence spectrum of anthracene in cyclohexane. (From Anacreon, R. E. and Ohnishi, Y., *Appl. Opt.*, 14, 2921, 1975. With permission.)

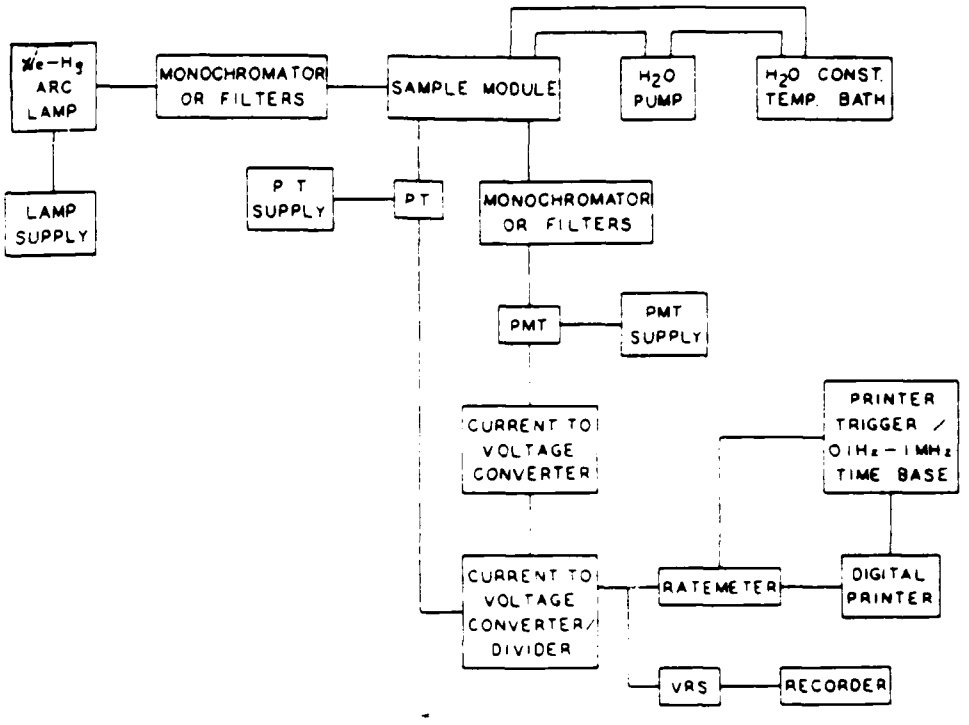

FIGURE 38. Block diagram of the general fluorescene reaction rate instrument (Reprinted with permission from Wilson, R. L. and Ingle, J. D., *Anal. Chem.*, 49, 1060, 1977. Copyright 1977 American Chemical Society.)

demonstrated using a fluorescence spectrum of anthracene dissolved in impure cyclohexane. The fluorescence of the impurity is evident in spectrum A of Figure 37. This corresponds to obtaining the anthracene spectrum vs. an air blank. Spectrum B shows the same solution run in the double-beam mode vs. a solvent blank.

The work presented by Anacreon and Ohnishi adequately demonstrates the utility of double-beam fluorescence for multicomponent analysis. However, one must recognize that this instrument does not solve all fluorescence blank problems. In many analysis schemes, the source of the fluorescence interference is unknown. Therefore, no blank solution is available for background compensation. For additional information on double-beam fluorescence spectroscopy, consult the review article by Porro and Terhaar.[93]

2. *Multicomponent Kinetic Studies by Fluorimetry*

Fluorescence spectroscopy has frequently been used to monitor multicomponent reaction rate kinetics. Wilson and Ingle[94] have recently described the design and operation of a fluorimetric reaction rate instrument. Figure 38 provides a block diagram of their system. In their paper, Wilson and Ingle provide a critical evaluation of the system, including precision of the measurements, background signal, and S/N ratio. The authors have also demonstrated the application of this system to the determination of silver.[95] This reaction rate method is based on the enhancement of the reaction between oxine-5-sulfonic acid and persulfate by silver ions. Figure 39 shows the emission spectrum of the fluorescent product produced in the Ag^+, oxine-5-sulfonic acid and persulfate. Figure 40 shows the silver calibration curve from this study and Table 7 gives a

Table 7
SUMMARY OF Ag^+ INTERFERENCE STUDY DATA

Species	Concentration (ppm[a])	Concentration (ppm[b])
Na(I)	300	—
K(I)	300	—
Mg(II)	300	—
Ba(II)	300	—
Sr(II)	300	—
Pb(II)	300	—
Ca(II)	30	150(I_2(0.95))
Cu(II)	30	300(I_2(0.13))
Fe(III)	3	30(I_2(0.70))
Hg(II)	3	30(I_2(0.52))
Cr(III)	30	150(I_1(0.98,0.88))
Co(II)	3	30(E_2(1.1))
Ni(II)	3	30(E_2(1.4))
Zn(II)	3	30(E_2(1.1))
Cd(II)	3	30(I_1(0.95,0.77))
Mn(II)	3	30(E_3(1.01,1.08))
Ti(II)	3	30(I_1(0.98,0.92))
V(IV)	0.03	0.3(I_1(0.96,0.80))
Sn(II)	0.3	3(E_3)
Sn(IV)	0.3	3(E_3)
Al(III)	0.3	3(E_2(1.1))
Zr(IV)	0.01	0.1(I_2(0.95))
Hf(IV)	0.1	1(I_2(0.76))
Pt(II)	0.3	3(I_1(0.93,0.70))
Au(III)	0.03	0.3(E (1.26,1.1))
SO_3^{2-}	0.18 *M*	—
PO_4^{3-}	0.15 *M*	—
ClO_4^-	0.12 *M*	—
NO_3^-	10^{-1} *M*	0.16 *M*(I_1(0.95,0.42))
Cl^-	10^{-4} *M*	10^{-1} *M*(I_1(0.95,0.88))
F^-	0.01 *M*	0.5 *M*(E_2(1.2))

[a] Concentration which had no effect on the rate of the blank or Ag-enhanced reaction.

[b] Concentration which increased or decreased the rate of either the blank or Ag-enhanced reaction. E_1 = ion enhances the Ag reaction more than the background reaction. E_2 = ion enhances both the Ag and background reactions equally. E_3 = ion enhances the background reaction more than the Ag reaction. I_1 = ion inhibits the Ag reaction more than the background reaction. I_2 = ion inhibits both the Ag and background reactions equally. Relative increase or decrease of blank and Ag-enhanced (0.5 ppm Ag^+) rates are given in parentheses.

list of interfering ions for this method. This example involves a one-component system, but one can easily conceive of using this system for multicomponent analysis.

As an example of another fluorimetric rate fluorimeter, Fogarty and Warner[96] have recently shown that the video fluorimeter could be used as both an initiator and probe of photochemical reactions. To demonstrate the utility of this approach, they chose to study

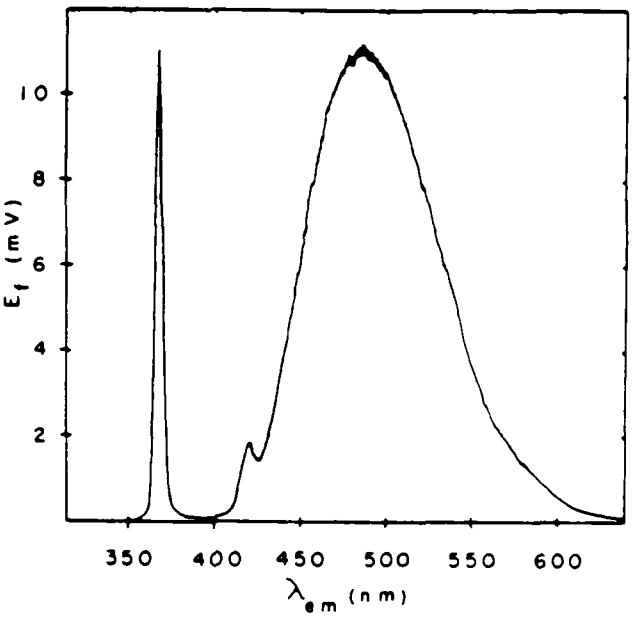

FIGURE 39. Ag^+ – OXSA – $S_2O_8^{=}$ emission spectrum. $[Ag^+]$ = 1 ppm, $[S_2O_8^{=}]$ = 0.1 *M*, [OXSA] = 10 ppm, R_f = 10 Ω, τ = 0.1 sec, E_{PMT} = 800 V, λ_{ex} = 366 nm, scan rate = 100 nm min, excitation slit = 2.0 nm, emission slit = 0.5 nm. (Reprinted with permission from Wilson, R. L. and Ingle, J. D., *Anal. Chem.*, 49, 1060, 1977. Copyright 1977 American Chemical Society.)

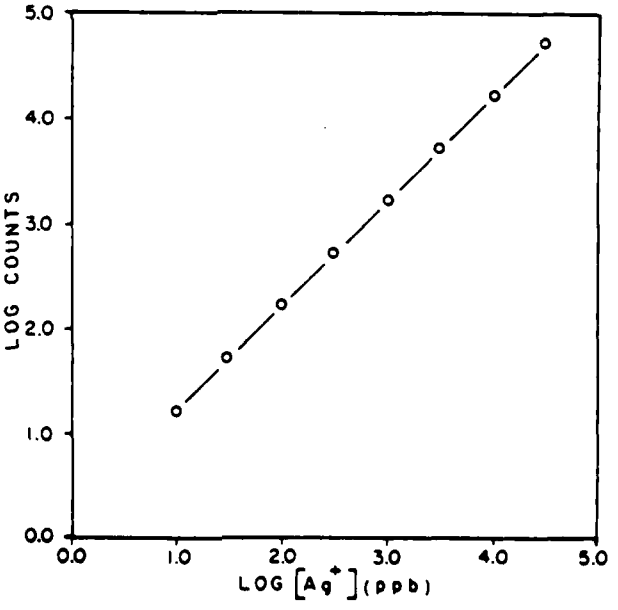

FIGURE 40. Ag calibration curve. [OXSA] = ppm, $[S_2O_8^{=}]$ = 0.1 M, ph = 2.2, other conditions are the same as in Figure 39. (Reprinted with permission from Wilson, R. L. and Ingle, J. D., *Anal. Chem.*, 49, 1060, 1977. Copyright 1977 American Chemical Society.)

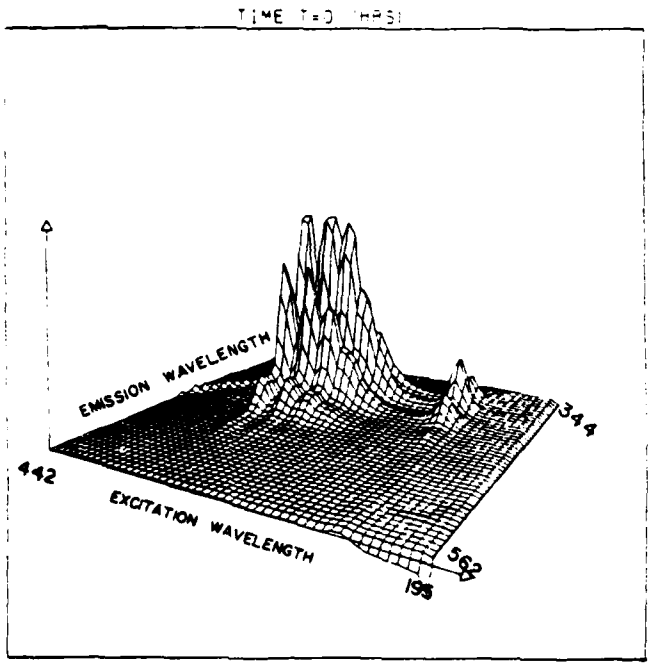

A

FIGURE 41. The EEMs of the reaction of chloroform with anthracene (A) T = 0, (B) T = 1.5 hr, (C) T = 3.0 hr. (From Warner, I. M. and Fogarty, M. P., *Appl. Spectrosc.*, 34, 438, 1980. With permission.)

the photo-induced reactions of anthracene in polychlorinated alkanes. For example, consider the data displayed in Figure 41. This diagram shows the EEMs of the reaction of chloroform with anthracene after photoinitiation of the reaction at times t = 0, 1.5 hr, and 3 hr. Figure 42 shows a spectral deconvolution of the data presented in Figure 41, while Table 8 presents a tabulated list of the calculated rate constants of the reactions. All reactions studied were found to be first order.

Based on the two studies presented here, it is reasonable to conclude that the use of fluorescence for multicomponent kinetic measurements will continue to be a valuable tool in the future.

3. *Fluorescence Detectors for Liquid Chromatography*

Perhaps one of the most useful aspects of fluorescence spectroscopy for multicomponent analysis is as a detector for separation methods such as liquid chromatography. This usefulness arises from the selectivity and sensitivity of fluorescence described earlier in our introductory section. The variation in designs for fluorescence detectors for liquid chromatography ranges from conventional fluorimeters to less conventional types such as the video fluorimeter. A number of examples of conventional detection can be cited and will not be discussed in detail here. For example, Johnson et al.[97] and Slavin et al.[98] have described conventional fluorimeters as detectors in high performance liquid chromatography. Less conventional designs have included the free-falling drop detector developed by Martin et al.,[99] which was designed to minimize the instrumental limitations of conventional flow-through fluorimeters such as large dead volumes. A

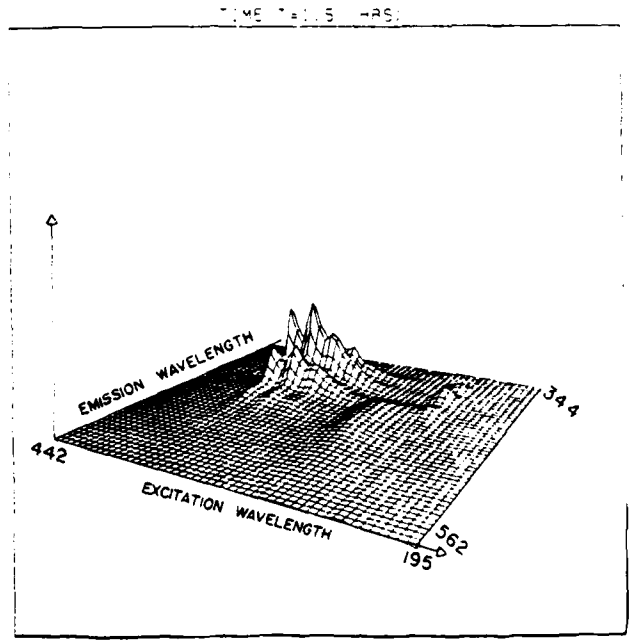

FIGURE 41B

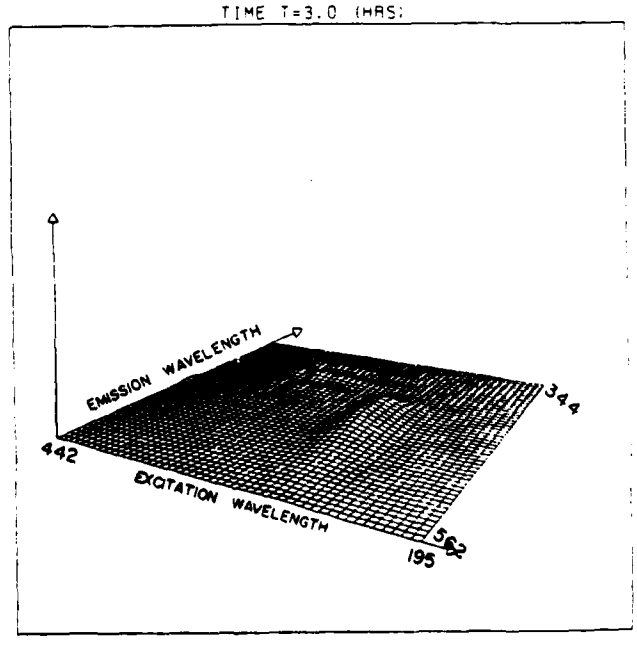

FIGURE 41C

diagram of this detector is shown in Figure 43. The detection chamber is spherical in design. The eluent enters this chamber in the form of a drop from a Teflon® needle connected to the chromatographic column. The drops are collected at a hole in the

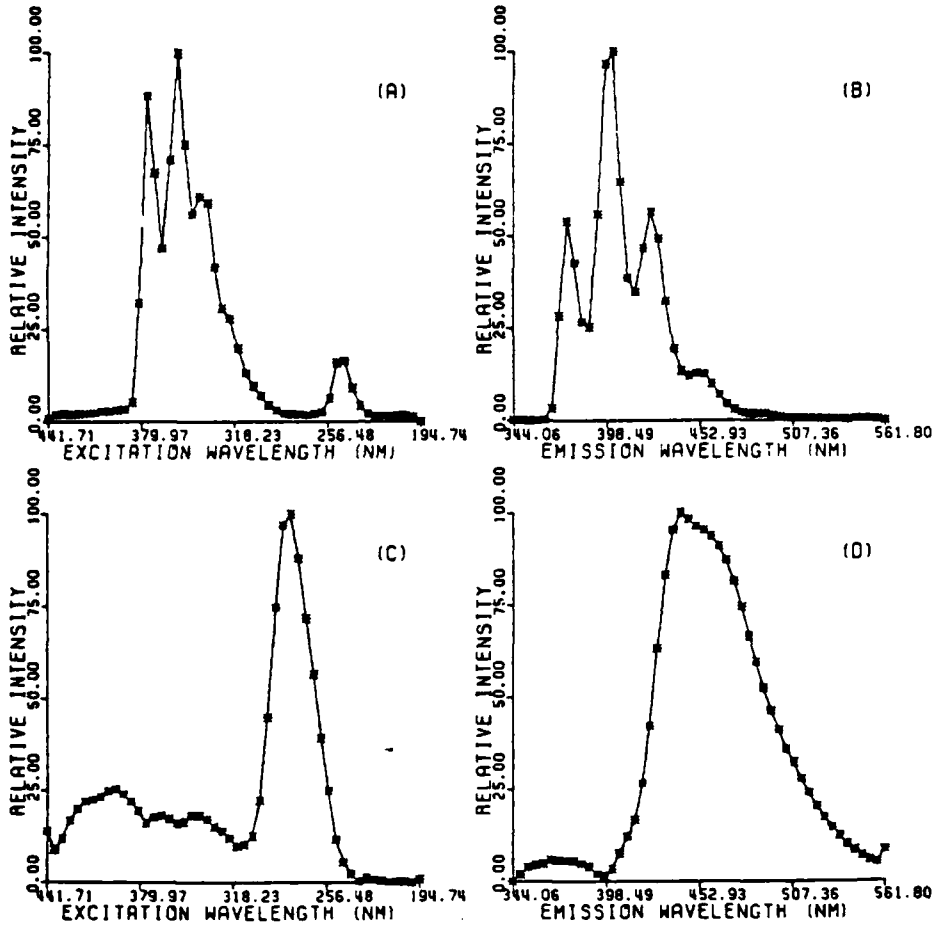

FIGURE 42. The ratio method deconvolution of the EEM of Fig. 41B. (A) Anthracene excitation spectrum. (B) Anthracene emission spectrum. (C) Photoproduct excitation spectrum. (D) Photoproduct emission spectrum. (From Warner, I. M. and Fogarty, M. P., *Appl. Spectrosc.*, 34, 438, 1980. With permission.)

Table 8
CALCULATED RATE CONSTANTS

Chlorinated alkane	Anthracene decay $\ln(I_A) = \ln(I_0) - kt$		Product formation $\ln(I_\infty - I_P) = \ln(I_\infty - kt)$	
	$k(s^{-1})$	std dev	$k(s^{-1})$	std dev
$CHCl_3$	1.14×10^{-4}	0.38×10^{-4}	1.43×10^{-4}	0.22×10^{-4}
CCl_4	2.00×10^{-1}	0.37×10^{-1}	1.78×10^{-1}	0.37×10^{-1}
C_2Cl_6	2.22×10^{-1}	0.44×10^{-1}	2.56×10^{-1}	0.95×10^{-1}
CCl_4(DMA)	2.26×10^{-1}	0.23×10^{-1}	3.59×10^{-1}	0.63×10^{-1}

From Fogarty, M. P. and Warner, I. M., *Appl. Spectrosc.*, 34, 438, 1980. With permission.

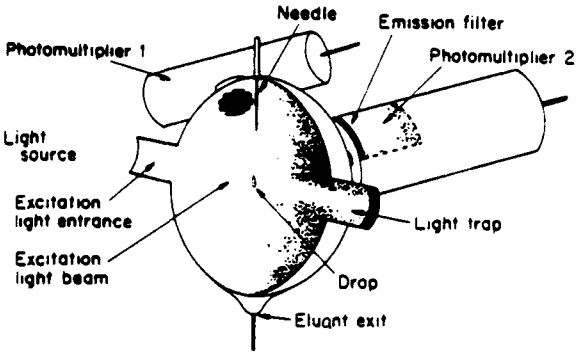

FIGURE 43. Free-falling drop detector. (From Martin, F., Maine, J., Swelley, C., and Holland, J. F., *Clin. Chem.*, 22, 1434, 1976. With permission.)

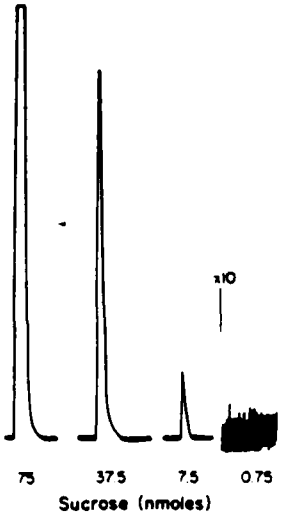

FIGURE 44. Typical sensitivity of free-falling drop detector. The indicated amounts of sucrose were applied to the anion exchange column 86 mmol ℓ borate buffer and eluted isocratically with 0.86 mol ℓ borate buffer (pH 8.8). (From Martin, F., Maine, J., Swelley, C., and Holland, J. F., *Clin. Chem.*, 22, 1434, 1976. With permission.)

bottom of the sphere which leads to a waste receptacle. A drop of eluent passing through the sphere scatters exciting light which is unfiltered and therefore corresponds to total light within the integration sphere. The output from photomultiplier 1 is used as a timing signal to process the fluorescence signal measured by photomultiplier 2. The light striking photomultiplier 2 is filtered to admit wavelengths in the range 320 to 395 nm. Figure 44 shows the typical sensitivity of this detector, and Figure 45 shows the chromatogram of a reference mixture of saccharides.

An objective of many detectors designed for liquid chromatography is to capture as

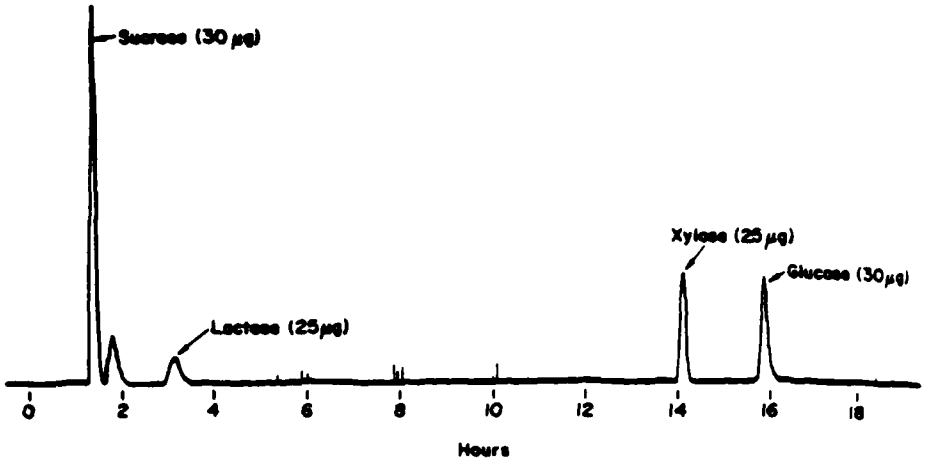

FIGURE 45. Chromatogram of a reference mixture of saccharides. The sample contained 75 nmol each of sucrose, lactose, globoside tetrasaccharide, GL3 trisaccharide, and 150 nmol of xylose and glucose in 0.15 mℓ of 86 nmol ℓ ("10%") borate buffer. The gradient maker initially contained 10% borate buffer in chamber 1, 30% borate buffer in chamber 2, 50% borate buffer in chambers 3 and 4, and 100% borate buffer in chambers 5 through 9. Each chamber contained 20 mℓ of solution. The solvent programmer was set to withdraw solvent from the gradient maker for 16 hr and then from the limit buffer reservoir for 6 hr. (From Martin, F., Maine, J. Swelley, C., and Holland, J. F., *Clin. Chem.*, 22, 1434, 1976. With permission.)

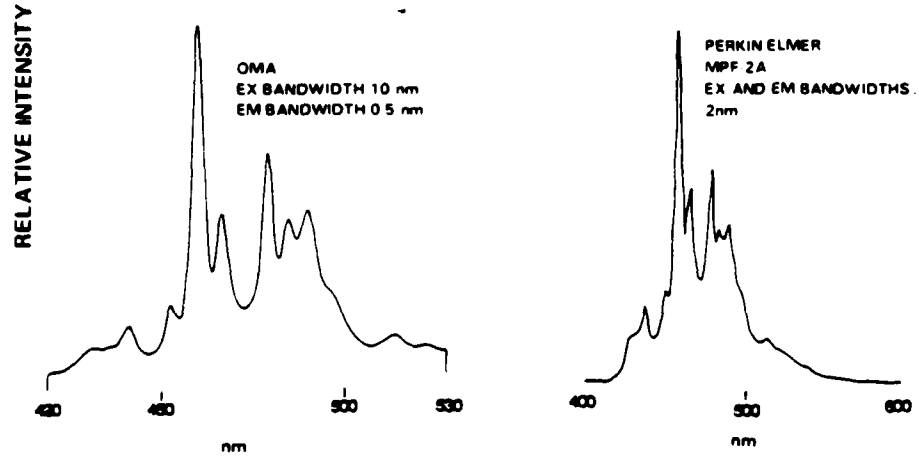

FIGURE 46. Fluorescence emission spectra of Ovalene (plastic std) Ex λ = 350 nm. (Reprinted with permission from Jadamec, J. R., Sauer, W. A., and Talmi, Y., *Anal. Chem.*, 49, 1316, 1977. Copyright 1977 American Chemical Society.)

much information as is possible in real time. Consequently, it is expected that rapid scanning multichannel detectors would find applications in liquid chromatography. One such system has been described by Jadamec et al.[100] This system uses a Princeton Applied Research Corporation (PARC) Optical Multichannel Analyzer (OMA, Model 1205A) to control an intensified vidicon detector (PARC Model 1205D) interfaced to a Farrand Optical Mark I Spectrofluorometer. The spectral coverage of the detector system was 110 nm. Figure 46 provides a spectral comparison of this system with a Perkin Elmer

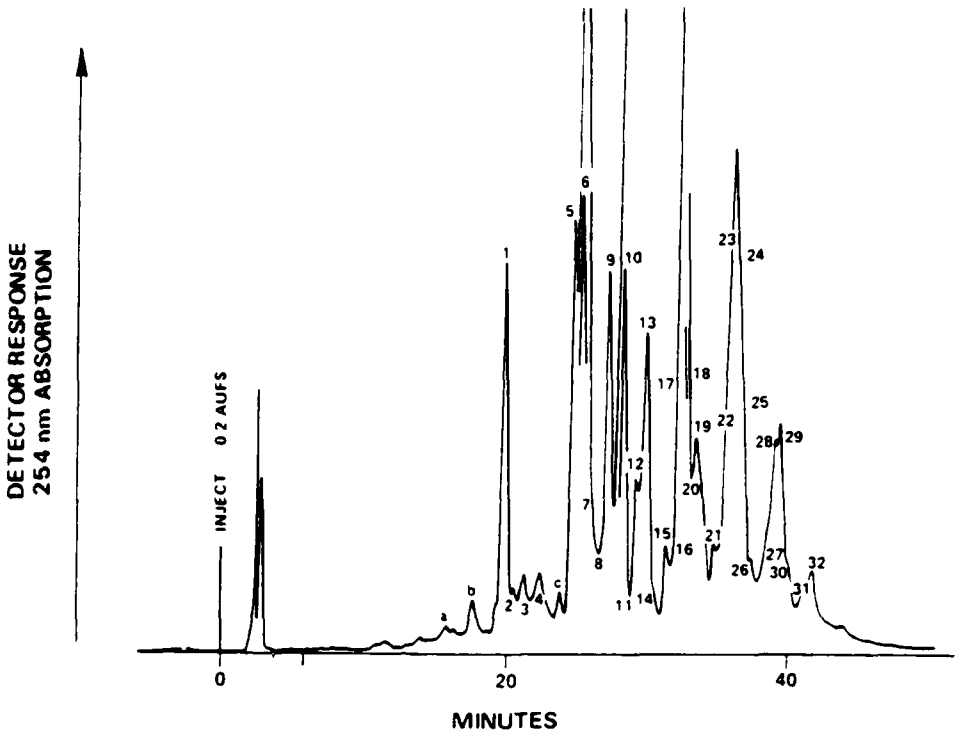

FIGURE 47. Liquid chromatogram of #2 fuel oil. (Reprinted with permission from Jadamec, J. R., Sauer, W. A., and Talmi, Y., *Anal. Chem.*, 49, 1316, 1977. Copyright 1977 American Chemical Society.)

MPF-2A spectrofluorimeter, and Figure 47 shows the chromatogram of a #2 fuel oil. Figure 48 shows the emission spectra captured in real time using the OMA detection system.

There are obvious advantages of capturing complete emission spectra of eluents on-the-fly. An even greater advantage would be to capture complete emission and excitation spectra on-the-fly. Thus, one can conceive of a video fluorimeter as a detector for HPLC. Two such approaches have been described, one by Herschberger et al.[101] and the other by Shelly et al.[102] In the latter approach, a flow cell (Precision Cells, Inc., P N 8830) with a flow cavity of square cross-section, and a 20-μl sample volume is coupled at the end of a reverse-phase chromatographic column. Data are then captured by using the video fluorimeter[83] as an eluant detector (Figure 49). Figure 50 shows a conventional absorption chromatogram for six polynuclear aromatic compounds, and Figure 51 shows the EEMs (background subtracted) captured on-the-fly. The quality of the spectra is noted to be as good or better than that obtained in a conventional cuvette.

The examples of fluorescence detectors for HPLC that combine fluorescence with a separation method show a very powerful approach to multicomponent analysis. Indicative of this realization is the increasing number of articles found on fluorimetric derivatization methods in HPLC.[103,104]

IV. MULTICOMPONENT FLUORESCENCE DATA REDUCTION

Up to this point, we have discussed instrumental techniques for multicomponent fluorescence analysis. Some of these techniques are inherently designed for spectral deconvolution such as the wavelength modulation technique of O'Haver and Parks.[55]

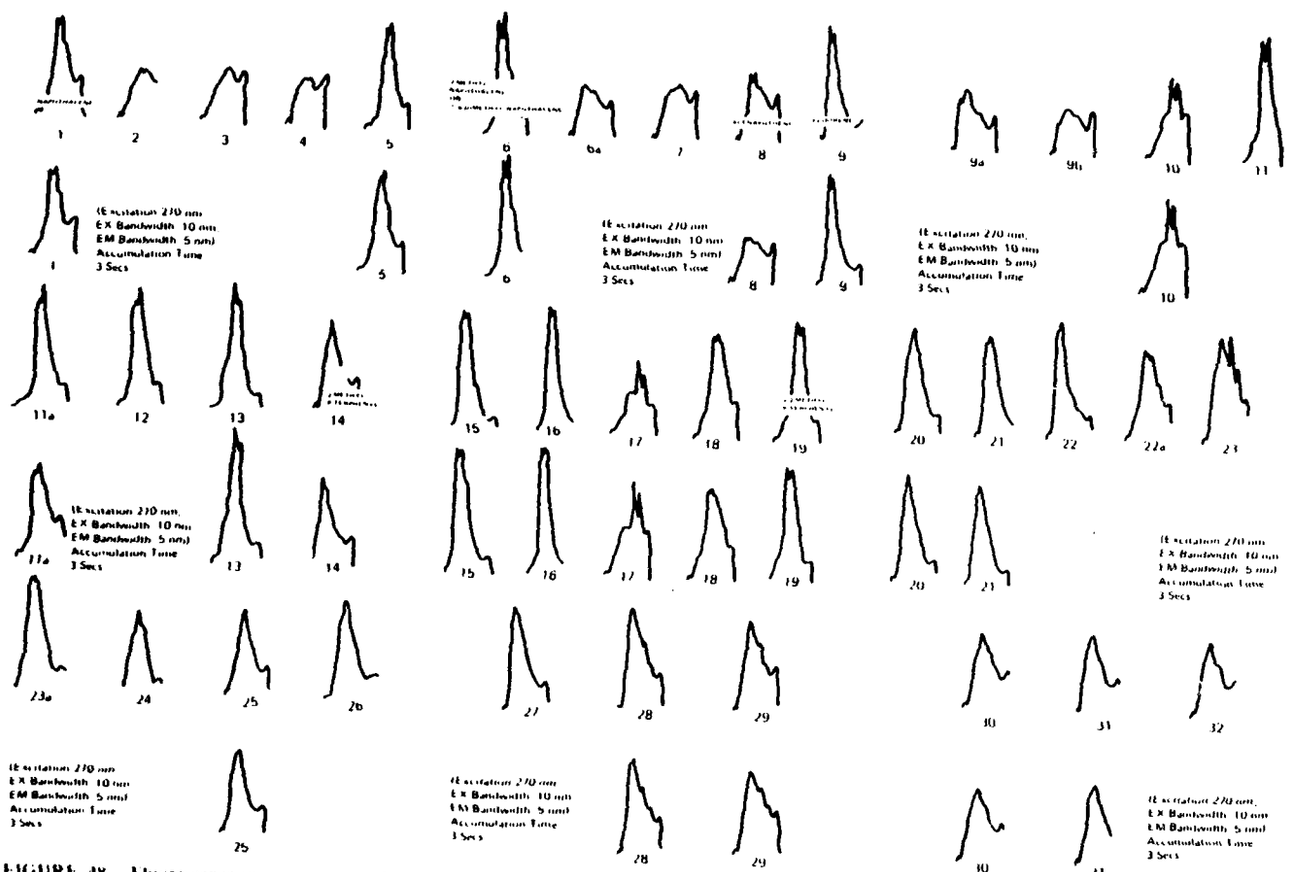

FIGURE 48 Fluorescence emission spectra (290 to 400 nm, 92 OMA scans each) of liquid chromatographic oil fractions taken during elution. (Reprinted with permission from Jadamec, J. R., Sauer, W. A., and Talmi, Y., *Anal. Chem.*, 49, 1316, 1977. Copyright 1977 American Chemical Society.)

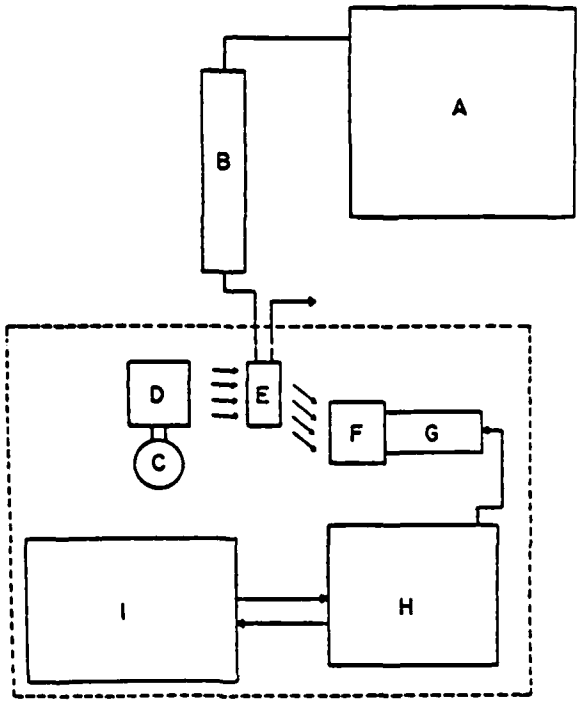

FIGURE 49. Video fluorimeter for chromatographic eluant detection. (A) Altex microprocessor controlled HPLC. (B) Column: 15 × 250 mm preparative or 4.6 × 250 mm analytical (cation exchange). (C) Light source. (D) Excitation polychromator. (E) Microfluorescence flow cell. (F) Emission polychromator. (G) SIT detector (intensified vidicon). (H) OMA-2 optical multichannel analyzer (I) HP9845T calculator. (From Warner, I. M., Fogarty, M. P., and Shelly, D. C., *Anal. Chim. Acta*, 109, 361, 1979. With permission.)

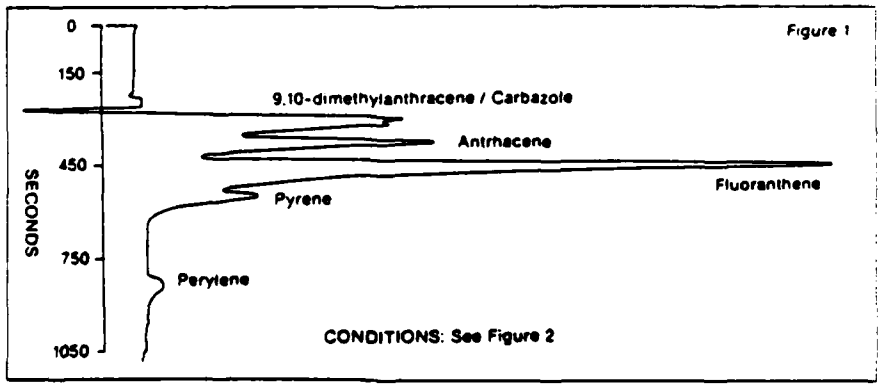

FIGURE 50. Separation of aromatic hydrocarbons with UV detection.

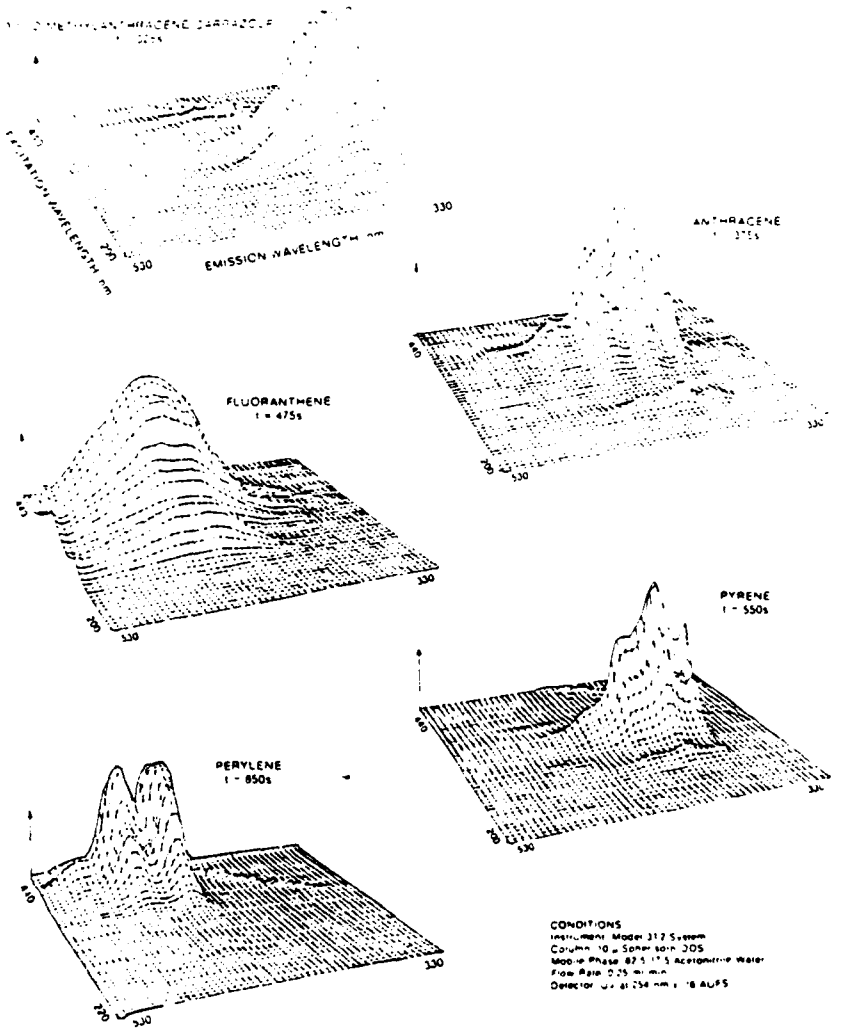

FIGURE 51. Three-dimensional fluorescent scans of aromatic hydrocarbons.

Others require algorithms to aid in spectral interpretation. This section will discuss data reduction algorithms common to most fluorescence techniques as well as novel algorithms developed in recent years to complement the development of novel instrumentation such as the video fluorimeter.[76,83]

A. General Algorithms

One of the most common algorithms used for fluorescence instrumentation is for spectral correction. Two types of spectral corrections are required, one for distortions in the excitation spectra due to the nonlinear output of the excitation source-optics combination, and the other for distortions in the emission spectra due to the detector-optics combination. Parker[23] has identified several approaches to spectral correction

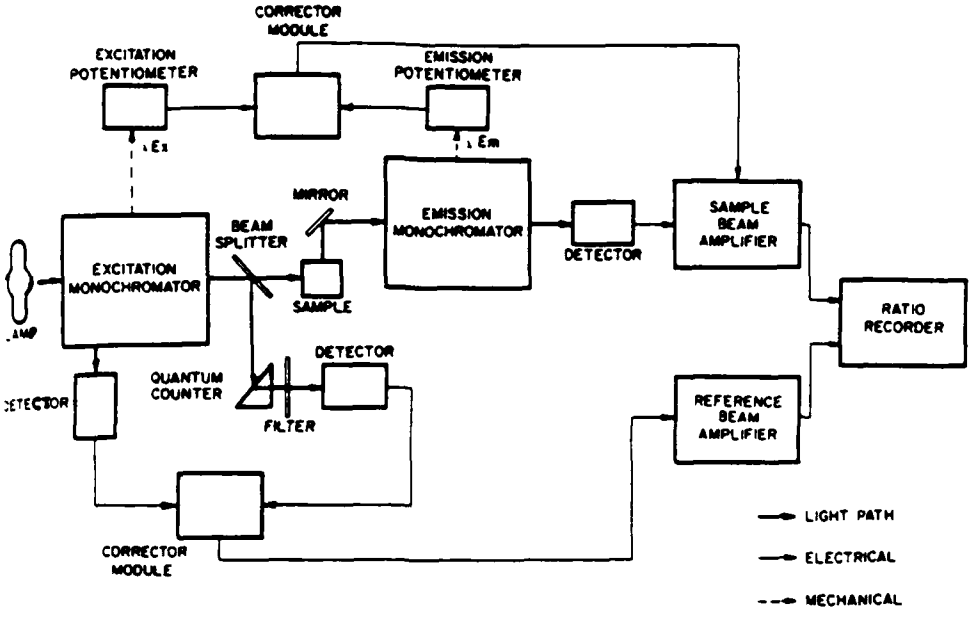

FIGURE 52. Block diagram of corrected excitation and emission system. (From Porro, T. J., Anacreon, R. E., Flandreau, P. S., and Fagerson, I. S., *J. Assoc. Off. Anal. Chem.*, 56, 608, 1972. With permission.)

which we will not discuss in detail here since we are mainly concerned with the implementation of algorithms to perform the spectral correction. A paper by Porro et al.[105] has identified and illustrated a number of principal uses of corrected spectral data using several polynuclear compounds as examples. Basically, a general diagram for a corrected-spectra fluorimeter is shown in Figure 52. A comparison of the corrected and uncorrected excitation spectra of anthracene is provided in Figure 53. Other examples of spectral correction instruments are cited by Shephard,[106] Tuan and Wild,[107] Budde and Dodd,[108] and Pailthorpe.[109]

In addition to spectral correction, it is often necessary to compensate for attenuation of the excitation beam due to strong absorption by the analyte. Recently, Holland et al.[110] developed an algorithm for this task. The authors defined the absorption correction factor as

$$fa = \frac{\ln T\,(W_2 - W_1)}{(T^{W_2} - T^{W_1})} \qquad (8)$$

where T is the transmittance and W_1 and W_2 are defined as the fractional distances across the cell at points X_1 and X_2, respectively. Most methods which correct for absorption by the analyte will generally use an equation of the form defined above. For detailed information on correction of inner-filter effects via right angle and front-surface illumination, a recent paper by Leese and Wehry[111] can be consulted.

B. Qualitative Analysis of Fluorescence Data

The simplest approach to qualitative multicomponent fluorescence data reduction involves a file searching system where the spectrum of an unknown compound is compared to spectra from a library of known compounds. Several systems have been described. More recently, Miller and Faulkner[112] developed a computer-assisted

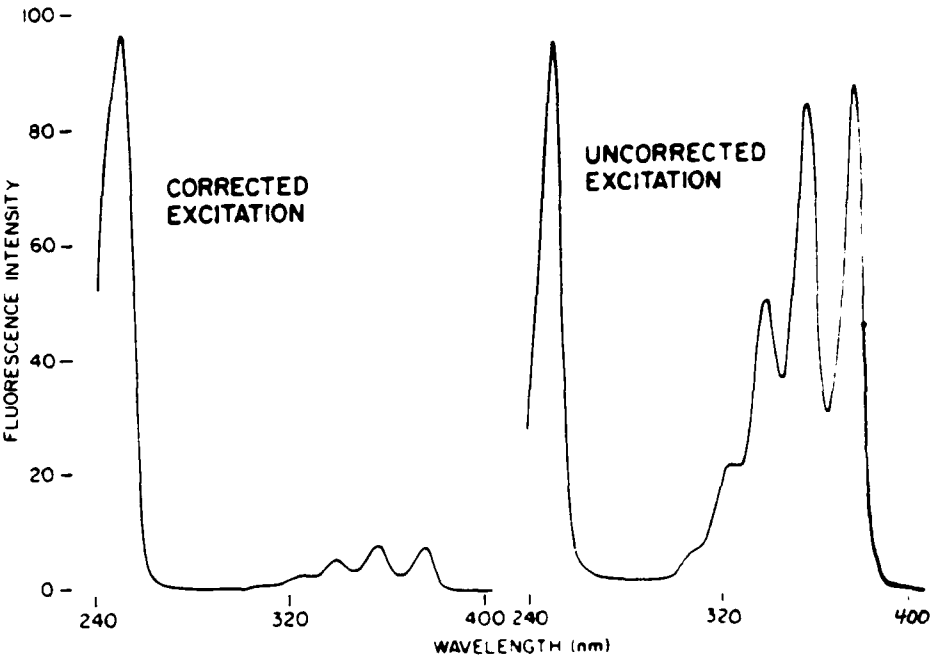

FIGURE 53. Anthracene in ethanol, corrected vs. uncorrected excitation spectra. (From Porro, T. J., Anacreon, R. E., Flandreau, P. S., and Fagerson, I. S., *J. Assoc. Off. Anal. Chem.*, 56, 608, 1972. With permission.)

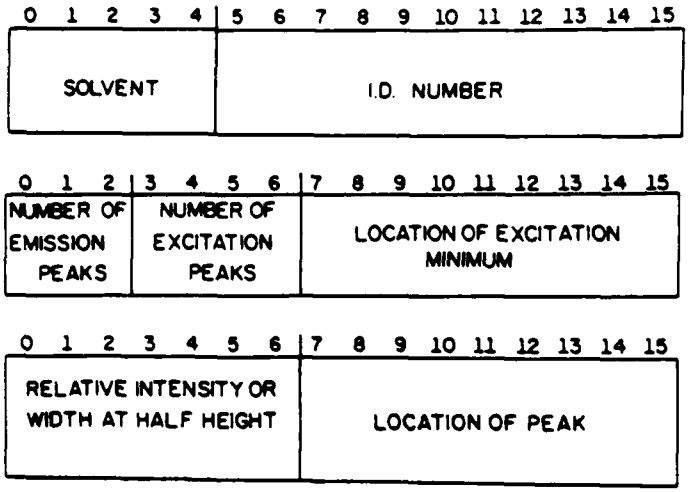

FIGURE 54. Packing of spectral information into 16-bit computer words. (Reprinted with permission from Miller, T. C. and Faulkner, L. R., *Anal. Chem.*, 48, 2083, 1976. Copyright 1976 American Chemical Society.)

structural interpretation program for fluorescence file searching. Their scheme employed a series of 16 bit computer words to store spectral information (Figure 54). A basic flow chart for their file searching program is depicted in Figure 55. Table 9 provides the results

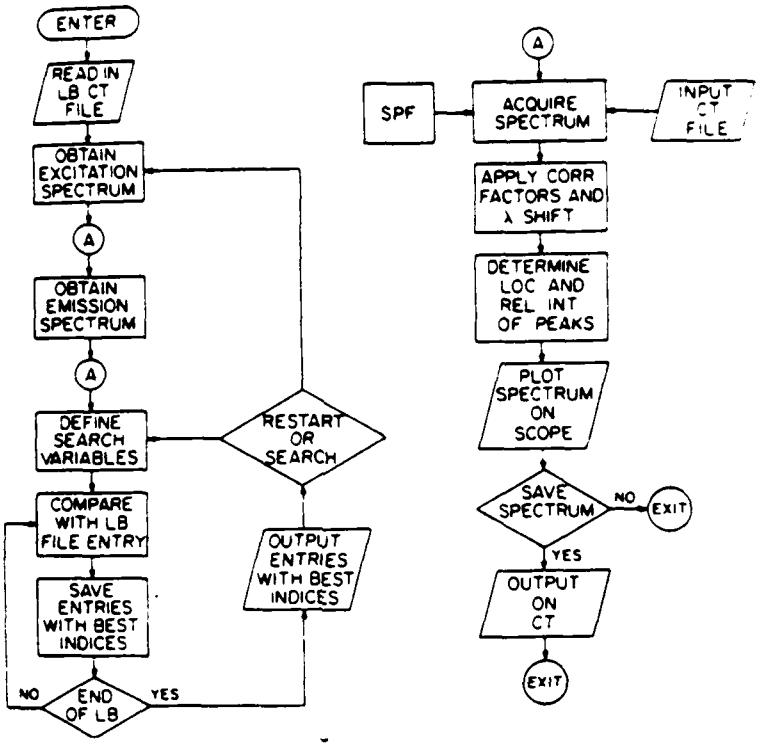

FIGURE 55. Flow chart for the file searching program. LB = library; CT = cassette. (Reprinted with permission from Miller, T. C. and Faulkner, L. R., *Anal. Chem.*, 48, 2083, 1976. Copyright 1976 American Chemical Society.)

of several searches on this system. The index column in this table refers to the degree of certainty in the spectral match. A value of "0" indicates a perfect match and less than perfect matches can extend to values as high as 65,000. Another paper from Faulkner's group[113] outlined the advantages of data compression of fluorescence spectral files by Fourier transformation.

An interesting algorithm has been developed by the research group of Buck[114] and applied to the analysis of binary fluorescent mixtures. This algorithm assumes that the fluorescence spectra of the components can be described by a series of Gaussian or asymmetric Gaussian curves. One example of qualitative analysis of binary mixtures was a study of single and binary component mixtures of anthracene, rubrene, naphthalene, and naphthacene in cyclohexane. These systems were chosen because of extensive spectral overlaps. The spectrum shown in Figure 56 is typical of the data obtained in this study. It was assumed that each binary mixture could be represented as a series of ten Gaussian peaks. Table 10 lists the peak parameters obtained for the individual standard compounds, and Table 11 provides a listing and assignment of the seven most dominant peaks determined by the algorithm for the mixture spectra. The agreement of the mixture data with standard data demonstrates the feasibility of this approach.

Since the development of the video fluorimeter which we described earlier, a number of algorithms have evolved to aid in qualitative analysis of data. Although a complete description is not practical in this paper, a brief synopsis is warranted. We previously stated that the data acquired on the video fluorimeter for a multicomponent mixture can

Table 9
RESULTS FROM SEARCH

Compound	Solvent[a]	Position of correct compound in list of results	Index
Anthracene	C	1	6
9,10-Dibromoanthracene	C	1	5
9-Methylanthracene	C	1	17
9,10-Diphenylanthracene	C	1	49
Diphenylamine	C	1	60
Diphenylamine	M	1	25
7-Hydroxycoumarin	M	1	61
7-Hydroxycoumarin	W	1	133
Quinine Sulfate	S	1	57
m-Methylanisole	C	2	17
3,5-Xylenol	C	53	76
3,5-Xylenol	M	9	17
Salicylamide	W	1	31
p-Toluidine	M	3	41
p-Cresol	M	4	15

[a] C = cyclohexane; M = methanol, S = 0.1 N H_2SO_4, W = water
[b] A perfect match has an index of zero

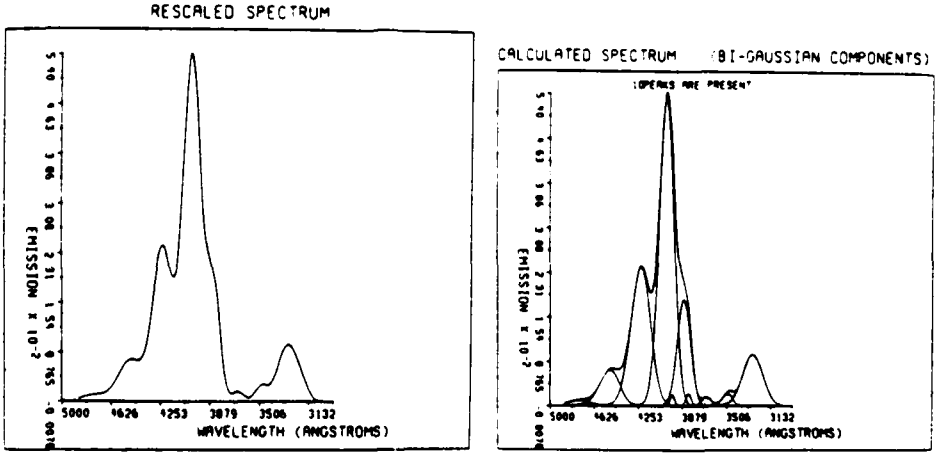

FIGURE 56. Spectra of binary mixtures. (A) Anthracene—naphthalene binary mixture spectrum. (B) Component peaks. Peaks with maxima at 364.5, 379.8, and 393.8 nm are attributed to noise. (From Rechsteiner, C. E., Gold, H. S., and Buck, R. P., *Anal. Chim. Acta*, 95, 51, 1977. With permission.)

Table 10
COMPONENT PEAK PARAMETERS FOR PURE REFERENCE MATERIALS

	Wavelength (nm)	Intensity	Peak parameter (+)	Peak parameter (−)
Anthracene	399.1	6.60	8.82	7.99
(85 μg mℓ$^{-1}$)	422.1	2.80	10.05	10.01
	447.8	0.86	9.15	10.23
	384.3	0.27	4.21	4.21
	475.1	0.17	12.91	14.33
Naphthacene	473.3	9.10	7.79	8.38
(11 μg mℓ$^{-1}$)	505.0	6.40	10.51	9.64
	541.0	1.70	17.80	13.59
	341.9	0.93	6.49	10.14
	360.3	0.61	7.69	36.32
Naphthalene	325.0	6.00	8.79	9.89
(136 μg mℓ$^{-1}$)	342.4	3.20	8.54	11.87
	363.0	0.68	13.62	19.07
	319.6	0.26	2.28	2.28
	335.4	0.75	3.76	4.46
Rubrene	551.2	1.37	14.21	16.89
(33 μg mℓ$^{-1}$)	588.0	0.75	18.14	21.38
	633.4	0.13	20.03	25.66
	472.3	0.03	6.64	7.43
	537.2	0.15	13.43	10.53

From Rechsteiner, C. E., Gold, H. S., and Buck, R. P., *Anal. Chim. Acta*, 95, 51, 1977. With permission.

be represented by

$$\underset{\sim}{M} = \sum_{i=1}^{n} \alpha(i)\, \underset{\sim}{x}(i)\, \underset{\sim}{y}(i)' \qquad (9)$$

where n is the number of fluorescent species and i is an index of each. Implicit in this equation is the assumption that the emission spectrum of each component is independent of the excitation wavelength and that the excitation spectrum of each component is independent of the monitored emission wavelength. This assumption has been found to be valid at low total absorbance (<0.01) where synergistic effects such as energy transfer and inner filter effects are negligible. In terms of linear algebra, the analysis scheme is simplified by these assumptions since for a pure component the expected linear dependence of the rows and columns would indicate a rank "1" matrix. That is, each row (column) is some linear multiple of another row (column). Additionally, the rank of a mixture matrix is a lower bound to the number of fluorescent components contributing to that matrix. However, the presence of noise in the data matrix complicates the analysis. Neglecting noise, it is reasonable to assume that a set of n vectors which form a basis for $\underset{\sim}{M}$ are related to the n desired spectral vectors. This approach to qualitative analysis of the EEM has been used with success.[115,116] Consider the positive definite square matrices $\underset{\sim}{M}\underset{\sim}{M}'$ and $\underset{\sim}{M}'\underset{\sim}{M}$. It is a simple algebraic procedure to show that the rows and columns of $\underset{\sim}{M}\underset{\sim}{M}^T$ are linear combinations of the columns of $\underset{\sim}{M}$ and that the rows and columns of $\underset{\sim}{M}^T\underset{\sim}{M}$ are linear combinations of the rows of $\underset{\sim}{M}$. Consequently, the n eigenvectors of $\underset{\sim}{M}\underset{\sim}{M}^T$ form a basis for the columns of $\underset{\sim}{M}$. Similarly, the n eigenvectors of $\underset{\sim}{M}^T\underset{\sim}{M}$ form a basis for the rows of $\underset{\sim}{M}$. Thus, the set of n basis vectors for the columns and rows of $\underset{\sim}{M}$ are easily obtained. However, it is well known that most eigenanalysis procedures will provide eigenvectors which form an orthogonal basis set. Thus, the

Table 11
COMPONENT PEAK PARAMETERS FOR BINARY MIXTURES

	Wavelength (nm)	Intensity	Parameter (+)	Parameter (−)	Contributing compound label[a]
Naphthalene	399.4	5.33	7.59	7.22	A
anthracene	421.6	2.42	10.00	9.52	A
	384.3	1.84	7.02	6.42	A
	325.0	0.89	11.04	9.49	Nl
	447.5	0.62	9.72	10.43	A
	345.6	0.21	4.43	5.98	Nl
	475.3	0.09	10.68	10.68	A
Naphthalene	325.2	4.52	8.78	9.99	Nl
naphthacene	341.2	2.69	7.49	10.19	Nl
	473.0	1.83	7.62	7.94	Nc
	504.9	1.27	9.49	9.71	Nc
	360.4	0.89	10.54	14.66	Nl
	541.3	0.33	18.02	13.04	Nc
	334.7	0.35	3.26	3.26	Nl
Naphthacene	473.3	2.31	7.60	7.80	Nc
rubrene	545.7	1.96	15.77	16.53	R
	505.1	1.59	9.81	9.71	Nc
	585.7	0.85	19.42	21.41	R
	342.5	0.28	7.21	11.19	Nc
	360.9	0.18	7.65	12.65	Nc
	630.5	0.13	17.39	23.22	R

[a] A = anthracene; Nl = naphthalene; Nc = naphthacene; R = rubrene

From Rechsteiner, C. E., Gold, H. S., and Buck, R. P., *Anal. Chim. Acta*, 95, 51, 1977. With permission.

eigenvectors for more than one component will usually contain negative elements. True spectral vectors are defined to be nonnegative. For more than one component, we then need to transform the eigenvectors to a nonnegative set of basis (spectral) vectors. Such a transformation has been described.[116] We will not discuss this transformation here, but two general observations can be made.

First, the transformation has only been applied to binary mixtures. Second, the transformation to a nonnegative basis set can be ambiguous depending on the degree of spectral overlap. As an example, consider the data presented in Figure 57. The spectrum derived from a mixture of anthracene and perylene (Figure 57A) is unambiguous due to a region of partial overlap between the emission and excitation spectra of the two compounds. Similar observations about the spectral overlap in Figure 57B and C predict that a mixture of anthracene and pyrene and a mixture of pyrene and fluoranthene would have one ambiguous spectrum each. Applications of this algorithm to a mixture of two porphyrin compounds also proved fruitful as shown by the deconvoluted spectra of Figure 58.

Another algorithm for qualitative analysis of the EEM has been developed by Fogarty and Warner.[117] This algorithm is similar to one previously developed by Hirschfeld for deconvolution of infrared data.[118] In application to fluorescence data, a major assumption of this algorithm is that each component in the mixture has some spectral region where it is a lone emitter. Consider another form of Equation 9:

$$\underline{M}_i = \sum_{i=1}^{n} C_i \underline{N}_i \qquad (10)$$

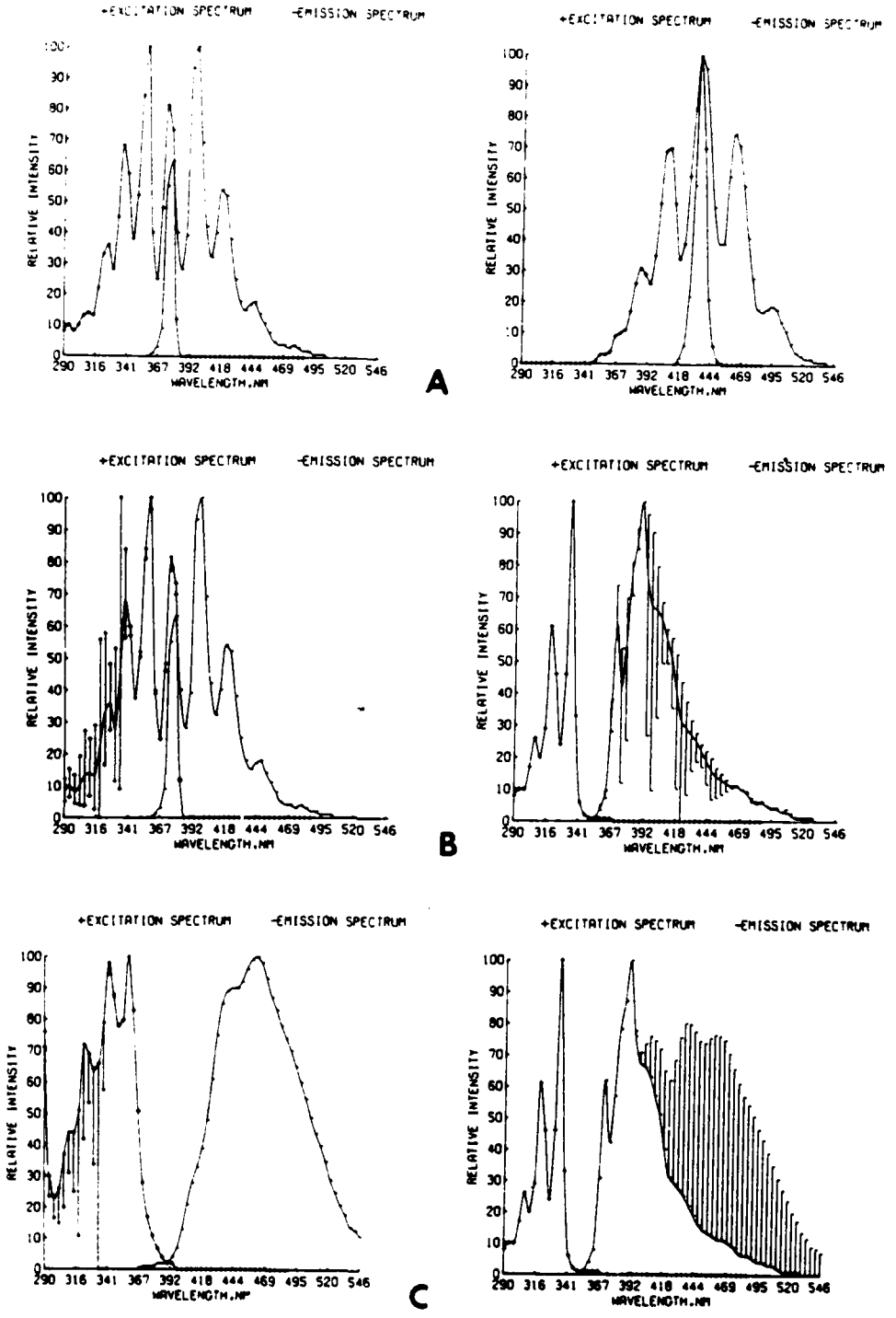

FIGURE 57. Ambiguities of binary mixtures of aromatic hydrocarbons. (A) Anthracene (left) and perylene (right). (B) Anthracene (left) and pyrene (right). (C) Fluoranthene (left) and pyrene (right). (Reprinted with permission from Warner, I. M., Davidson, E. R., and Christian, G. D., *Anal. Chem.*, 49, 564, 1977. Copyright 1977 American Chemical Society.)

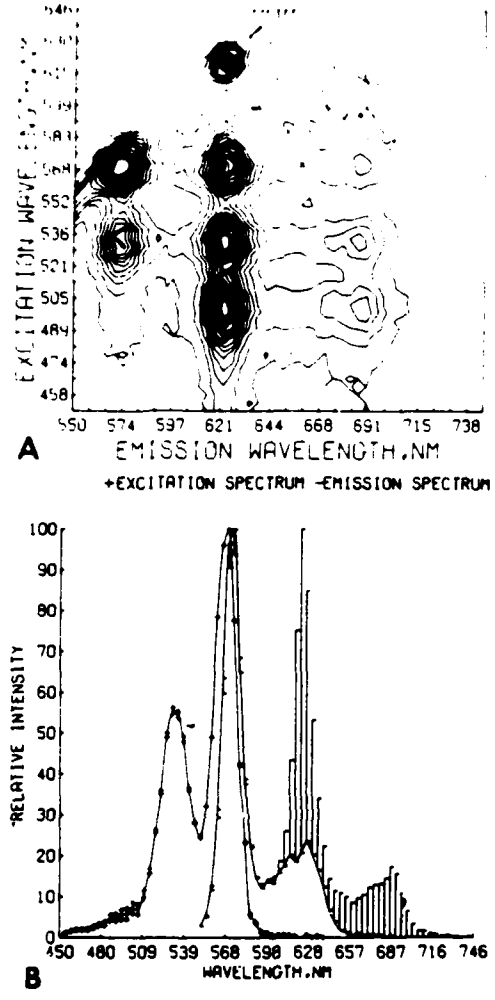

FIGURE 58. Resolved two-dimensional spectra. (A) Contour plot of data of experimentally acquired two-component mixture of ZnOEP and H_2OEP. (B) Resolved two-dimensional spectra of component 1 (ZnOEP). (C) Resolved two-dimensional spectra of component 2 (H_2OEP). (Reprinted with permission from Warner, I. M., Davidson, E. R., and Christian, G. D., *Anal. Chem.*, 49, 564, 1977. Copyright 1977 American Chemical Society.)

where $\underline{N}_i$ is an arbitrary standard matrix whose spectral characteristics are not known and C_{ij} is the concentration of the i^{th} component in $\underline{M}_j$ divided by its concentration in $\underline{N}_i$. If we can obtain a set of n matrices containing the n components of Equation 10, we will have a set of n equations in n unknowns. In matrix form, this is expressed as

$$\underline{M}^* = \underline{A}\,\underline{N}^* \qquad (11)$$

where $\underline{A}$ is the set of C_{ij} coefficients, $\underline{M}^*$ is the series of mixture matrices, and $\underline{N}^*$

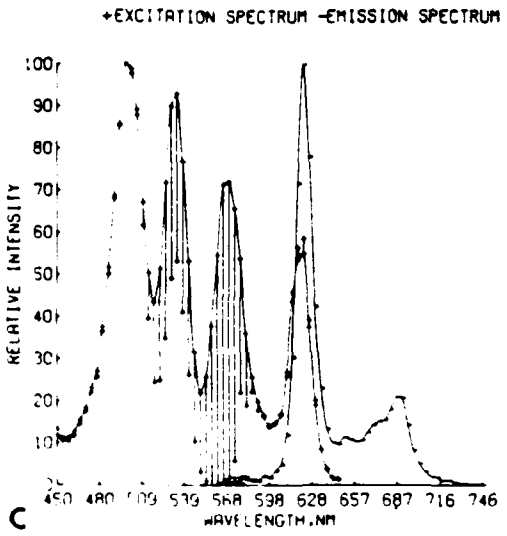

FIGURE 58C

represents the series of standard component matrices. Then, if $\underset{\sim}{A}$ is invertible, the solution to Equation 11 is

$$\underset{\sim}{N}^{\bullet} = A^{-1}\,\underset{\sim}{M}^{\bullet} \tag{12}$$

Fogarty and Warner have shown that estimates of C_n can be obtained in regions where the components are lone emitters by obtaining a ratio of one of the mixture matrices and *the other n − 1 matrices*. The authors have also shown that quenching can be an aid in this ratio deconvolution. Consider the example shown in Figure 59A which corresponds to a mixture of anthracene and 9,10-dimethylanthracene. Figure 59B corresponds to the addition of the quencher methyliodide, while Figure 59C is the matrix obtained by ratioing Figure 59A and B. The resulting deconvolution is shown in Figure 60.

Both of the algorithms which we have described for the analysis of data from a video fluorimeter are limited to mixtures of only a few components. The eigenanalysis method has only been applied to binary mixtures while the ratio method has been applied to tertiary mixtures. The ratio method has the advantage of requiring less computer time for convergence.

C. Quantitative Analysis of Fluorescence Data

The determination of the concentration of known components in a fluorescent mixture is a problem routinely confronting the analyst. These routine determinations will more often than not involve the use of standard solutions of the known compounds. Such is the approach used for quantitative evaluation of the emission-excitation matrix. Recall that we stated that Equation 9 could be rewritten as Equation 10 or, in another notation, we can write

$$\underset{\sim}{M} = \sum_{i=1}^{n} C_i(\underset{\sim}{M})_i \tag{13}$$

where C_i and $(\underset{\sim}{M})_i$ are the previously defined C_n and $\underset{\sim}{N}_n$, respectively. The best least squares approximation to $\underset{\sim}{M}$ would require a minimization of the weighted square of the elements of the error matrix $\underset{\sim}{E}$, i.e.,

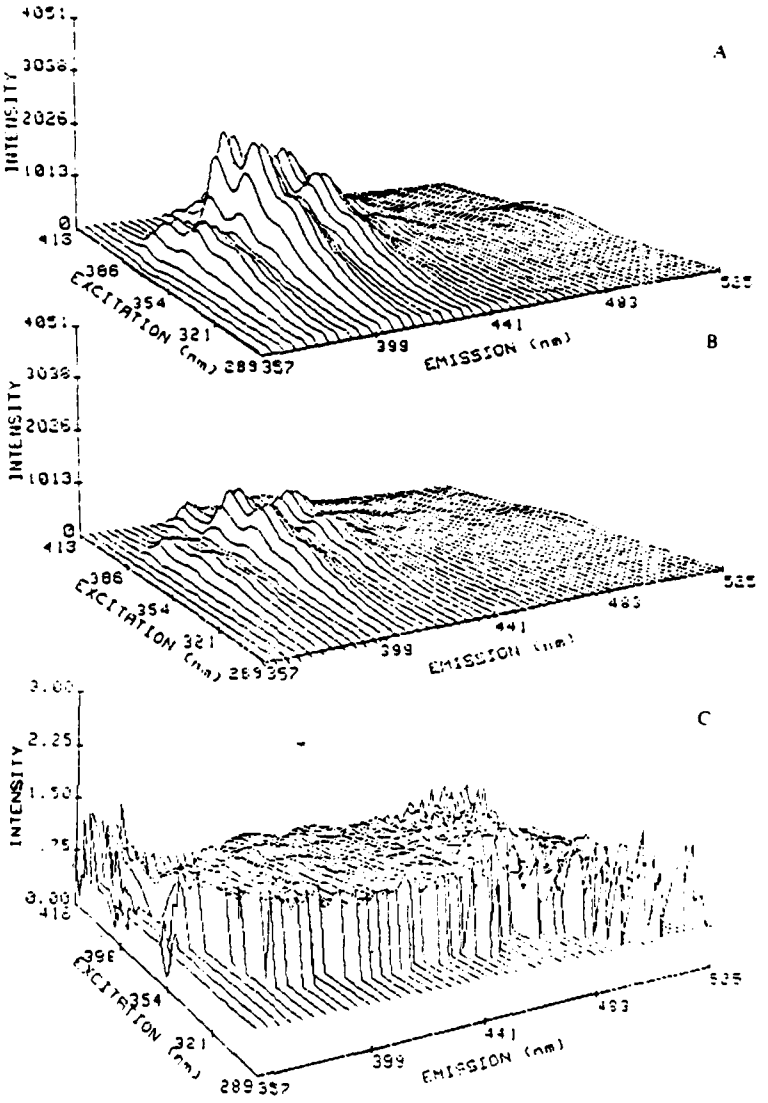

FIGURE 59. (A) Three-dimensional spectrum of anthracene mixed with 9,10-dimethylanthracene. (B) Quenched with methyl iodide. (C) Ratio of A and B. (Reprinted with permission from Fogarty, M. P. and Warner, I. M., *Anal. Chem.*, 53, 259, 1981. Copyright 1981 American Chemical Society.)

$$\sum T_{kl} E_{kl}^2 = \sum T_{kl} [M_{kl} - \sum_i C_i (M_{kl})_i]^2 = \min \qquad (14)$$

where T_{kl} represents weighting factors which we shall assume are unity for simplicity. Derivation of the least squares equation gives

$$\sum_j [\sum_{kl} (M_{kl})_i (M_{kl})_j] C_i = \sum_{kl} (M_{kl})_i M_{kl} \qquad (15)$$

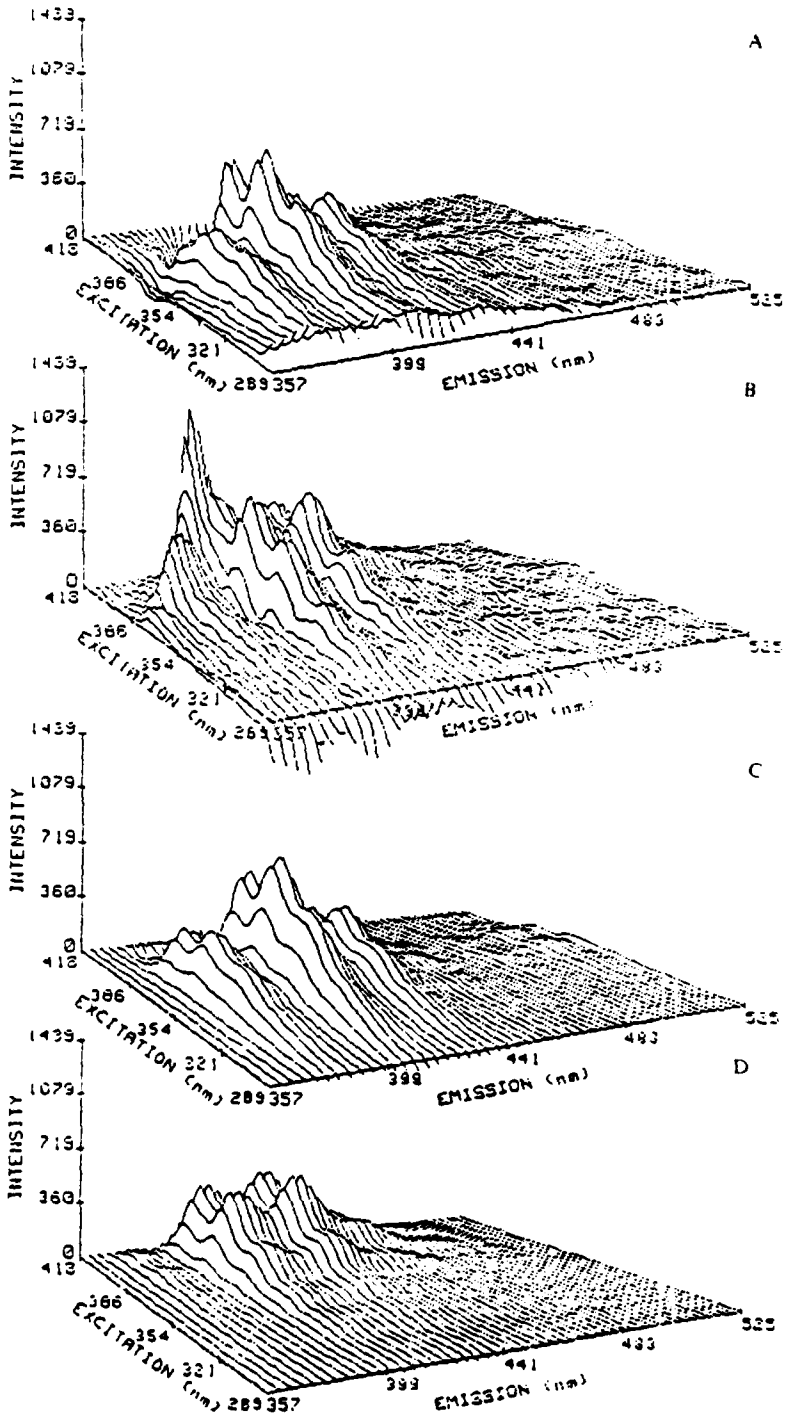

FIGURE 60. Deconvoluted spectra of Figure 59C. (A) Ratio deconvoluted spectrum of anthracene. (B) Ratio deconvoluted spectrum of 9,10-dimethyl anthracene. (C) Eigenanalysis deconvolution of anthracene. (D) Eigenanalysis deconvolution of 9,10-dimethyl anthracene. (Reprinted with permission from Fogarty, M. P. and Warner, I. M., *Anal. Chem.*, 53, 259, 1981. Copyright 1981 American Chemical Society.)

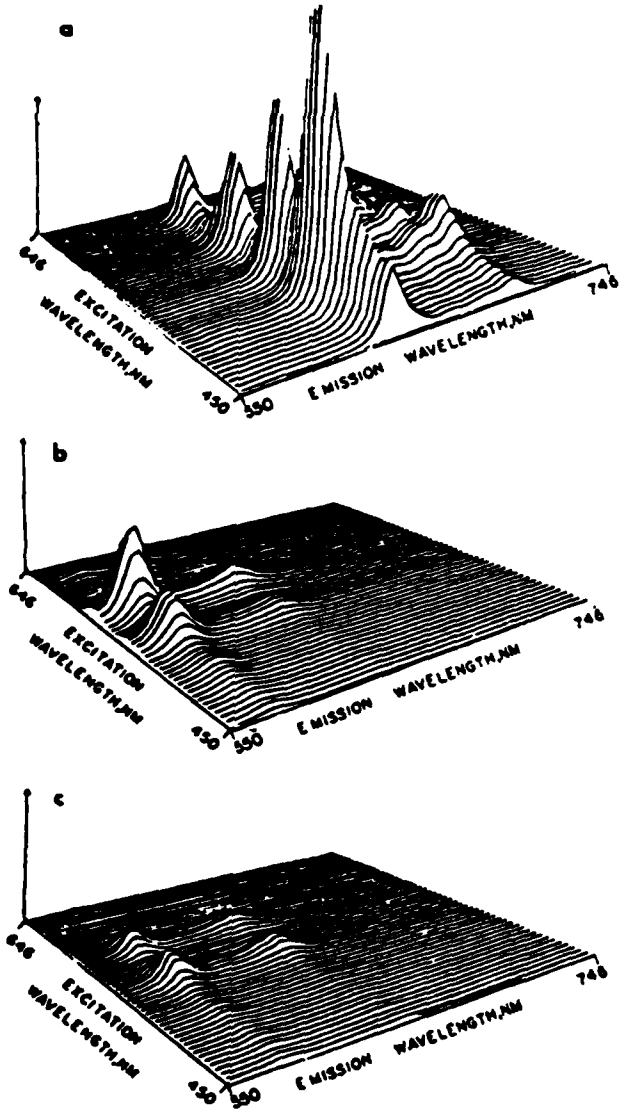

FIGURE 61. Quantitative analysis of EEM. (a) Rank one H_2OEP standard EEM. (b) Rank one ZnOEP standard EEM. (c) Rank one $SnCl_2$ OEP standard EEM. (d) Mixture with scattered light removed (data collected at 4-nm increments). (Reprinted with permission from Warner, I. M., Davidson, E. R., and Christian, G. D., *Anal. Chem.*, 49, 2155, 1977. Copyright 1977 American Chemical Society.)

where M_{kl} is an element of $\underset{\sim}{M}$ and $(M_{kl})_i$ and $(M_{kl})_j$ are elements of i^{th} and j^{th} standard matrices. An alternative approach uses linear programming to maximize the function

$$\square = \sum_{i=1}^{n} A_i C_i \qquad (16)$$

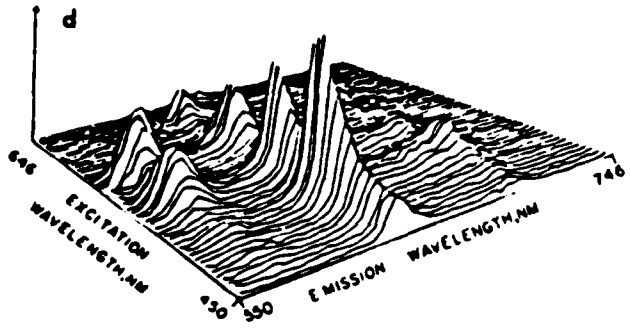

FIGURE 61D

Table 12
LEAST SQUARES AND LINEAR PROGRAMMING ANALYSIS OF EXPERIMENTALLY ACQUIRED TERNARY MIXTURE OF H_2OEP, $SnCl_2OEP$, AND ZnOEP

Component	True concentration 10^{-7} *M*	Least squares concentration 10^{-7} *M*[a]	Estimated std dev	Simplex concentration 10^{-7} *M*[a]
H_2OEP	2.42	2.46	0.02	2.38
ZnOEP	21.4	21.6	0.5	21.0
$SnCl_2OEP$	3.04	3.44	0.23	3.22

[a] Calculated using the spectrum of a 4.83×10^{-7} *M* H_2OEP solution, a 2.14×10^{-6} *M* ZnOEP solution, and a 6.07×10^{-7} *M* $SnCl_2OEP$ solution as standards.

subject to the constraints

$$E_{kl} = M_{kl} - \sum_i C_i (M_{kl})_i \geq 0 \qquad (17)$$

where

$$A_i = \sum_{kl} (M_{kl})_i \qquad (18)$$

Both of these methods have been applied to quantitative analysis of the EEM with success.[119] As an example, Figure 61 shows typical data in this study, while Table 12 displays the input and computed results of the analyses. This study demonstrated that the least squares method was satisfactory when all of the components are known. However, the linear programming method is preferred over the least squares method when all of the components are not specified.

An alternative to the least squares and linear programming method has been proposed and applied by Ho et al.[120,121] This method is termed the "method of rank annihilation" and is more useful than either the least squares or linear programming method when all of the components are not specified. Briefly, one can approximate $\underset{\sim}{M}$ by a matrix M′ formed from the eigenvalues ξ_k and eigenvectors U_k and V_k^T. I.e.,

$$\underset{\sim}{M}' = \sum_{k=1}^{s} \xi_k U_k V_k^T \qquad (19)$$

Table 13
RESULTS OF LEAST SQUARES AND RANK ANNIHILATION FOR A ONE-COMPONENT PERYLENE SOLUTION

	Relative concentrations[a]					
	20.0	**10.0**	**2.00**	**0.200**	**0.100**	**0.020**
Least squares	19.99	10.07	2.23	0.250	0.114	0.022
Annihilation	20.03	10.09	2.23	0.249	0.115	0.023
annihilation	20.07	10.10	2.23	0.250	0.114	0.022
b_i	0.9978	0.9969	0.9987	0.9998	0.9991	0.9500
a_i	0.9997	0.9984	0.9998	0.9999	0.9[illegible]	0.9852
ξ_i	2.97×10^{-11}	7.52×10^{-12}	3.86×10^{-11}	4.59×10^{-9}	9.56×10^{-7}	4.04×10^{-7}

[a] The concentrations are relative to the standard 5.0×10^{-5} *M* perylene solution. For this standard $\alpha_i^2 = 7.37 \times 10^{10}$.

Reprinted with permission from Ho, C. N., Christian, G. D., and Davidson, E. R., *Anal. Chem.*, 50, 1108, 1978. Copyright 1978 American Chemical Society.

where $s \leq n$. If the test compound is present, then the vectors $\underline{x}$ and $\underline{y}^I$ (Equation 9) and u_k and v_k^I should satisfy the conditions

$$\sum_{k=1}^{n} a_k^2 = (u_k^I x)^2 = 1 \tag{20}$$

and

$$\sum_{k=1}^{n} b_k^2 = (v_k^I y)^2 = 1 \tag{21}$$

Bessel's inequality requires that

$$\sum_{k=1}^{n} a_k^2 \leq 1 \tag{22}$$

and thus the nearness of

$$\left(\sum_{k=1}^{n} a_k^2\right)\left(\sum_{k=1}^{n} b_k^2\right) \tag{23}$$

to unity is the estimate of whether the test compound is present. If Equations 20 and 21 are satisfied, then the matrix

$$E' = \underline{M} - \beta N \tag{24}$$

will have rank $n - 1$ when evaluated at $\beta = C_i - C_i^0$ where C_i is the concentration of the test compound in the mixture and C_i^0 is the concentration of its standard. Simply stated, the rank annihilation method measures the value of β at which the test component is exactly eliminated from the mixture matrix. Table 13 shows the results of the least squares and rank annihilation methods for a one-component system.[120] Table 14 shows the results of rank annihilation for perylene in this mixture while Figure 62 is an eigenvalue plot of the same data.[121] It is apparent from these results that the rank annihilation method shows the greatest promise for quantitative analysis of the EEM when the identities of all components are not specified.

Table 14
RESULTS OF THE METHOD OF RANK ANNIHILATION USING THE EXTENDED RANK PROCEDURE

		Relative perylene concentrations[a]					
r[b]	Eigenvalue[c]	20.00	10.00	2.00	1.00	0.20	0.10
2	2	20.04	10.08	2.11	1.11	0.85	0.78
3	2	20.04	10.08	2.05	1.29	0.79	0.71
	3	14.66	9.18	2.11	0.99	0.34	0.26
4	2	20.04	10.08	2.05	1.28	0.75	0.68
	3	14.66	9.19	2.10	0.96	0.20	0.10
6	3					0.20	0.10

[a] Solutions and standards are the same as in Table 13.
[b] Dimension of e matrix before extension.
[c] Index of eigenvalue minimized.

Reprinted with permission from Ho, C. N., Christian, G. D., and Davidson, E. R., *Anal. Chem.*, 52, 1071, 1980. Copyright 1980 American Chemical Society.

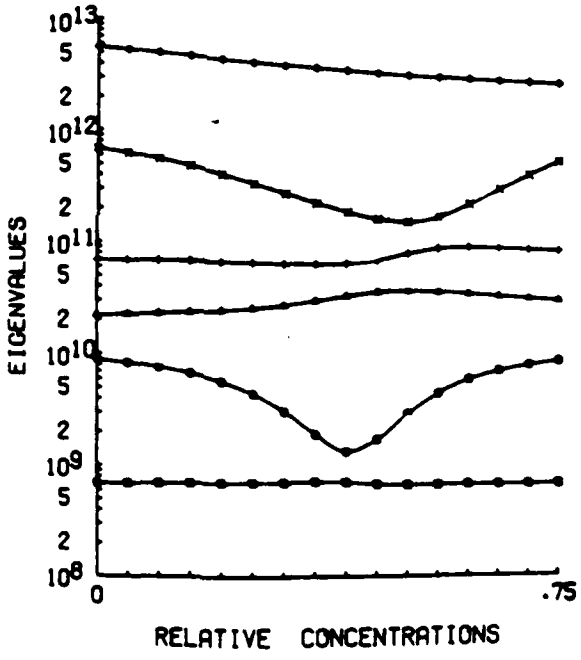

FIGURE 62. Plot of eigenvalues vs. relative concentration. Plot of the eigenvalues μ with R = 6 against the relative concentration (β) of the standard subtracted for anthracene in Sample I. The relative concentration plotted must be multiplied by 2.5 (gain factor) to obtain the actual relative concentration. (Reprinted with permission from Ho, C. N., Christian, G. D., and Davidson, E. R., *Anal. Chem.*, 52, 1071, 1980. Copyright 1980 American Chemical Society.)

V. SUMMARY AND CONCLUSIONS

In this manuscript, we have presented several examples of the recent advances in multicomponent fluorescence analysis. Our discussion has concentrated mainly on developments in instrumental methods, although we have also provided a brief review of the increasingly important area of multicomponent data reduction. No single critical review article can reasonably cover all possible aspects of a given topic, and for those topics not included, we have referred the reader to other review articles. One such topic which we feel is noteworthy is matrix isolation spectroscopy. In this technique, the constituents of a multicomponent mixture are analyzed at low temperatures after isolation through vaporization and large dilution by an inert gas. The spectra obtained are comparable in sharpness to those obtained by the low temperature Shpol'skii method.[122] A number of applications of the use of this technique in fluorescence spectroscopy are cited by Wehry and co-workers.[123-125] A general review on matrix isolation spectroscopy has been given by Wehry and Mamantov.[126]

Another important area which we should mention here is the application of lasers to multicomponent fluorescence analysis. Several advantages accrue from the use of these high intensity, narrow line excitation sources, including increased sensitivity and selectivity. A recent review was written by Wright and Wirth on the use of lasers for multicomponent fluorescence analysis.[127] Applications in fluorescence line narrowing spectrometry are becoming increasingly important.[128-130]

Finally, we would like to emphasize that multicomponent fluorescence analysis is a very new field experiencing rapid growth in recent years. New instrumental techniques and data reduction strategies are being developed at a fast pace, and we look forward to their increased application in chemical analysis.

ACKNOWLEDGMENT

I. M. Warner is grateful for support from the Office of Naval Research and the Department of Energy (DE-AS05-80EV10404) during the preparation of this manuscript.

REFERENCES

1. **O'Donnell, C. M. and Solie, T. N.,** *Anal. Chem.*, 50, 189R (1978)
2. **O'Donnell, C. M. and Solie, T. N.,** *Anal. Chem.*, 48, 175R (1976)
3. **Aaron, J. J. and Winefordner, J. D.,** *Talanta*, 22, 707 (1975)
4. **Karasek, F. W.,** *Res/Dev*, 27, 28 (1976).
5. **Bridges, J. W.,** *Methodol. Dev. Biochem.*, 5, 25 (1976)
6. **Gibson, E. P.,** *J. Forensic Sci.*, 22, 403 (1977).
7. **Guilbault, G. G.,** *Photochem. Photobiol.*, 25, 403 (1977).
8. **Klainer, S. M.,** *Opt. Eng.*, 15, SR14, (1976).
9. **Lloyd, J. B. F.,** *Chem. Br.*, 11, 442 (1975).
10. **Haddad, P. R.,** *Talanta*, 24, 1 (1977)
11. **Krause, L.,** *Adv. Chem. Phys.*, 28, 267 (1975)
12. **Richardson, F. S. and Riehl, J. P.,** *Chem. Rev.*, 77, 773 (1977)
13. **Boutilier, G. D., Bradshaw, J. D., Weeks, S. J., and Winefordner, J. D.,** *Appl. Spectrosc.*, 31, 307 (1977).
14. **Cooney, R. P.,** Detector and Other Instrumental Effects on Signal-To-Noise Ratio in Gas and Liquid Phase Fluorescence, Dissertation, University of Florida, Gainesville, 1977
15. **Lim, C. S. and Miller, J. N.,** *Anal. Chim. Acta*, 100, 235 (1978)
16. **White, J. U.,** *Anal. Chem.*, 48, 2089 (1976).
17. **Anacreon, R. E. and Ohnishi, Y.,** *Appl. Opt.*, 14, 2921 (1975).
18. **Porro, T. J. and Terhaar, D. A.,** *Anal. Chem.*, 48, 1103A (1976)

19. **Jameson, D. M., Spencer, R. D., and Weber, G.,** *Rev. Sci. Instrum.*, 47, 1034 (1976).
20. **Glushko, V., Caley, R., and Karp, C.,** *Anal. Chem.*, 48, 2077 (1976).
21. **Wehrly, J. A., Williams, J. F., Jameson, D. M., and Kolb, D. A.,** *Anal. Chem.*, 48, 1424 (1976).
22. **Bowen, E. J.,** *Luminescence in Chemistry*, Van Nostrand, London, 1968.
23. **Parker, C. A.,** *Photoluminescence of Solutions*, Elsevier, New York, 1968.
24. **Wehry, E. L.,** *Modern Fluorescence Spectroscopy*, Vols. 1 and 2, Plenum Press, New York, 1976.
25. **Guilbault, G. G.,** *Practical Fluorescence*, Marcel Dekker, New York, 1973.
26. **Lewis, G. N. and Kasha, M.,** *J. Am. Chem. Soc.*, 66, 2100 (1944).
27. **St. John, P. A. and Winefordner, J. D.,** *Anal. Chem.*, 39, 500 (1967).
28. **Freed, S. and Salmre, W.,** *Science*, 128, 1341 (1958).
29. **Freed, S. and Vise, M. H.,** *Anal. Biochem.*, 5, 338 (1963).
30. **Winefordner, J. D. and Latz, H. W.,** *Anal. Chem.*, 35, 1517 (1963).
31. **Hollifield, H. C. and Winefordner, J. D.,** *Chem. Instrum.*, 1, 341 (1969).
32. **Keirs, R. J., Britt, R. D., and Wentworth, W. E.,** *Anal. Chem.*, 29, 202 (1957).
33. **O'Haver, T. C. and Winefordner, J. D.,** *Anal. Chem.*, 38, 602 (1966).
34. **O'Haver, T. C. and Winefordner, J. D.,** *Anal. Chem.*, 38, 1258 (1966).
35. **Winefordner, J. D.,** *Acc. Chem. Res.*, 2, 361 (1969).
36. **Fisher, R. P. and Winefordner, J. D.,** *Anal. Chem.*, 44, 948 (1972).
37. **O'Donnell, C. M., Harbaugh, K. F., Fisher, R. P., and Winefordner, J. D.,** *Anal. Chem.*, 45, 609 (1973).
38. **Harbaugh, K. F., O'Donnell, C. M., and Winefordner, J. D.,** *Anal. Chem.*, 46, 1206 (1974).
39. **Badea, M. G. and Georghiou, S.,** *Rev. Sci. Instrum.*, 47, 314 (1976).
40. **Steinograber, O. J. and Berlman, I. B.,** *Rev. Sci. Instrum.*, 34, 524 (1963).
41. **Hazan, G., Grinvald, A., Maytal, M., and Steinberg, I. Z.,** *Rev. Sci. Instrum.*, 45, 1602 (1974).
42. **Thomaz, M. F., Barrades, I., and Ferreira, J. A.,** *J. Luminesc.*, 11, 55 (1975).
43. **Yguerabide, J.,** *Methods in Enzymology*, Vol. 26, Part C, Colowick, S. P. and Kaplan, N. O., Eds., Academic Press, New York, 1972.
44. **Weissler, W.,** *Anal. Chem.*, 46, 500R (1974).
45. **Cundill, R. B. and Palmer, T. F.,** *Annual Reports on the Progress of Chemistry*, Vol. 70, Sec. A, The Chemical Society, London, 1973, p. 31.
46. **Loper, G. L. and Lee, E. K. C.,** *Chem. Phys. Lett.*, 13, 140 (1972).
47. **Yoshihara, K., Kasuya, T., Inove, A., and Nagakura, S.,** *Chem. Phys. Lett.*, 9, 469 (1971).
48. **Deinum, T., Werkhoven, C. J., Langelaar, J., Pettschnick, R. P., and van Voosot, J. D. W.,** *Chem. Phys. Lett.*, 12, 189 (1971).
49. **Shaver, L. A. and Love, L. J. C.,** *Appl. Spectrosc.*, 29, 485 (1975).
50. **Love, L. J. C., Upton, L. M., and Ritter, A. W.,** *Anal. Chem.*, 50, 2059 (1978).
51. **Love, L. J. C. and Shaver, L. A.,** *Anal. Chem.*, 48, 364A (1976).
52. **Aaron, J. J., Sanders, L. B., and Winefordner, J. D.,** *Clin. Chim. Acta*, 45, 375 (1973).
53. **Shaver, L. A.,** Critical Evaluation of Time-Resolved Fluorescence for the Analysis of Multicomponent Fluorescent Mixtures, Dissertation, Seton Hall University, South Orange, N.J., 1978.
54. **Busch, G. E. and Rentzepeis, P. M.,** *Science*, 194, 276 (1976).
55. **Flemming, G. R., Morris, J. M., and Robinson, G. W.,** *Aust. J. Chem.*, 30, 2337 (1977).
56. **Porter, G., Sadkowski, P. J., and Tredruell, C. J.,** *Chem. Phys. Lett.*, 49, 416 (1977).
57. **Spencer, R. D. and Weber, G.,** *Ann. N.Y. Acad. Sci.*, 158, 361 (1969).
58. **Weber, G.,** *J. Chem. Phys.*, 66, 4081 (1977).
59. **Schurer, K., Ploegaert, P. G. F., and Wennekes, P. C. M.,** *J. Phys. E*, 9, 821 (1976).
60. **Itoh, K. B.,** *Gifu Daigaku Igakubu Kiyo*, 25, 97 (1977).
61. **Pohoski, R. and Zachara, S.,** *Zesz. Nauk. Wydz. Mat., Fiz. Chau., Univ. Gdanski, Fiz.*, 1, 107 (1972).
62. **Reseuitz, E. P. and Lippert, E.,** *Ber. Bunsenges Phys. Chem.*, 78, 1227 (1974).
63. **Hauser, M. and Heidt, G.,** *Rev. Sci. Instrum.*, 46, 470 (1975).
64. **Mousa, J. J. and Winefordner, J. D.,** *Anal. Chem.*, 46, 1195 (1974).
65. **O'Haver, T. C. and Parks, W. M.,** *Anal. Chem.*, 46, 1886 (1974).
66. **O'Haver, T. C., Green, G. L., and Keppler, B. R.,** *Chem. Instrum.*, 4, 197 (1973).
67. **Green, G. L. and O'Haver, T. C.,** *Anal. Chem.*, 46, 2191 (1974).
68. **Brownrigg, J. T., Hornig, A. W., and Coleman, H. J.,** Paper 396 presented at the 28th Pittsburgh Conference on Analytical Chemistry and Applied Spectroscopy, March 1977.
69. **Giering, L. P.,** *Ind. Res.*, 20, 134 (1978).
70. **Parker, C. A.,** *Photoluminescence of Solutions*, Elsevier, New York, 1968, p. 21.
71. **Guilbault, G. G.,** *Practical Fluorescence: Theory Methods and Techniques*, Marcel Dekker, New York, 1973.
72. **Haugen, G. H., Raby, G. A., and Rigdon, L. P.,** *Chem. Inst.*, 6, 205 (1975).
73. **Bentz, A. P.,** *Anal. Chem.*, 48, 455A (1976).

74. **Adlard, E. R.**, *J. Inst. Petrol*, 58, 63 (1972).
75. **Gaugh, T. H.**, *Science*, 203, 1330 (1979).
76. **Johnson, D. W., Gladden, J. A., Callis, J. B., and Christian, G. D.**, *Rev. Sci. Instrum.*, 49, 54 (1978).
77. **Warner, I. M., Callis, J. B., Davidson, E. R., and Christian, G. D.**, *Clin. Chem.*, 22, 1483 (1976).
78. **Johnson, D. W., Callis, J. B., and Christian, G. D.**, *Anal. Chem.*, 49, 747A (1977).
79. UFS-200 Flat Field Spectrograph, Product of Instruments SA, Inc., 08840, Metuchen, N.J.
80. **Talmi, Y.**, *Anal. Chem.*, 47, 697A (1975).
81. **Talmi, Y.**, *Anal. Chem.*, 47, 685A (1975).
82. **Talmi, Y., Baker, D. C., Jadamec, J. R., and Saver, W. A.**, *Anal. Chem.*, 50, 936A (1978).
83. **Warner, I. M., Fogarty, M. P., and Shelly, D. C.**, *Anal. Chim. Acta*, 109, 361 (1979).
84. **Lloyd, J. B. F.**, *Nat. Phys. Sci.*, 231, 64 (1971).
85. **Lloyd, J. B. F.**, *J. Forensics Sci. Soc.*, 11, 83 (1971).
86. **Lloyd, J. B. F.**, *Analyst*, 100, 82 (1975); 99, 729 (1974).
87. **John, P. and Soutar, I.**, *Anal. Chem.*, 48, 520 (1976).
88. **Lloyd, J. B. F. and Evett, I. W.**, *Anal. Chem.*, 49, 1710 (1977).
89. **Vo-Dinh, T.**, *Anal. Chem.*, 50, 396 (1978).
90. **Vo-Dinh, T. and Gammage, R. B.**, *Anal. Chem.*, 50, 2054 (1978).
91. **Latz, H. W. Ullman, A. H., Winefordner, J. D.**, *Anal. Chem.*, 50, 2148 (1978).
92. **Anacreon, R. E. and Ohnishi, Y.**, *Appl. Opt.*, 14, 2921 (1975).
93. **Porro, T. J. and Terhaar, D. A.**, *Anal. Chem.*, 48, 1103A (1976).
94. **Wilson, R. L. and Ingle, J. D.**, *Anal. Chem.*, 49, 1060 (1977).
95. **Wilson, R. L. and Ingle, J. D.**, *Anal. Chem.*, 49, 1066 (1977).
96. **Fogarty, M. P. and Warner, I. M.**, *Appl. Spectrosc.*, 34, 438 (1980).
97. **Johnson, E., Abu-Shumays, A., and Abbott, S. R.**, *J. Chromatogr.*, 134, 107 (1977).
98. **Slavin, W., Rhip Williams, A. T., and Adams, R. F.**, *J. Chromatogr.*, 134, 121 (1977).
99. **Martin, F., Maine, J., Swelley, C., and Holland, J. F.**, *Clin. Chem.*, 22, 1434 (1976).
100. **Jadamec, J. R., Sauer, W. A., and Talmi, Y.**, *Anal. Chem.*, 49, 1316 (1977).
101. **Hershberger, L., Callis, J., and Christian, G.**, *Anal. Chem.*, 51, 1444 (1979).
102. **Shelly, D. C., Ilger, W. A., Fogarty, M. P., and Warner, I. M.**, *Altex Chromatogram*, 3(1), November 1979.
103. **Lawrence, J. F.**, *J. Chrom. Sci.*, 17, 147 (1979).
104. **Dunges, W., Meyer, A., Muller, K., Muller, M., Pietschmann, R., Plachetta, C., Sehr, R., and Tuss, H.**, *Z. Anal. Chem.*, 288, 361 (1977).
105. **Porro, T. J., Anacreon, R. E., Flandreau, P. S., and Fagerson, I. S.**, *J. Assoc. Off. Anal. Chem.*, 56, 608 (1972).
106. **Shepherd, T. M.**, *Chem. Ind.*, No. 7, 332 (1973).
107. **Tuan, V. D. and Wild, U. P.**, *Appl. Opt.*, 13, 2899 (1974).
108. **Budde, W. and Dodd, C. X.**, *Appl. Opt.*, 12, 2607 (1971).
109. **Pailthorpe, M. T.**, *J. Phys. E: Sci. Instrum.*, 8, (1975).
110. **Holland, J. F., Teits, R. E., Kelly, P. M., and Timnick, A.**, *Anal. Chem.*, 49, 706 (1977).
111. **Leese, R. A. and Wehry, E. L.**, *Anal. Chem.*, 50, 1193 (1978).
112. **Miller, T. C. and Faulkner, L. R.**, *Anal. Chem.*, 48, 2083 (1976).
113. **Yim, K. W., Miller, T. C., and Faulkner, L. R.**, *Anal. Chem.*, 49, 2069 (1977).
114. **Rechsteiner, C. E., Gold, H. S., and Buck, R. P.**, *Anal. Chim. Acta*, 95, 51 (1977).
115. **Weber, G.**, *Nature (London)*, 190, 27 (1961).
116. **Warner, I. M., Christian, G. D., Davidson, E. R., and Callis, J. B.**, *Anal. Chem.*, 49, 564 (1977).
117. **Fogarty, M. P. and Warner, I. M.**, *Anal. Chem.*, 53, 259 (1981).
118. **Hirschfeld, T.**, *Anal. Chem.*, 48, 721 (1976).
119. **Warner, I. M., Davidson, E. R., and Christian, G. D.**, *Anal. Chem.*, 49, 2155 (1977).
120. **Ho, C. N., Christian, G. D., and Davidson, E. R.**, *Anal. Chem.*, 50, 1108 (1978).
121. **Ho, C. N., Christian, G. D., and Davidson, E. R.**, *Anal. Chem.*, 52, 1071 (1980).
122. **Kirkbright, G. F. and De Lima, C. G.**, *Analyst*, 99, 338 (1974).
123. **Stroupe, R. C., Tokousbalides, P., Kickinson, R. B., Wehry, E. L., and Mamantov, G.**, *Anal. Chem.*, 49, 701 (1977).
124. **Tokousbalides, P., Hinton, E. R., Dickinson, R. B., Belotta, P. V., Wehry, E. L., and Mamantov, G.**, *Anal. Chem.*, 50, 1189 (1978).
125. **Dickinson, R. B. and Wehry, E. L.**, *Anal. Chem.*, 51, 780 (1979).
126. **Wehry, E. L. and Mamantov, G.**, *Anal. Chem.*, 51, 643A (1979).
127. **Wright, J. C. and Wirth, M. J.**, *Anal. Chem.*, 52, 989A (1980).
128. **Personov, R. I. and Kharlamov, B. M.**, *Opt. Commun.*, 7, 417 (1973).
129. **Eberly, J. H., McGolgin, W. C., Kawaoka, K., and Marchetti, A. P.**, *Nature*, 251, 215 (1974).
130. **Brown, J. C., Edelson, M. C., and Small, G. J.**, *Anal. Chem.*, 50, 1394 (1978).


DATE
FILME
7 — 8